EFFECT OF BODY MASS INDEX ON THE BIOMECHANICAL PROPERTIES OF ANTERIOR VAGINAL WALL TISSUE OF PROLAPSED PATIENTS

by

SANDRA GABRIELA OCHOA LOPEZ

Presented to the Faculty of the Graduate School of

The University of Texas at Arlington in Partial Fulfillment

of the Requirements

for the Degree of

MASTER OF SCIENCE IN BIOMEDICAL ENGINEERING

THE UNIVERSITY OF TEXAS AT ARLINGTON

May 2013

Acknowledgements

I take this opportunity to express my very great appreciation to the members of my thesis committee for their willingness to give their time and useful recommendations and guidance during the development of my research work and this document. Special thanks to Dr. Cheng-Jen Chuong, my research advisor, for his valuable support, advice and assistance in keeping my progress on schedule throughout the course of my degree. I am also deeply thankful to Dr. Robert Eberhart and honored for his time taken to revise my thesis document and his valuable input to help me improve it. My grateful thanks are also extended to Dr. Philippe Zimmern and his medical students at the University of Texas Southwestern Medical Center, who trusted me with patient data from the experiments they conducted so I could do the analysis reported in this document. Thanks to Larry Perry from SLRI Nashville, Tennessee, for the generous loan of BTC-2000^{TM} instrument and to Mr. Jimmy and Howard of the UTA physics shop for the useful modifications of the BTC-2000^{TM} probe. Also thanks to Dr. Doyle Hawkins for taking a special interest in improving the statistical analysis for the publication that might result from this study.

I owe a debt of gratitude to the Bioengineering department and to the University of Texas at Arlington for accepting me into their Master's program, as well as to all of the professors that I had during my degree. I learned a lot from all of you. I would also like to express a deep sense of gratitude to the Mexican National Council for Science and Technology (CONACYT) for providing me a scholarship that gave me the opportunity to achieve one of my professional goals by completing my Master's degree in my second language.

This thesis is dedicated to my wonderful family: my father Jorge Ochoa, my mother Maria Antonieta Lopez, my sister Tony and my brother Jorge, who have always been my motivation. I would like to thank them for their endless love and support throughout my life and for always believing in me, even when I faced difficult situations. Thank you for your words of encouragement and for providing me all the tools I needed for this success. You kept me strong while being apart from you and focused on my objective. I love you. Lastly, I wish to thank my best friend Roberto, and all of my amazing friends and colleagues that supported me throughout the course of my graduate degree. All of you contributed to this accomplishment.

April 19, 2013

Abstract

EFFECT OF BODY MASS INDEX ON THE BIOMECHANICAL PROPERTIES OF ANTERIOR VAGINAL WALL TISSUE OF PROLAPSED PATIENTS

Sandra Gabriela Ochoa Lopez, MS

The University of Texas at Arlington, 2013

Supervising Professor: Cheng-Jen Chuong

Anterior Vaginal Wall (AVW) prolapse is a bothersome condition that affects thousands of women. Its onset and progression is not well understood but is thought to be multifactorial. Biomechanical properties of AVW tissue from prolapsed patients have been measured in-vitro using excised tissue specimens with great variability found in results, possibly from differences in tissue preparation, setting, preservation time, temperature, hydration, etc. In-vivo test using a BTC-2000^{TM} cutometer-like device has recently been developed that measures the tissue uplift under suction pressure load. In this study, a systematical analysis of biomechanical property measurements from AVW tissues was done, including both in-vitro and in-vivo tests, derived from 28 patients requiring vaginal surgical repair. Immediately after in-vivo measurement, AVW tissue sample was excised from consenting patients and subjected to in-vitro uniaxial tensile test to measure its intrinsic biomechanical properties. Data from both in-vivo and in-vitro tests were then correlated with each of four known risk factors: obesity, parity, age and menopause. Results from in-vitro test showed that obesity could affect AVW biomechanical properties, with overweight patients (BMI > 25, n=15) developing higher tissue stiffness than patients with normal weight (BMI < 25, n=13), possibly due to tissue

remodeling. Patients with higher parity numbers (3-6) are seen to have higher tissue compliance than patients in the other group (0-2). Although age and menopause did not show statistically significant differences in biomechanical properties, they exhibit trend lines suggesting alterations in tissue biomechanical properties associated with these factors. Combining data from both in-vitro and in-vivo tests could aid in the development of improved prosthetic meshes and better planning for surgical repair.

Table of contents

List of Illustrations

List of Tables

List of Abbreviations

1. 10%TM=Tangent modulus at 10% strain
2. 25%LSE=Loading strain energy at 25% stretch
3. 25%HSE=Hysteresis strain energy from 25% loading-unloading strain
4. 25%TM= Tangent modulus at 25% strain
5. 25%USE=Unloading strain energy from 25% stretch
6. AVM= Anterior Vaginal Muscularis
7. AVW= Anterior vaginal wall
8. BMI= Body mass index
9. ECM= Extracellular matrix
10. FDA= Food and Drug Administration
11. FSE= Failure strain energy
12. IAP= Intra-abdominal pressure
13. KLC= Potassium chloride
14. LOX=Lysyl Oxidase
15. LOX1=Lysyl Oxidase-like 1
16. MMPs= Matrix metalloproteinases
17. MRI=Magnetic resonance Imaging
18. MTM=Maximal tangent modulus
19. POP= Pelvic organ prolapse
20. POP-Q= Pelvic organ prolapse quantitative system
21. PTU= Peak tissue uplift
22. SD= Standard deviation

23. TVL=Total vaginal length
24. UTS= Ultimate tensile strength
25. YSE=Yielding strain energy

Chapter 1

Introduction

1.1 Female pelvic organ prolapse background

Pelvic organ prolapse (POP) is a bothersome condition for women and occurs when pelvic organs become weakened or stretched and either descend or shift within the pelvis, sometimes protruding against the walls of the vagina. This is a common disease affecting an estimated 3.3 million women in the United States [1] having a great impact in women's quality of life. POP can present in different ways depending on the organ that descent. The most common form is anterior vaginal wall (AVW) prolapse [2], also known as cystocele, which involves the bladder descent by lack of vaginal wall support (Figure 1).

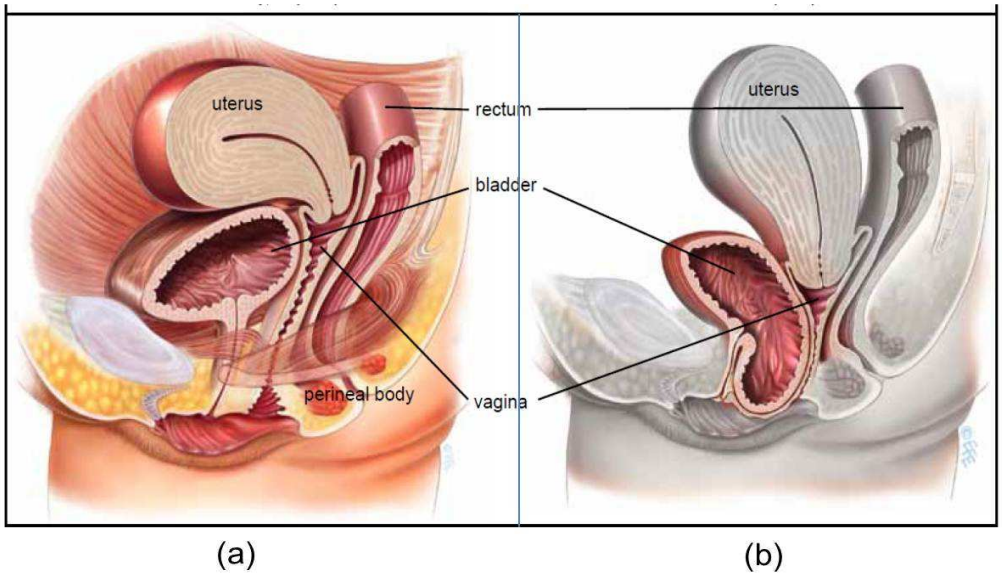

Figure 1 (a) Normal position of vagina relative to the rest of pelvic organs (b) Anterior vaginal wall prolapse responsible for bladder descent [3].

As it progresses outside the vaginal introitus the prolapsed bladder may not empty well, which can lead to urinary problems such as loss of bladder control and recurrent bladder infections [3]. Other types of prolapse include: Rectocele, which is the herniation of the rectum into the posterior wall of the vagina; Uterine prolapse, when the uterus descend into and eventually out of the vagina; Enterocele, which is when a space develops between the vagina and rectum into which a small bowel can bulge, and vaginal prolapse after hysterectomy [4].

1.1.1 Anatomy of the vagina

The vagina is a fibromuscular tube that connects the lower portion of the uterus to the outside environment. It functions as a supporting hammock for the pelvic viscera [5], and its position relative to the other pelvic organs resembles a finger of a glove which is tucked inside the rest of the glove, as illustrated in Figure 2a.

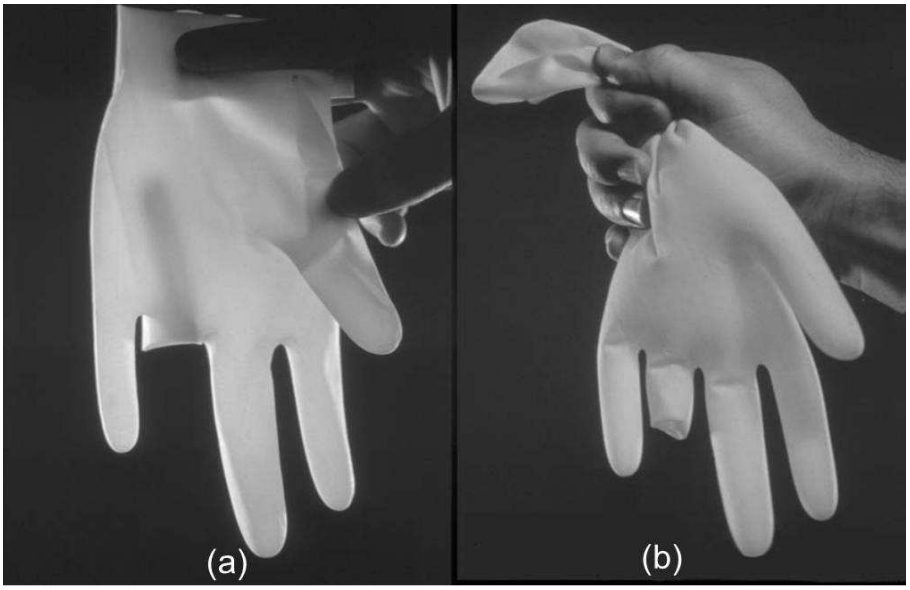

Figure 2 (a) Representation of the position of the vagina relative to the rest of pelvic organs (b) Prolapse of vagina due to pressure from the other pelvic organs [6].

Thus, the vaginal walls are the interface where forces are transmitted among pelvic organs in the pelvic cavity, and if the pressure in that enclosed area increases, the vagina tends to be pushed downward, and sometimes protrudes outward when POP occurs, as illustrated in Figure 2b.

The area of the average female pelvis is 94 cm^2 [50]. The pelvic floor (Figure 3) a complex system comprised of striated muscle, smooth muscle and connective tissue [4], prevents the vagina to protrude out by supporting it when forces are transmitted in the pelvic cavity. Contraction of the striated muscle component, referred to as the Levator Ani, provides support to the pelvic organs by acting as a shelf upon which they rest. Anatomical interruptions afford passage of the urethra, vagina and rectum. The mid-vagina is attached to the arcus tendineus fasciae pelvis, also known as white line, on each side [7]. The connective tissue and striated muscle from mid and lower vagina share loading support to assist in resisting the downward forces resulting from a combination of abdominal pressure and gravity. The upper vagina rests on the levator plate and is stabilized by superior and lateral connective tissue attachments as well [7].

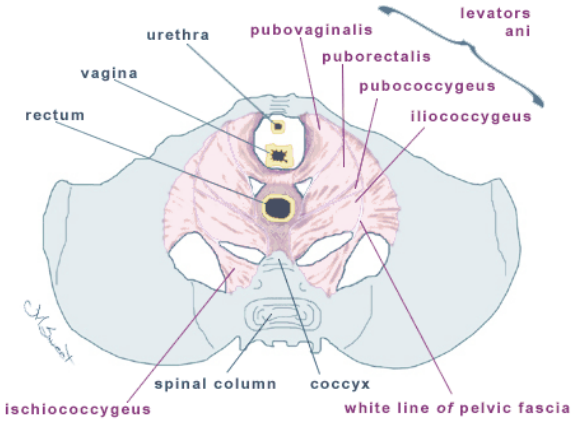

Figure 3 Pelvic floor: Levator Ani complex and connective tissue that forms the White Line [3].

The load in the pelvic cavity, when the person is standing, comes from a combination of different forces: The hydrostatic load due to the fluid abdominal contents beneath the diaphragm; The load coming from the weight of genital organs; The intra-abdominal pressure (IAP) due to the postural tone of the abdominal muscle group (Transversus and Rectus Abdominis, and internal and external obliques) and diaphragm muscle; and respiratory activity [53]. In the supine position the load is approximately 19 Newtons (N), and it rises up to 37 N when standing, and up to 129 N when coughing or performing Valsava maneuvers [51].

The entire vaginal wall thickness in a menstruating woman ranges from 2 to 4 mm [7]. It is composed of three layers, the mucosa, muscularis and the adventitia, shown in Figure 4 .

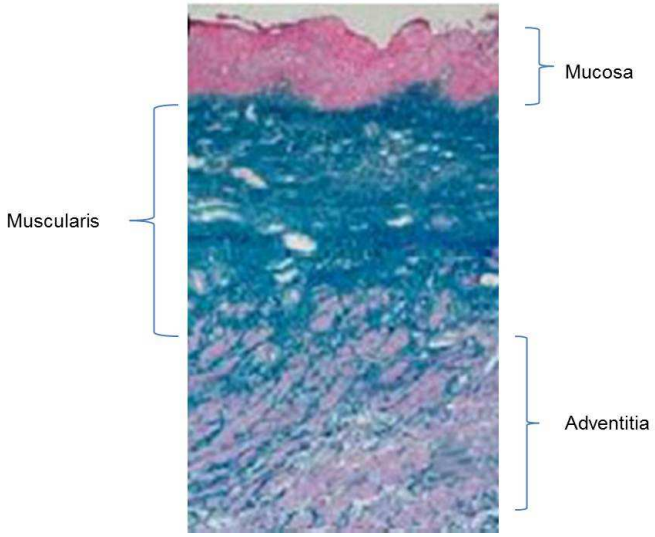

Figure 4 Histological trichrome image of the vaginal wall [4]

The mucosa contains the epithelium, which measures 0.15 to 0.30 mm from surface to basement membrane and is composed mainly of squamous cells at various stages of maturation that are constantly being turned over due to hormonal changes.

Beneath there is a stromal layer named lamina propria, which consists of a thin, dense collagen layer with intermixed elastin that acts as a membrane responsible for the passive mechanical properties [57], and thus provides physical stability of the vagina during the transferring of forces [4,58]. Following is the vaginal muscularis, a fibromuscular layer that consists of smooth muscle admixed with elastin and collagen, and provides the active mechanical properties of the tissue (the forces exerted when the muscle is stimulated [59]) as well as longitudinal and central support to the vagina [7]. The adventitia, the deepest layer, is a loose connective tissue layer shared with the bladder anteriorly and the rectum posteriorly. Normal connective tissue from adventitia contains abundant discontinuous extracellular matrix (ECM) composed of collagen, elastin, water and ground substance [8], as well as adipose tissue, nerve fibers and blood vessels [8].

1.1.2 Causes of anterior vaginal wall prolapse

There are two main theories to explain AVW Prolapse: distention and displacement [9]. Distention is caused by damage to the vaginal wall that leads to alterations in the connective tissue composition. Displacement is due to the overstretched or detached anterolateral vaginal supports from the arcus tendineus fasciae pelvis, causing prolapse without damage to vaginal tissue [9]. This thesis is focused on the distention type of prolapse.

The alterations of tissue composition of the vaginal wall in the distention type of prolapse may occur due to vaginal delivery trauma. As many as 50% of women who have given birth one or more times have some degree of genital prolapse [1], and therefore it is considered the primary risk factor. However, it has been discovered that the causes of POP are multifactorial [10,11]. Approximately half of all women over age 50 complain of symptoms associated with prolapse [1]. Moreover, prevalence of POP appears to

gradually increase in the elderly [11]. Therefore there is strong evidence that age is a contributor to POP. Additionally, recent research has reported a relationship between the hormone loss induced by menopause and POP [10]. Another important risk factor is obesity. Studies based on questionnaires have shown that the risk of having a cystocele is 50% higher in women with Body Mass Index (BMI) of 25 or higher [12]. However, the relationship between obesity and prolapse has not been well studied. Other factors such as cigarette smoking leading to chronic cough, previous hysterectomy and constipation have also been implicated in the etiology of pelvic organ prolapse [6].

1.1.3 Current diagnostic methods of vaginal wall prolapse

Pelvic Organ Prolapse Quantitative System (POP-Q) is a standard system used for staging POP and approved by the International Continence Society (ICS), the American Urogynecologic Society, and the Society of Gynecologic Surgeons [29]. According to POP-Q system patients with POP can be classified in five different stages depending on the length of the most severe portion of the protrusion. It considers a -2 cm buffer to compensate for vaginal distensibility and the inherent imprecision of the measurement of total vaginal length (TVL). The hymen is used as a fixed point of reference [29]. An illustration of the stages of POP according to POP-Q system is shown in Figure 5, and their description is shown in Table 1. Stages can be further sub-grouped according to which portion of the lower reproductive tract is the most distal part of the prolapse by use of letter qualifiers (a = anterior vaginal wall, p = posterior vaginal wall, c = vaginal cuff and Cx = cervix) [29].

The severity of POP is usually diagnosed during a pelvic exam. With the patient in the dorsal lithotomy position, the doctor assesses the ability of the patient to contract and relax her pelvic muscles selectively. A forceful Valsalva maneuver will demonstrate maximum organ descent [13]. The downside of this diagnostic procedure is that the

doctor cannot actually see how weak the muscles are and cannot effectively determine the prolapse stage. An optimal vaginal examination is obtained intraoperatively under general anesthesia [13].

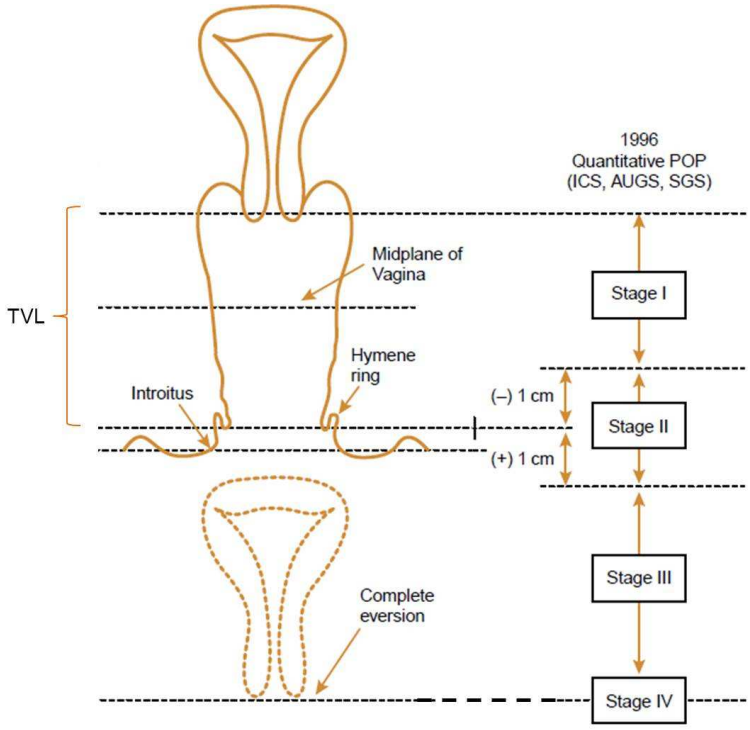

Figure 5 Illustration that describes POP stages according to POP-Q staging system [56]

Table 1 POP-Q staging system [56]

Stage	Leading edge of POP in relation to hymen
0	< -3 cm
I	< - 1 cm and > -3 cm
II	≥ - 1 cm and ≤ + 1 cm
III	> +1 cm and < (+TVL -2) cm
IV	≥ (+ TVL -2) cm

A variety of imaging techniques, including ultrasound, magnetic resonance imaging (MRI) and X-ray imaging, have been used to visualize pelvic floor anatomy, support defects, and relationships among adjacent pelvic organs [14]. These techniques may be more accurate than physical examination in determining which organs are involved in pelvic organ prolapse. However, the limitations include lack of standardization, validation, and availability [15].

All of the procedures mentioned above have an important limitation which is that they tell very little about the actual mechanical properties of the affected tissue. Currently there are no standardized methods that analyze the properties of the tissue in order to effectively understand the biomechanical causes of the prolapse.

1.1.4 Vaginal wall prolapse repair

Physiotherapy to increase muscle strength and pharmacological treatment are currently available therapeutic options [13]. In addition, women can get temporary support by wearing a device called a vaginal pessary, which supports the wall as a knee or ankle brace supports a weak joint. When these options are inadequate surgery is conduced to repair the defect and return the bladder and other internal organs to their original position [13].

Approximately 250,000 procedures to correct pelvic organ prolapse are performed each year in the United States [16]. Moreover, 29% of women have to undergo repeat surgery for recurrent prolapse [16].The relatively high re-operation rate suggests that the methods of surgical repair need improvement. Additionally, POP surgical repair costs over one billion dollar per year and 28% of that amount goes to repairing cystocele and rectocele [1].

AVW repair surgery, also known as anterior colporrhaphy, is the surgical procedure for reinforcing the fascial support layer between the bladder and the vagina.

The technique involves plicating the layers of vaginal muscularis and adventitia overlying the bladder to reduce the protrusion of the bladder. Plicating the patient's own damaged tissue may fail, with failure rates reported in the range of 40–60% [16]. Therefore, modifications of the anterior colporrhaphy were proposed involving the placement of a stabilizing mesh in the anterior compartment in order to strengthen the repair [1]. However, according to a recent FDA report, including a mesh did not result in less recurrent prolapse and furthermore, post-operative complications were significantly higher for patients with mesh including mesh erosion or detachment, infection, pain with intercourse and rarely death [17].

Chapter 2

Theoretical background

2.1 Literature review: Biochemical and biomechanical properties of AVW

The biomechanical properties of tissues provide quantitative information regarding the responses to applied physiological and non-physiological forces. The mechanisms undergoing tissue deformation are dependent on inherent biochemical composition and spatial organization [4]. Therefore, analyzing the biochemical and biomechanical properties of the AVW of prolapsed and non-prolapsed tissue might help our understanding of how the cited risk factors alter the vaginal tissue progression to the point of prolapse. Analysis could also help explain why there are failures associated with surgical techniques and to improve the results of surgical repair, by providing vital information and guiding the design and development of a better mesh. A better mesh could provide needed support to help restoring the AVW physiological functions. However, obtaining fresh human prolapsed and especially non-prolapsed vaginal tissue is a major limitation for researchers. Not many studies have been carried out to characterize the mechanical properties of AVW tissues. A few studies have used tissues from human cadaver or from four-legged animals for characterization of AVW properties [18]. However, those tissues cannot truly describe the actual properties of human AVW tissue due to composition and structural differences.

When a load is applied to a soft biological tissue, such as the AVW, the load-elongation and stress-strain curves exhibit a non-linear response (Figure 6). This is because biological tissues often stiffen as they are deformed, a process known as strain stiffening, which allows biological tissue to respond adaptively to varying external

mechanical conditions [61]. Strain stiffening allows the AVW tissue to be compliant at normal physiological strain levels and strengthen at larger deformations that could threaten tissue integrity [61]. This non-linear response, critical for the physiological function of normal non prolapsed AVW can be divided into 3 regions: the initial non-linear toe region, a 'linear' region (which is not truly completely linear), and the failure region [4]. From these response curves, the biomechanical properties of the AVW tissue can be extracted [4].

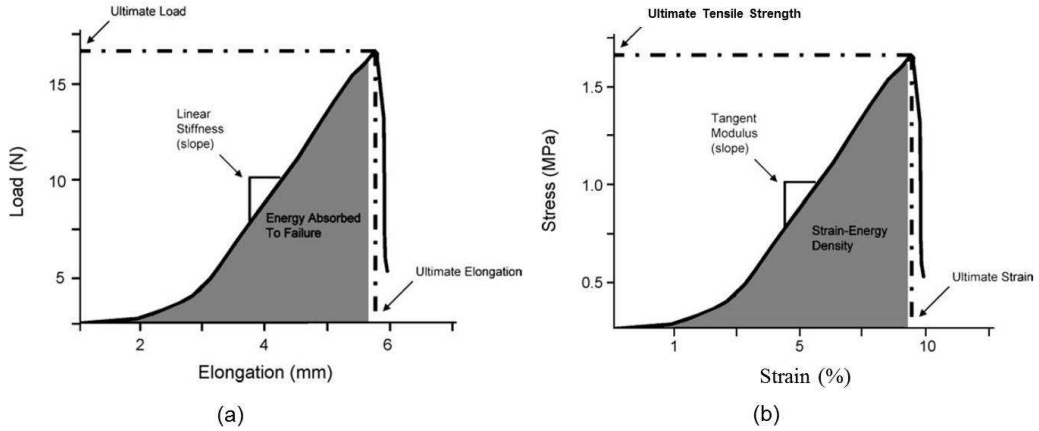

Figure 6 Non-linear response curve of AVW tissue (a) Parameters that describe structural properties of tissues from a load-elongation curve (b) Parameters that describe the mechanical properties of tissues from a stress-strain curve [4]

The biomechanical properties of tissues are divided into structural and mechanical properties [4,19]. Even though they are related to each other, these properties describe different characteristics of the tissue.

Structural properties describe how much deformation the specimen of arbitrary dimensions undergoes in response to an applied load. This is without considering any anatomical or geometric characteristics of the tissue such as its natural shape, size,

cross-sectional area or length. The structural properties obtained from one type of loading, a uniaxial tensile test, are shown in Figure 6a. Parameters extracted from this test include: the ultimate load, which is the maximal force applied up to the point of rupture; maximal elongation, which is the amount that the tissue stretched up until the maximal load; linear stiffness, which corresponds to the slope of the load–elongation curve within the 'linear' region observed. This parameter reflects the resistance of the tissue to elongation and therefore a higher stiffness means a larger force is needed to deform the tissue [19]. Another important parameter is energy absorption, which is the area underneath the load–elongation curve; when integrated to the ultimate elongation point it represents the energy required for tissue failure.

The mechanical properties incorporate tissue dimensions, and thus give specific information, for example, about the stiffness and the compliance of specific tissues [4]. In this dimensionally specific model the stiffness is described by the relationship between the amount of stress applied to the specimen versus the amount of strain that the tissue undergoes. Stress is defined as force divided by cross-sectional area and strain is defined as the change in elongation relative to the initial length [4]. Therefore, mechanical properties describe the composition and microstructural arrangement of a tissue independent of its size and geometry. From a uniaxial tensile test to failure, the obtained parameters that describe the mechanical properties (Figure 6b) are: the ultimate tensile strength (UTS), which corresponds to the maximal stress before failure; Ultimate strain, which is the strain corresponding to UTS; tangent modulus, which is the slope of the stress–strain curve in the 'linear' region, and indicates the compliance (low tangent modulus) or stiffness (high tangent modulus) of the tissue. The tangent modulus of the linear portion of a stress-strain curve is called Young's modulus in linear response materials, and therefore sometimes is incorrectly referred to as Young's modulus by

some researchers; and the strain energy density, which corresponds to the area underneath the stress–strain curve [4].

Another important tissue biomechanical property, one that can be observed in a uniaxial tensile test, is whether it exhibits elastic or viscoelastic response. When a material behaves in an elastic manner, the stress–strain curve will follow the same path upon loading and unloading of the tissue, meaning that the tissue will return to its original shape once the load is removed. Moreover, if the tissue is stretched and relaxed repetitively, it will not change this mechanical response over time [9]. This is not the case for soft biological tissues. These tissues, including AVW, show both viscous fluid-like and elastic solid-like (viscoelastic) response, which means that the mechanical properties are both time-dependent and rate-dependent. This behavior is thought to result from the complex interactions of the collagen, elastin, proteoglycan, and water molecules within the tissue [4]. Thus, the stress–strain curves during repetitive loading and unloading of viscoelastic tissue will not follow the same path.

2.1.1 Studies related to tissue composition

Tissue composition is widely thought to directly impact both passive and active mechanical properties [57]. Thus, several studies attempted to analyze the differences of AVW tissue composition between prolapsed and non-prolapsed subjects.

Collagen I, collagen III and elastin, the fibrillar components of AVW, are thought to contribute the most to the passive mechanical behavior of the tissue [57,58]. Collagen in tissues arranged into bundles, which are rod-like structures conformed by cross-linked collagen molecules that consist of triple helix polypeptide chains [58]. The crosslinking of collagen molecules is catalyzed by lysyl oxidase (LOX) [63]. Collagen I is the major structural protein in soft tissues, and is primarily responsible for resistance to deformation, as in the tensile strength test [20]. Type III collagen forms smaller fibers

than type I, suggesting lower stiffness, and is predominant in tissues that require increased distensibility [20]. Elastin fibers gives tissues the ability to stretch and to recoil [22]. The role of elastin in maintaining AVW tissue integrity is thought to be critical [62] and some studies suggest that the passive mechanical properties of AVW connective tissue depend not only in elastin content alone, but rather in the organization of elastin fibers relative to collagen I and collagen III fibers, which act together to provide the mechanical strength [42, 45, 57, 58]. An electron micrograph of a stretched sample of healthy AVW tissue from loose connective mucosa layer is shown in Figure 7a. The configuration of both, elastin, and tightly packed collagen bundles can be identified. Figure 7b shows the electron micrograph of the same layer from a stretched prolapsed sample, showing an irregular network of collagen and elastin fiber fragmentation [62].

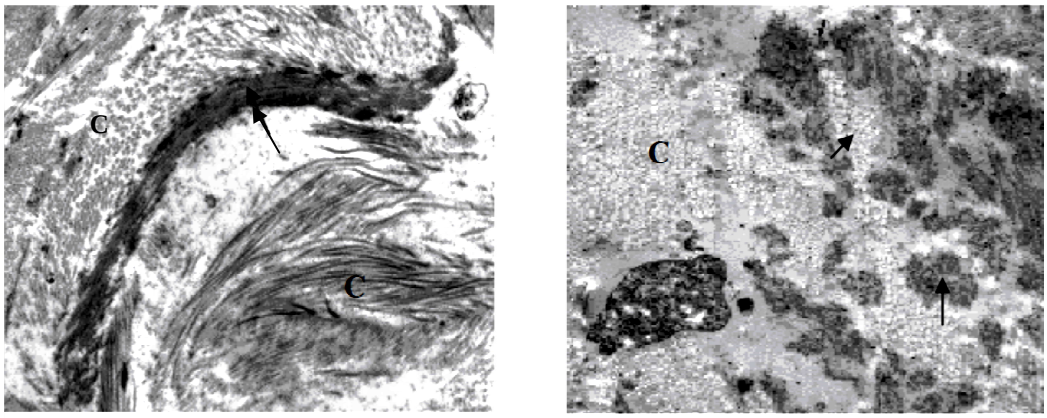

Figure 7 Electron micrographs showing elastin fibers (↑) and collagen bundles (C) arrangement in stretched samples of AVW (a) Non-prolapsed AVW tissue (magnification of x2156) showing elastin fiber long and continuous and tightly arranged collagen bundles (b) Prolapsed AVW tissue (magnification of x2784) showing elastin fiber fragmentation and alteration in collagen network [62].

Karam et al. (2007) compared elastin expression and individual elastic fiber width in the AVW of postmenopausal women, with and without POP. Samples were obtained from the upper lateral AVW from 43 POP patients undergoing cystocele repair, and from the same region for 10 control non-POP patients that were undergoing radical cystectomy for unrelated reasons. The percentages of elastin, and the elastic fiber widths were measured by immunohistochemistry, using image analysis software. The results indicated that the elastin expression and fiber width were significantly lower in the AVW of patients with cystocele compared to controls of a similar age, which suggests that disruptions in elastic fibers might contribute to the onset of prolapse [23].

Matrix Metalloproteinases (MMPs) play important roles in ECM remodeling by aiding its programmed degradation [4,24,20]. Mosier et al. (2009) studied the expression of mRNA from ECM proteins in 45 patients with AVW prolapse and 6 patients without prolapse. Patients were all postmenopausal as in the Karam research, and the procedure of sample acquisition was the same. Total RNA was isolated, cDNA was synthetized and the polymerase chain reaction was done to asses mRNA expression of collagens type I and III, proelastin and three different MMPs. A significant increase in collagen type I and collagen type III mRNA was found in tissues with prolapse compared to control specimens. The ratio of type III to type I collagen was lower in POP patients compared to controls. An increasing trend in pro-elastin and MMP and mRNA expression was found in the prolapse category but was not statistically significant. This research was relevant because it suggested that unbalanced type I and type III collagen mRNA expressions in tissue, with unbalanced collagen supply and demand, might be another cause of AVW tissue prolapse [20].

Zong et al. (2010) studied elastin metabolism in 87 patients [25]. Twenty premenopausal patients with no prolapse were used as a control group, and POP

patients were divided in 3 groups: Premenopausal, postmenopausal without hormone therapy and postmenopausal on hormone therapy. The epithelium was excised leaving the sub-epithelium, muscularis and adventitia for analysis. The elastin precursor, tropoelastin, was measured by immunoblotting and mature elastin protein by a desmosine crosslink radioimmunoassay. MMPs 2 and 9 were quantitated by gelatin zymography. The results indicated that tropoelastin, mature elastin, pro-MMP-9 and active MMP-9 were increased in women with prolapse, while active MMP-2 was decreased relative to controls. Comparison of tropoelastin and mature elastin values obtained from the same women showed them to be independently regulated. Their findings resembled those of Karam's research in that elastin metabolism was shown to be altered in the vagina of women with prolapse relative to controls. Furthermore, they related chronic conditions that increase intra-abdominal pressure, such as obesity and chronic cough, to the development and progression of POP. They concluded that elastin metabolism is altered in the vagina of women with prolapse possibly due to vaginal tissue remodeling in response to an increased mechanical stretch [25].

Additionally, vaginal tissue remodeling is shown to be powerfully regulated immediately before and after delivery [29, 63]. Pregnancy has been related to a profound connective tissue remodeling [42]. Akins et al. (2011) performed a biochemical analysis in the cervix and analyzed changes in the factors that modulate collagen structure during early mice pregnancy, including expression of proteins involved in processing of procollagen, assembly of collagen fibrils, cross-link formation, and deposition [63]. They conducted this study because previous research suggest that the cervical ECM must be disorganized during labor to allow birth, followed by a rapid repair postpartum [64, 65]. Cervical tissue was dissected from the reproductive tract, and vaginal tissue was carefully removed from cervical tissue. Cervices were flash-frozen in liquid nitrogen

immediately following their extraction. Quantitative real-time PCR (QPCR), immunofluorescence and immunoblotting were used for the biochemical analysis.

Collagen content and crosslinks were analyzed with electron microscopy. They concluded that early changes in tensile strength during cervical softening result in part from changes in the number and type of collagen crosslinks and are associated with a decline in expression of two matricellular proteins thrombospondin 2 and tenascin C, as well as a decline in expression of LOX [63]. It is important to note that electron micrographs of cervical ECM at early pregnancy (Figure 8a) and late pregnancy (Figure 8b) presented in their research show a similar arrangement in collagen and elastin fibers shown previously in Figure 7a (non-prolapsed tissue) and Figure 7b (prolapsed tissue), respectively, from AVW tissue.

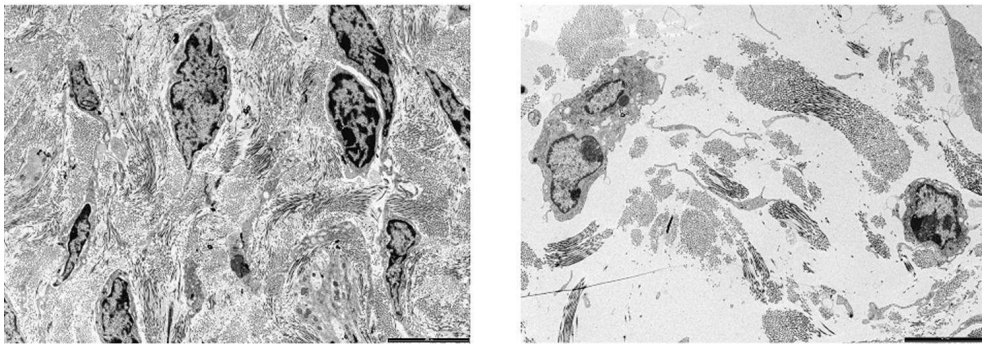

(a) (b)

Figure 8 Electron micrographs of cervical ECM tissue taken at a magnification of x4200 on (a) early pregnancy (day 6 gestation) (b) late-pregnancy (day 18 gestation, with birth occurring at day 19) of mice. Bar-1000nm [63]

Cellular components and electron-dense components of the ECM appeared to be in close proximity during early pregnancy (Figure 8a), while in late gestation, collagen fibers were more dispersed and not associated with cellular components of the tissue

(Figure 8b). By comparing these images it is tempting to imply that POP patients develop a similar irregular network of collagen and elastin fibers in their pelvic tissues, including AVW tissue, similar to the remodeling the pelvic tissues undergo during pregnancy.

Since the sub-epithelium and muscularis of the vagina are thought to confer the majority of tensile strength and active mechanical properties to the vaginal wall [26], Northington et al. (2011) focused on the contractility of the Anterior Vaginal Muscularis (AVM) from women with and without POP. A prior study had documented a decrease in the fractional area of smooth muscle in the anterior and posterior vaginal walls of women with prolapse compared to controls [27]. Therefore, Northington performed in-vitro experiments in instrumented muscle contraction baths to measure the peak force generated by AVM tissue in response to potassium chloride (KCL) and phenylephrine. They found that there were no differences in the mean amplitudes of forces generated in response to KCl normalized to either wet weight or muscle cross-sectional area (muscle stress), between women with and without POP. However, AVM from women with prolapse produced a significantly higher mean force response to KCl normalized to total cross-sectional area (tissue stress), compared to controls. While the control samples demonstrated a consistent response to phenylephrine, there was no response to this stimulant generated by AVM tissue from women with POP. They concluded that molecular changes of the contractile apparatus of prolapsed vaginal muscularis may be a compensatory mechanism to maintain force and that is why there is no change in muscle stress between prolapsed and control patients (in response to KCL). They also stated that the absent response to phenylephrine by AVM from women with prolapse may be related to a lower expression of α1A adrenergic receptors in vaginal smooth muscle in this group [27]. This could be related to what happens in congestive heart failure, where as the contractility of ventricular muscle decreases, the ventricle increases in size.

2.1.2 Studies related to structural behavior

Several studies have attempted to analyze the structural behavior of AVW tissue. Lei et al.[10] (2007) measured the elastic structural properties of AVW by taking excised human vaginal wall samples from 43 women undergoing transvaginal hysterectomy. The patients were classified as: 9 premenopausal POP, 14 premenopausal control without any type of prolapse, 12 postmenopausal with POP and 8 postmenopausal without prolapse. POP patients were also subclassified as mild (patients with stage I-II POP), moderate (patients with stage III POP), and severe (patients with stage IV POP) according to POP-Q staging system. Patients with previous surgical procedures for prolapse or on hormone therapy were not included in this research. Excised tissues were frozen at -70 degrees Celsius. The frozen tissue was thawed less than 24 hours after the excision, for 1 hour at room temperature, and then trimmed to rectangular shape of 5 x 25 mm in size. For the uniaxial tensile testing, both ends of the tissue were secured to metal hooks by sutures. One hook was fixed and the other one was connected to a computerized tissue puller system. The tissue was pulled at a constant rate of 0.8 mm/s up to an elongation of 8 mm. Superimposed on this linear elongation was a sine wave with a vibration frequency at 50 Hz. The measurement was repeated every minute with increasing length up to the rupture point. They found a significant increase in elastic modulus in premenopausal POP patients compared to premenopausal control group, as well as in postmenopausal POP patients compared to postmenopausal controls. In addition, ultimate load and relative elongation were significantly decreased in menopausal groups compared to their respective control groups. The collected results suggested that the connective tissue for POP patients, whether they are pre or postmenopausal, is less elastic and stiffer than controls. However, between POP patients there were only significant differences between properties of mild and moderate

categories, where patients with moderate POP showed higher elastic modulus, lower ultimate load and lower elongation mean values than patients with mild POP. No significant differences were observed between moderate and severe prolapse groups. Lei et al. [10] concluded that degeneration of structure in AVW, possibly due to lower collagen content in AVW epithelium, lowers the biomechanical properties and leads to POP; once prolapse occurs, the tissue degeneration becomes such that the mechanical properties do not present further changes [10].

Moalli et al. (2008) analyzed the impact of the removal of ovarian hormones estrogen and progesterone on the properties of AVW tissue in mice [11]. They obtained 5 mm from the distal portion of the AVW from rats after performing ovariectomy (OVX) surgery. They compared results with healthy AVW tissue from non-ovariectomized control rats of the same age. OVX was performed on young (4 months) and older rats (9 months). They performed a uniaxial tensile test up to failure point, and calculated the structural properties. The results showed a 40% decrease in linear stiffness and 30% decrease in ultimate load at failure in young rats following OVX. However, the addition of estrogen and progesterone following removal of the ovaries eliminated the decrease in linear stiffness and ultimate load in the vaginal wall [11]. Meanwhile, for the older animals, there were no significant changes due to OVX, nor was there obviation by hormone replacement. This research suggests that ovariectomy at a young age without hormone therapy is a risk factor for the development of POP. However, a major limitation in this study is that rats may have differences in connective tissue metabolism compared with humans and may respond differently to hormones [11].

In the same year, Alperin et al. researched the impact of Lysyl Oxidase-like protein 1 (LOXL1) deficiency on the vagina and its supportive tissues. Previous studies had demonstrated that extracellular matrix stability is assured by the intra- and

intermolecular covalent cross-linking of elastin and collagen, initiated by lysyl oxidase (LOX), a copper-dependent amine oxidase [29]. Alperin et al. wanted to investigate whether LOXL1 is crucial to maintain the structural integrity of the vagina and its supportive tissues. They analyzed sample tissues of LOXL1 deficient mice and compared their data with the control mice using uniaxial tensile loading up to the failure point. The groups demonstrated statistically significant differences, with LOXL1 animals displaying a 31% decrease in ultimate load at failure, suggesting that animals without LOX1 and its encoding gene, have mechanically weaker tissues. However, the maximum linear stiffness, or yield point, was not significantly different between the groups. They attributed this to a similarity in both groups tissue response in what they defined the 'linear' region, since in fact the response was not linear. The second region of the response, which corresponded to point past the yielding point, differed between the two groups since in control mice additional vaginal support tissues began to resist downward distension, producing the second region of increasing force with increasing distension. However, in the LOXL-deficient animals this did not occur. They concluded that in LOXL1 knockout mice, animals would spontaneously develop prolapse following vaginal delivery and with increasing age, suggesting that genetic predispositions may contribute to this multifactorial condition [29]. This research may also suggest a modification in vaginal wall connective tissue in pregnant patients that is related to the onset of POP.

Epstein et al. (2006) researched the in-vivo biomechanical properties of POP patients with a cutometer device [30]. Cutometers are suction-based devices that have been used in dermatology to measure the biomechanical properties of the dermal component of skin, which is the richest site of collagen and elastin, in a non-invasive manner [30]. They used the device with a 10 mm DermaLab skin probe that exposes the tissue to vacuum, to measure the elongation that occurs on skin in the forearm and in the

left vaginal sidewall in patients with and without prolapse. The amount of vacuum force needed for elongating tissue to pass 2 infrared gates in the probe is recorded to measure extensibility. The device also calculates a stiffness index, which is an approximate Young's modulus of the tissue. The suction was done at different times to allow comparison between probe measurements for one tissue. This demonstrated the fatigue effect in tissue, or creep, thought to be due to a temporary breakdown in ECM crosslinking after repeated exposure to a load. Patients were divided into 25 POP patients with prolapse stage from I-IV, and patients without prolapse. The results showed no statistically significant differences between measurements done in forearm skin for POP and non-POP patients. However, results were statistically significant when comparing vaginal tissue measurements. The force needed to reach both gates was higher for control group tissue than for prolapse, and the stiffness index was higher in control group, indicating that POP patients have a greater extensibility in vaginal tissue than patients without prolapse. These findings contradict research that suggests that women with POP have a systemic collagen or elastin disorder such as Alperin et al. study, and demonstrate that prolapse may be due to local alterations in biomechanical properties of the vaginal wall. Moreover, increasing extensibility of the tissue in the Epstein study was associated with linearly increasing prolapse severity, indicating that as POP gets more severe, the vaginal tissue becomes more compliant [30]. It is tempting to relate this to an increase in AVW collagen III in POP patients observed in other researches, such as the one by Mosier et al. [20].

Mosier et al. (2011) similarly tested the reliability of using a cutometer-like device BTC-2000™ for in vivo vaginal tissue measurements [31]. With a 10 mm diameter probe, they applied a ramped suction pressure from 0 to 150 mmHg in 6 seconds to the prolapsed AVW at a fixed point just below the level of the bladder neck area. The

pressure was selected at this maximum value because it is similar to physiological conditions of pressure the tissue is exposed to when coughing or doing the Valsava maneuver [31]. Twenty four patients with symptomatic stage 2-3 AVW prolapse requiring surgical repair were studied under general anesthesia (to avoid patient anxiety factor) to provide a precise location of the probe. The measurements were first done with an empty bladder; they were repeated after the bladder was filled to 300 ml to represent a typical loading condition for a supine patient. External suprapubic measurements were done for each patient and taken as controls. All biomechanical parameters displayed by the instrument were assessed for reliability, in preparation for a clinical measurement series. These parameters included: laxity, which is the percentage of acute elastic deformation that occurs at very low pressure values and can be defined by a change in the pressure-deformation curve slope; elastic deformation, which is the amount of deformation obtained at the point of the maximum suction pressure; modulus, which is calculated as the slope of the linear portion of the stress vs. strain curve; energy absorption, which is the total area beneath the stress-strain curve; and another parameter is elasticity,which is the amount of elastic recovery that occurs immediately upon release of negative pressure [34]. Measurements were made in duplicate by the primary surgeon and a separate, randomly chosen tester. The results showed that the calculated biomechanical parameters were not statistically different at the two bladder volumes. Moreover, data collected from the duplicate primary surgeon tests were not statistically different. However, duplicate values between randomly chosen testers were less reliable. They concluded that BTC-2000™ is reliable for biomechanical measurements on the human prolapsed AVW [31].

2.1.3 Studies related to mechanical properties

Different experimental protocols for in-vitro characterization of the properties of AVW have also been done. However, due to the extensive and complex testing protocols, samples are usually frozen and stored, and then thawed preceding the test, which may alter the mechanical properties of biological tissues. Therefore, Rubod et al. (2006) researched the effect of thawing vaginal tissue samples from ewes in the tissue's biomechanical properties [5]. Uniaxial tension measurements were made with the fresh extracted tissue and then frozen to -18C for a day. Then, the tissue was defrosted and the same uniaxial tension test was performed. The test was done up to the point of failure with an Instron TM 4302 apparatus, a machine that clamps the tissue from opposite sides and stretches it at a constant deformation rate. Special grips were made for the tissue to avoid slippage [5]. They also tested the influence of room temperature and humidity after removing the samples from isotonic solution, and the influence of taking samples from different locations and performing the test in different orientation of fibers. Finally, they tested with different Instron deformation rates. Their results showed that the effect of frozen storage was negligible in terms of the mechanical properties of the vagina, since the strain-stress curve was practically the same between fresh and frozen/thawed samples. However, the stress-strain curves were significantly different when samples were tested after removal from saline solution, which indicated that sample storage in saline plays a major role in test quality. Sample location did not present significant differences in response. However, for this comparison they took samples from both the AVW and posterior vaginal wall, and this is not the case for human vaginal tissue, since the support, and the forces that the walls are subjected to are different than in ewes. Tissues tested for changes in deformation rate showed that behavior is changed for longer tests due to tissue dehydration. They also concluded that the anisotropy of the

tissue is an important factor to consider and the tissue should be tested in its longitudinal direction. They concluded by providing a protocol for Instron testing which consists in freezing the tissue after excision at -18 C in physiological solution for maximum of 24 hours before being tested [5].

For most of the tests described thus far, authors assumed that the AVW tissue behaves as an elastic material. Since it is important to recognize that tissues are in fact viscoelastic and to truly characterize tissue behavior simulating in vivo loading, in 2008 the same research group of Rubod et al. analyzed the biomechanical properties of AVW tissue using cyclic loadings. They obtained tissue samples from 5 patients undergoing AVW prolapse surgical repair and from 5 cadavers without noticed pelvic floor dysfunction. They did cyclic tensile loading followed by a failure test, using the same procedure as in the previous research. For both groups, all rupture tests showed large strain before rupture, as well as a non-linear response. However, the non-linear response was more pronounced in POP tissues, exhibiting a hyper-elastic nature under large deformation [2]. Since it was a small group of patients no statistical analysis was done. For cyclic loading tests, they repeated the test at different levels of maximum strain. The results also showed non-linear behavior as well as hysteresis between loading and unloading paths, thereby demonstrating the viscous behavior of the material. In conclusion, they suggested that a comparison of Young's modulus in POP and non-POP patients to characterize the mechanical properties of AVW tissue, as done previously by other researchers, is inaccurate due to the tissue's viscoelastic and non-linear behavior [2].

In 2009 Zimmern et al. proposed a different method for uniaxial testing using fresh instead of frozen/thawed AVW tissue samples [32]. The rationale behind this was that protocols that include freezing of samples lead to formation of ice crystals in the

tissue which can lead to damage in the ECM [32]. He and his group also studied the biomechanical properties of the human AVW tissue subjected to two different types of transportation methods within the span of two years. Group 1 consisted in tissue samples immersed with saline and group 2, tissues from similar patients, were wrapped in gauze and moistened with drops of saline solution. These samples were mounted between two aluminum blocks that had self-adhesive grip tape to prevent slippage and excessive tissue clamping stress. A uniaxial tensile test up to failure was performed following a protocol similar to Rubod's testing, employing a MTS Bionix tensile testing machine. The results showed that tissues immersed in saline had a lower Young's modulus but higher ultimate tensile strength. They suggested that hyaluronic acid found in connective tissue retained water and caused swelling. Therefore, they reassured that tissue preservation during transport from the operating room to the laboratory may influence biomechanical testing; they recommended that freezing and thawing of the tissue should not be permitted before performing experimental testing, as results might be incorrect. They proposed to test freshly collected samples within 2 hours of harvest. [32].

In 2010 Feola et al. researched the alterations in collagen composition after parity in rhesus macaques and correlated it to the mechanical behavior of the tissue. Rhesus macaques were used because the size of the fetal head relative to the vaginal diameter places the mothers at a high risk to sustain an injury at the time of vaginal delivery, which is similar to humans, unlike rats that are used by other researchers. Collagen ratios and alignment were quantified by fluorescent microscopy and picrosirius red staining. After obtaining 11 tissues from rhesus macaques, 5 nulliparous and 6 parous, a uniaxial tensile test was done up to rupture with clamping from opposite sides of the specimen, restraining one side and pulling the other. Results showed that the nulliparous tissues group exhibited a more non-linear response beyond 3% strain

compared to the parous group, resulting in a 52% higher local tangent modulus, and 3 times higher tensile strength than parous animals. They also found that the ratio of collagen I to III was similar between the two groups. They concluded that parity has a significant long-term negative impact on collagen alignment and thus on the biomechanical properties of the vagina [18].

2.2 Problem statement

Since most of these research groups only analyzed the elastic properties of the AVW tissue, they usually conducted uniaxial tensile tests up to failure point and concentrated on comparing Young's modulus or the ultimate failure point, even though the vaginal wall has been shown to have a viscoelastic nature. Therefore, these studies cannot provide complete insight into understanding the true causes of the changes in properties of prolapsed tissue. Furthermore, some studies were done with animal tissue to obtain samples large enough for analysis. However, vaginal tissue might behave differently, especially for quadruped animals, since humans are bipedal and their vaginal tissue is subjected to different gravitational forces [18]. Moreover, most human studies have been done on cadaveric tissues or frozen/thawed tissues that can lead to measurement errors due to changes in tissue structure. Additionally, in-vivo studies of the vaginal wall are limited to analysis of the structural behavior, and biomechanical properties have to be analyzed with in-vitro testing, due to lack of suitable methods to characterize properties of living tissue. Furthermore, all of the information provided by these tests cannot be part of pre-operative surgical planning, nor can it be used to track disease progression before the operation, or postoperative healing. Finally, current diagnosis involves qualitative pelvic examination; surgery is sometimes necessary using native tissue or a mesh to correct the hernia defect. An algorithm explaining quantitative data to guide this repair is not available. In addition, high rates of postsurgical recurrence

including recent FDA alerts about complications due to mesh usage in POP repair [17] reinforced the need for more research in effective means of detection, characterization and preoperative assessment. Thus, obtaining a reliable non-invasive in vivo method that quantitates the mechanical properties of the affected tissues may allow more reliable preoperative and postoperative assessments. Such information may allow better modeling of the vaginal wall and lead to better preventive methods against the development or progress of prolapse.

2.3 Aim of the present study

The aim of this study was firstly, to use a better protocol for in-vitro testing, and also to employ in-vivo testing to simulate forces that AVW prolapsed tissue undergoes, evaluating parameters that have not been analyzed in previous studies that define the nature of the tissue. The rationale was to obtain more accurate biomechanical properties that could be useful in the clinical setting. The second aim was to individually analyze several risk factors: Obesity, parity, age, and menopause and assess alterations of the biomechanical properties of the tissue, if any, to realize how much each factor contributes to the development or progression of AVW prolapse.

Finally, this study was intended to correlate the structural behavior parameters obtained from cutometer-like in-vivo measurements done with the BTC-2000^{TM} obtained in those same patients with the in-vitro properties. This comparison was done within the context of each risk factor, in order to determine if the in-vivo test is a reliable tool that provides useful information on the tissue's properties, and severity of prolapse. The results of this systematical analysis are intended to be useful so clinicians can do a better pre-surgical assessment of the severity of AVW prolapse, in order to determine the best repair solution.

Chapter 3

Materials and methods

3.1 Biomechanical properties from in-vivo measurements

Following IRB approval, 28 women with symptomatic stage 2-3 AVW prolapse requiring surgical repair were consented for the study. Procedure and measurements were performed by Dr. Philippe Zimmern of UT Southwestern Medical Center. At the time of surgery, under general anesthesia and with an empty bladder, a 10 mm diameter BTC-2000™ probe was applied at a standardized fixed point on the midline of the prolapsed AVW, corresponding to the level of the bladder neck, as identified by the balloon of a Foley catheter. A picture of the device and the probe is shown in Appendix A. A suction pressure ramp was applied to the probe chamber, from 0 to -150 mmHg in 6 seconds, and the corresponding peak tissue uplift was measured by triangulation within the probe employing a laser altimeter, as shown in Figure 9a. The chamber was then returned to atmospheric pressure via an external valve, pressure promptly dropping to 0 mmHg; recoil of the distended tissue through the ensuing relaxation was recorded for 14 seconds. The 150 mmHg peak pressure was chosen since it is similar to pressure that the tissue is subjected to physiologically (pelvis area is approximately 94 cm^2, and maximal stresses occur at 129 N, which results in a pressure of 1.372 N/cm^2, or 103 mmHg [30,53]).

Directly from the device, two parameters reflecting in-vivo biomechanical properties of the AVW were obtained: Peak tissue uplift (PTU) and energy absorption at PTU, illustrated in Figure 10. PTU (in millimeters) is the maximum tissue uplift recorded at the moment of maximum suction pressure delivery when time is equal to 6 seconds, a

measure of tissue compliance [33]. Energy absorption (in mmHg*mm), derived from the area underneath the pressure-uplift curve, reflects the overall elastic energy absorbed in the regional tissue under pressure load [34].

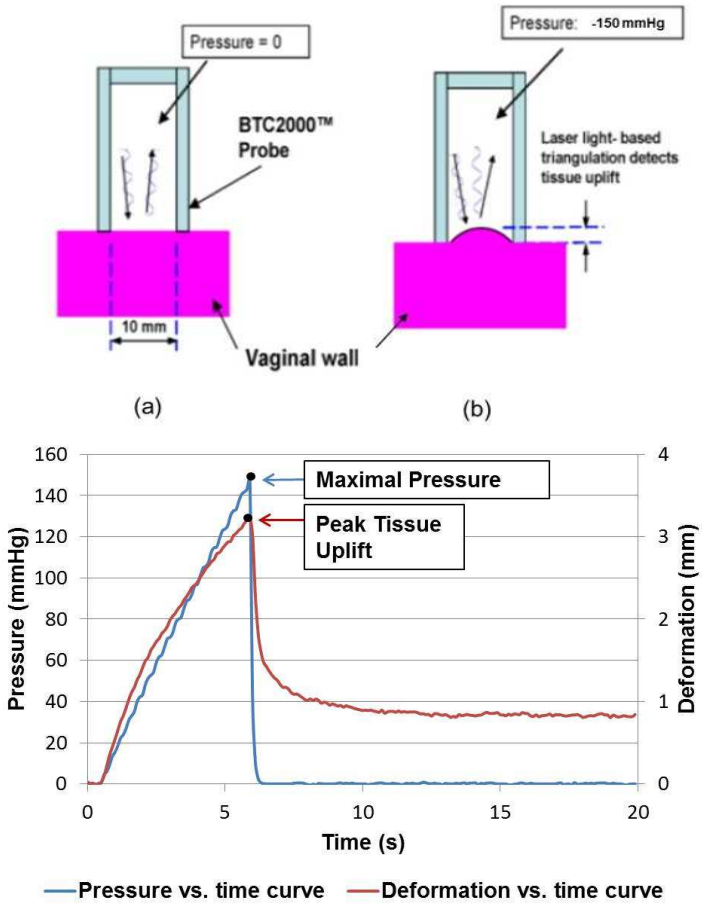

Figure 9 Schematic illustration of the BTC-2000™ measurement (a) Probe before the applied pressure (b) Ramped pressure applied to tissue up to -150 mmHg which produces a peak tissue uplift measured by laser light-based triangulation [32] (c) Plot of ramped pressure applied to the tissue (blue) and typical tissue deformation response (red) against time.

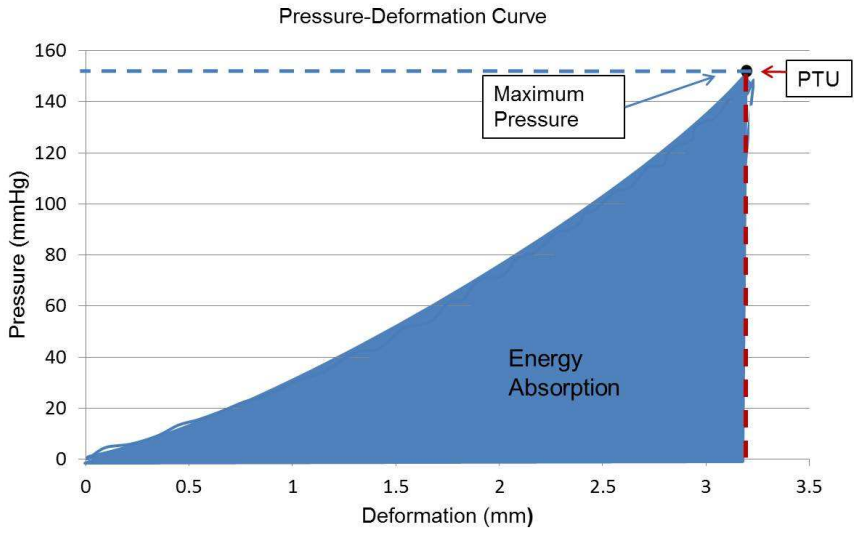

Figure 10 Force-deformation curve from AVW tissue response from which the structural parameters (PTU and energy absorption) are obtained

3.2 Biomechanical properties from in-vitro measurements

During prolapse repair tissue samples approximately 1 cm x 3 cm were taken from the same position as described in Zimmern et al [32]. A description of the protocol for 'Instron' mechanical testing performed by trained medical students is given in Appendix B. The raw data from these 'Instron' tests included time, stress and strain of the complete experiment.

In order to characterize tissue performance under real-life conditions instead of doing just a tensile failure test, cyclic loading at lower peak force was applied in our protocol. Since the main goal was to correlate the behavior of the strained tissue from in-vitro testing with the uplift presented by in-vivo measurements, in-vitro testing cyclic loading had to be adjusted to match or approximate the strain caused by the suction pressure of the cutometer. Based on a mathematical model calculation previously done (Appendix C), a maximum tissue strain of 23% is associated with a PTU of 3 millimeters

(mm) and a 28% strain is associated with a PTU of 4 mm. Since Mosier et al. [31] have shown BTC-2000^{TM} peak tissue uplifts ranged from 1 to 3.5 mm, the in-vitro test was done by stretching each specimen up to 25% strain followed by complete unloading. This was repeated for three cycles followed by stretching the sample up to failure.

3.2.1 Extracting parameters of biomechanical properties from data of cyclic stretch

Representative uniaxial stress-strain data of a freshly excised AVW specimen subjected to 'Instron' testing is shown in Figure 11a.

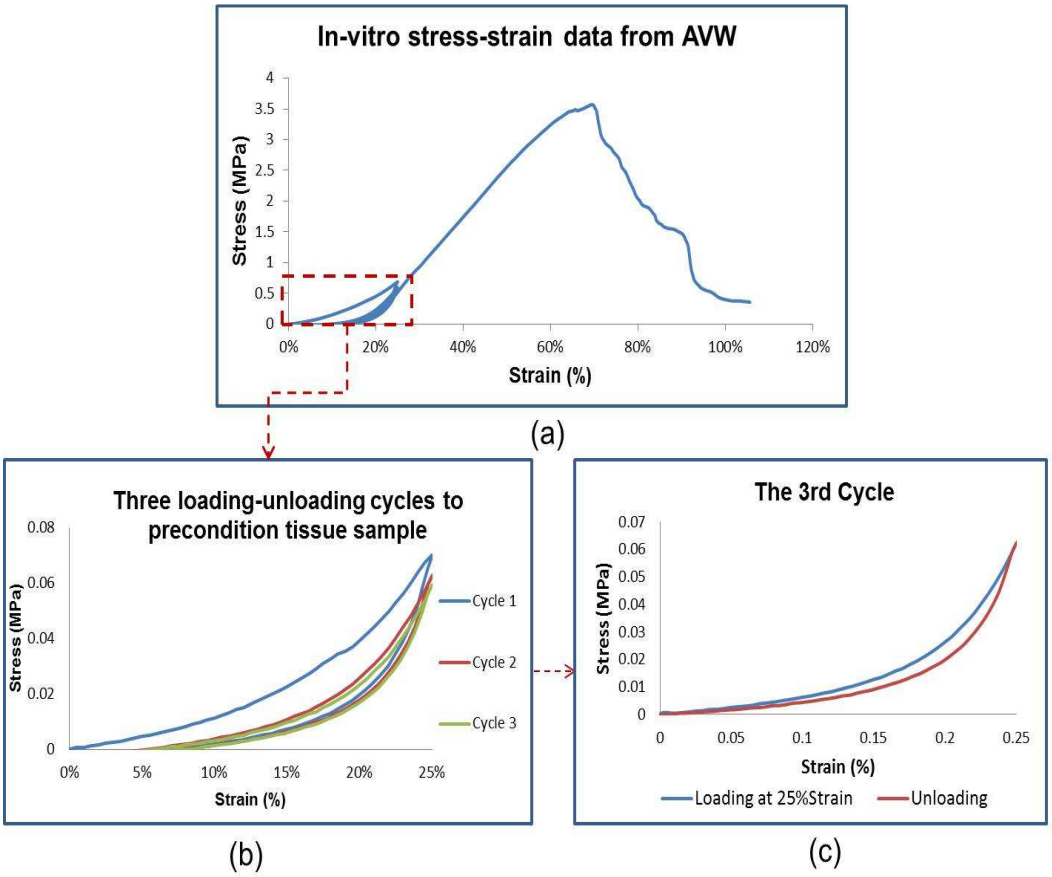

Figure 11 (a) AVW tissue response from Instron testing showing 3 cyclic loadings followed by a failure test (b) Cyclic loading (c) Third cycle used for analysis showing different paths for loading and unloading due to viscoelastic properties.

The third loading-unloading cycle was used for the analysis, since the first two cycles were done to pre-condition the tissue sample (Figure 11b and c). Pre-conditioning allows the tissue to converge to a consistent repeatable loading/unloading response [54].

The tangent modulus at 10% Strain (10%TM) was calculated from the stress-strain data by obtaining the slope that corresponds to the point where strain reached the 10% level and the five previous data points, as shown in Figure 12. The tangent modulus at 25% strain (25%TM) was also calculated from the stress-strain curve by obtaining the slope d(Stress)/d(Strain) of the last 5 points at 25% strain state for each patient.

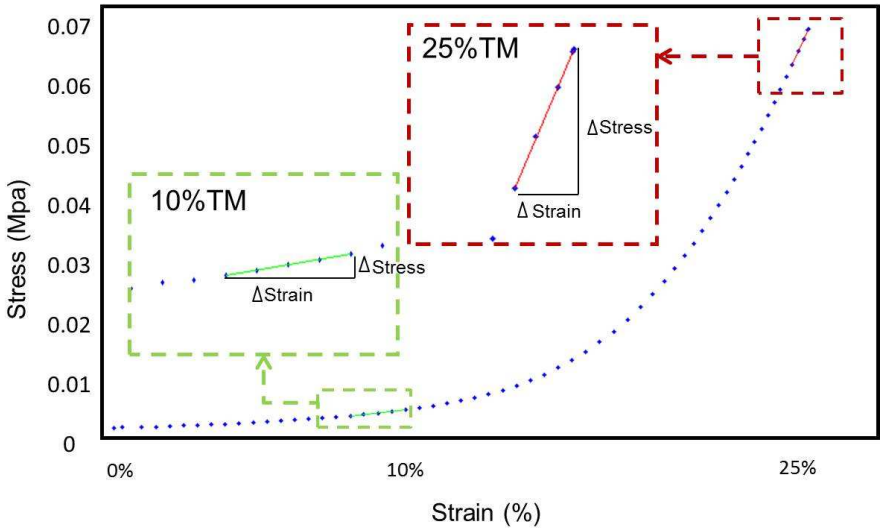

Figure 12 Illustration of tangent modulus at 10% strain and tangent modulus at 25% strain

Additionally, the loading strain energy up to 25% stretch (25%LSE) was calculated. It represents the strain energy stored in the specimen at the strained state and corresponds to the area underneath the loading path showed in Figure 13a.

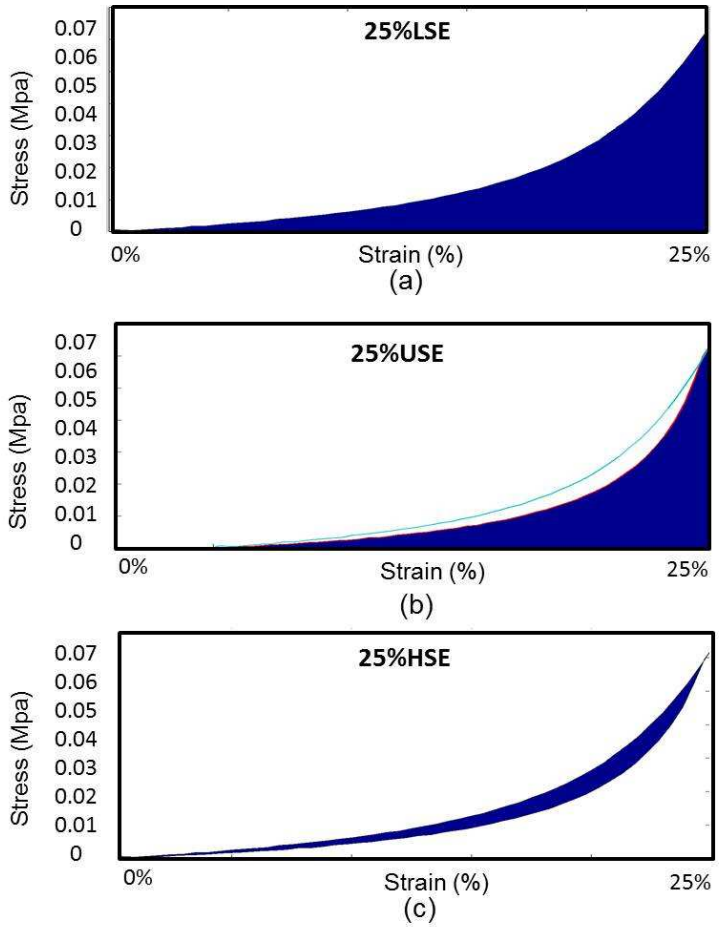

Figure 13 (a) 25%LSE: Area under the loading curve (b) 25%USE: Area under the Unloading curve (c) 25%HSE: Area between the loading and unloading curve.

The unloading strain energy (25%USE), calculated as the area under the unloading path, was also obtained, which represents the recovered upon unload strain energy (Figure 13b). The more recovered energy the more elastic the tissue is since it does not suffer permanent deformation [34]. The hysteresis strain energy (25%HSE), calculated as the difference between 25%LSE and 25%USE, was obtained which represents the energy loss through the loading-unloading cycle (Figure 13c).

25%LSE and 25%USE were obtained with the trapezoidal numerical integration method using MATLAB R2011 built-in function ‘z=trapz(x,y)’. This function computes the integral of Y(Stress) with respect to X (Strain) by dividing the area underneath the curve into a larger number of trapezoids and sum their total area (Figure 14).

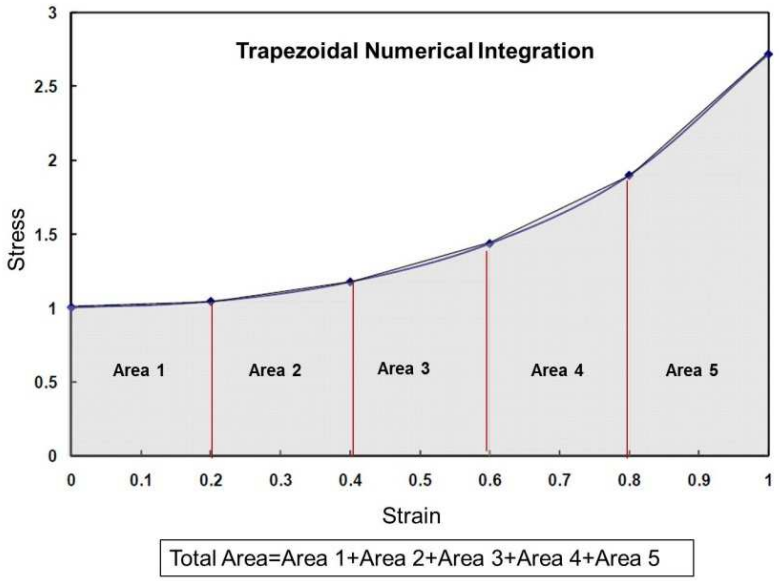

Figure 14 Illustration of the trapezoidal numerical integration to obtain the area under the nonlinear stress-strain curve [35]

Since the 25%LSE values for all patients were between 50 and 60 points, the error for the approximation, when fitting the responses to a Gaussian function curve, was less than 2% error and thus the approximation provided a reasonable value. The 25%HSE was evaluated by subtracting the 25%USE from the 25%LSE.

3.2.2 Extracting parameters of biomechanical properties from data stretching to failure

The stress-strain curve from ‘Instron’ failure test was used to extract additional parameters of biomechanical properties, similar to that of Chuong et al. [36] on the biomechanical properties of canine diaphragmatic central tendon. Matlab R2011a was

used for the calculation, and a function, shown in Appendix D, was programmed to obtain each patient parameters.

Three parameters are derived from stress-strain responses at the point at which the tangent stiffness or d(Stress)/d(Strain) reaches its maximum (MTM), beyond which the tangent stiffness starts to drop due to progressive failure of the tissue's underlying microstructure. The parameters are yielding strain, yielding stress and yielding strain energy (YSE). Additionally, three parameters are derived from the failure point at which the tissue fails to carry further load as seen from the stress-strain data. These three parameters are failure strain, ultimate tensile strength (UTS) and failure strain energy (FSE). All these parameters are illustrated in Figure 15.

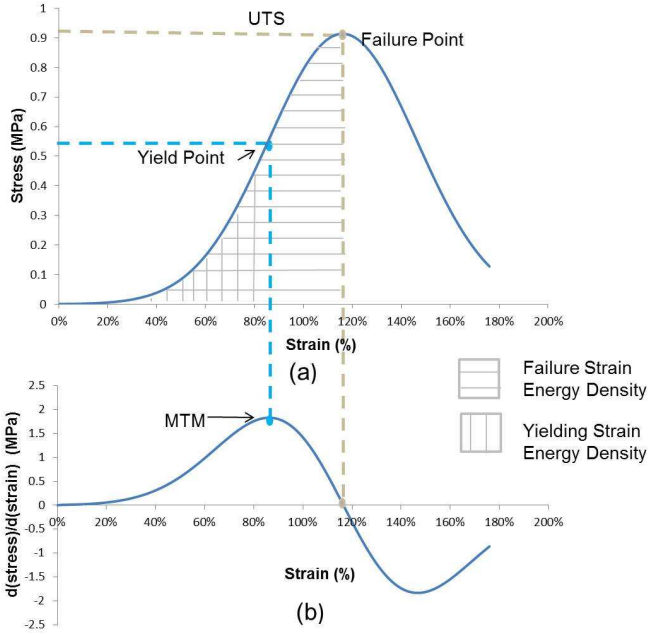

Figure 15 Parameters obtained from (a) Instron failure test of AVW tissue (b) First derivative of the stress-strain curve. The maximal tangent modulus (MTM) corresponds to the yielding point, and when the derivative is equal to 0, it corresponds to the failure point.

The stress-strain data was fitted to a sixth order polynomial for smoothing, since the raw data from Instron test can make the data appear irregular leading to noise in d(Stress)/d(Strain) curve and erroneous results [37,35]. From the fitted curve, the yielding point and the failure point were identified, based on the criteria that the first derivative of the stress-strain curve reached maximum or became zero, respectively. The respective strain energy was then determined by using the trapezoidal numerical integration with the built-in function 'z=trapz(x,y)' of Matlab, as described in the previous section. The error of the approximation, were found to be 0.14 ± 0.06% for strain energy up to yielding point and 0.018 ± 0.026% for the strain energy up to failure point.

3.3 Associating risk factors from patients with prolapse

The patients with AVW prolapse were divided in four different risk factor groups in order to compare any biomechanical parameter sensitivity from in-vivo and in-vitro tests: Obesity (changes in Body Mass Index, or BMI), parity number, geriatric age and menopausal age. For each risk factor, the patients were further divided into two groups to assess for statistical differences (Table 2).

Table 2 Subgroups division of each analyzed risk factor

Risk Factor	Group 1	Group 2
Obesity	BMI < 25	BMI ≥ 25
Parity	Parity: 0-2	Parity: 3-6
Geriatric age	Age: 40-65	Age: 65-83
Menopause	Age: 40-53	Age: 60-83

3.3.1 Effect of BMI

According to the National Center for Health Statistics, 69% of adults in the United Stated are either overweight or obese. Moreover, the prevalence of obesity is higher among older women compared with younger women [38]. Obesity is defined as a

significant gain above ideal weight, with the latter being classified as the weight that maximizes life expectancy [39]. Overweight and obesity are associated with POP, but there is no documented evidence that relate the biomechanical and structural properties of AVW tissue from overweight patients to the development or progression of prolapse [39].

BMI is calculated as body mass divided by the square of the patient's height. It is a measure used to approximate body fat percentage among the weight-height ratio [39]. According to it, patients with a BMI lower than 25 are considered have a normal healthy weight, and those with a BMI of 25 or higher are considered overweight. Patients with a BMI of 39 or higher are considered obese [38]. In this study, due to the sample size, overweight and obese were analyzed in the same group. Group 1 was considered to have a healthy weight with a BMI range from 20.18 to 24.84. Group 2 was considered overweight with a BMI range from 25.5 to 43.4. For each group, the mean and standard deviation (SD) for each biomechanical parameter described above was obtained. The means in age and parity were also obtained for each group along with their standard deviation, to verify that the differences between groups were only due to BMI and were not influenced by the other two parameters.

3.3.2 Effect of parity

Since injury to the vagina and its supportive tissues at the time of vaginal birth is considered a major risk factor for prolapse [18], patients were divided according to number of child delivery in two groups with the parity number ranging from 0 to 2 in group 1 and the parity number in group 2 ranging from 3 to 6. From 28 patients, 2 patients had both vaginal delivery and C-section, and 1 patient was nulliparous. The rest of the patients had vaginal deliveries. For each group, the mean and standard deviation for each biomechanical parameter was obtained. The means in age and BMI were obtained

for each group along with their respective standard deviation, to verify that the differences between groups were only due to parity number and not influenced by the other two parameters.

3.3.3 Effect of geriatric age

The older adult, people whose age exceeds 65, represented 12.9% of the population in United States in 2009 [40]. Aging is considered a risk factor of prolapse due to changes in composition in connective tissue [12,22]. Patients were divided according to geriatric age in group 1 with age ranging from 40 to 64 and in group 2 with age ranging from 66 to 80. For each group, the mean and standard deviation for each biomechanical parameter was obtained. The means in parity and BMI were obtained for each group along with their respective standard deviation to verify that the differences between groups were only due to menopause and were not influenced by the other two parameters.

3.3.4 Effect of menopause

The impact of menopause in the biomechanical properties of AVW tissue has been studied. These studies however led to differences in conclusions due to differences in the definition for menopausal age [4,11]. In this study, patients were grouped in premenopausal, with age ranging from 40 to 53, and postmenopausal with age ranging from 60 to 83. There were no patients in between the ages 54 to 59. For each group, the mean and standard deviation for each biomechanical parameter was obtained. The means in parity and BMI were obtained for each group along with their respective standard deviation, to examine any differences between groups due to menopause alone and not influenced by the other two parameters.

3.4 Statistical analysis

Welch 2-tailed t-tests were used compare the means between each group to examine any statistical differences. The statistics were calculated with a confidence interval of 95% (α=0.05). Furthermore, a post-hoc retrospective power analysis using Cohen's d tables [41] was done for each parameter that showed no statistical significance to obtain the approximate sample size needed to avoid missing an effect due to sampling size. The statistical power was set for 80% power, with a 20% probability risk of a type II error. All statistics analysis was done using Excel 2010 (Microsoft).

3.5 Correlating in-vivo and in-vitro measurements

Biomechanical parameters from in-vitro properties were plotted against peak tissue uplift from in-vivo BTC-2000TM test to see any trend between the progression of POP and each BMI group. The same was done for parity groups, and groups in the geriatric age analysis and menopause analysis. To analyze the strength and direction for each trend, the correlation coefficient (r) was calculated, and after a linear regression was performed the coefficient of determination (R^2) was calculated to determine the percentage of the data that was represented by the linear fit.

3.6 Finding outliers

After peak tissue uplift and energy absorption from BTC-2000TM test were plotted, a comparison of the points of each patient was made. Since peak tissue uplift and energy absorption were shown to increase linearly as the severity of prolapse increases [19,31], each point was analyzed to see if they followed the expected trend line. From Instron testing, each patient's stress-strain response was plotted and analyzed for noise from the experiment. A description of the analysis done to find possible outliers is found in Appendix E. All of the 28 patients' data was used for the analysis and the results.

Chapter 4

Results

4.1 Effects of BMI

From the 28 patients, 13 had a BMI <25 (group 1) and 15 had a BMI ≥25 (group 2). In the BMI analysis, when analyzing patient attributes, there were no significant differences due to age or parity number between groups, indicating the differences found in biomechanical parameters only account for differences in BMI. Table 3 summarizes the data (mean ± SD) for each group with the corresponding P Value from the t-test.

4.1.1 Effect of BMI from in-vivo test results

Results from in-vivo BTC-2000^{TM} tests (peak tissue uplift and energy absorption) did not present significant differences between BMI groups as summarized in Table 3. A plot of both BTC-2000^{TM} parameters, shown in Figure 16, indicates that there is a positive correlation between tissue uplift an energy absorption, and that as POP stage increases the compliance of the tissue increases in a linear fashion for both groups,confirming the accuracy of the device. The coefficient of determination (R^2) shows that the linear regression represents the data in 95% and 75% of the cases, respectively.

4.1.2 Effect of BMI from in-vitro test results

All of the parameters obtained from cyclic tensile loading (Table 3) presented significant differences among BMI groups. The 10%TM (Figure 17a) and 25%TM (Figure 17b) were significantly higher for group 2 than BMI<25 group. These indicates a steeper response and therefore the development of higher stresses at same levels of strain, suggesting a stiffer tissue for patients with BMI≥25 compared to patients with BMI <25.

Table 3 Summary of parameters results from in-vivo and in-vitro tests (mean ± SD) for each of the BMI groups with corresponding P-values. n= number of patients, values in red represent statistically significant differences between groups ($p<0.05$)

			BMI<25 (n=13)	BMI≥25 (n=15)	P-Value
Patient Attributes		Age	63 ± 9	64 ± 12	0.75
		Parity	2 ± 1	3 ± 1	0.11
In-vivo (BTC-2000^{TM})		Peak tissue uplift (mm)	1.98 ± 0.95	1.99 ± 0.94	0.99
		Energy absorption (KPa)	7.33 ± 2.92	7.65 ± 3.91	0.81
In-vitro (1D Tensile stretch)	Cyclic stretch to 25%	10%TM (MPa)	0.075 ± 0.049	0.023± 0.18	0.0053
		25%TM (MPa)	0.42 ±0.39	2.10 ± 2.39	0.0053
		25%LSE (KPa)	2.88 ± 2.01	10.01 ± 9.02	0.0091
		25%USE (KPa)	2.25 ± 1.57	7.71 ± 6.91	0.0091
		25%HSE (KPa)	0.62 ± 0.45	2.29 ± 2.12	0.0091
	Stretch to failure	MTM (MPa)	1.87 ± 0.84	3.69 ± 2.68	0.023
		Yielding Strain (%)	81.10± 24.19	55.88 ± 24.49	0.011
		Yielding Stress (MPa)	0.51 ±0.73	0.73 ± 0.33	0.048
		YSE (MPa)	0.099 ± 0.049	0.11 ± 0.062	0.65
		Failure Strain (%)	118.65 ± 37.41	95.50 ± 35.81	0.11
		Failure Stress (MPa)	0.93 ± 0.34	1.44 ± 0.57	0.0081
		FSE (MPa)	0.39 ± 0.21	0.54 ± 0.20	0.038

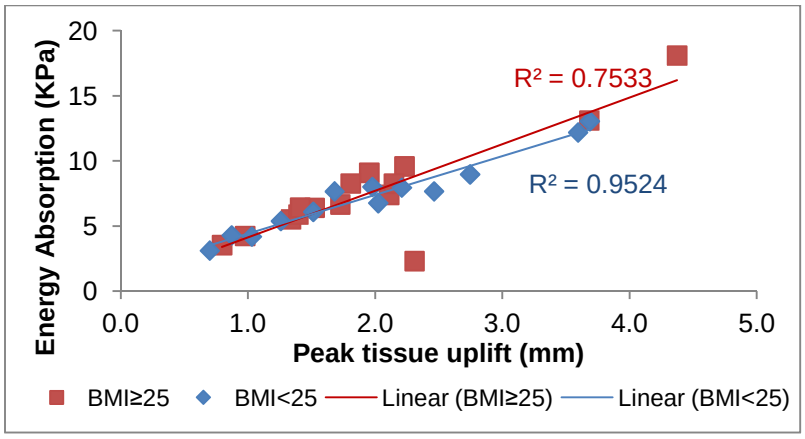

Figure 16 Association between BTC-2000™ parameters (Peak tissue uplift and energy absorption) for each BMI group and coefficient of determination (R^2) for each linear regression

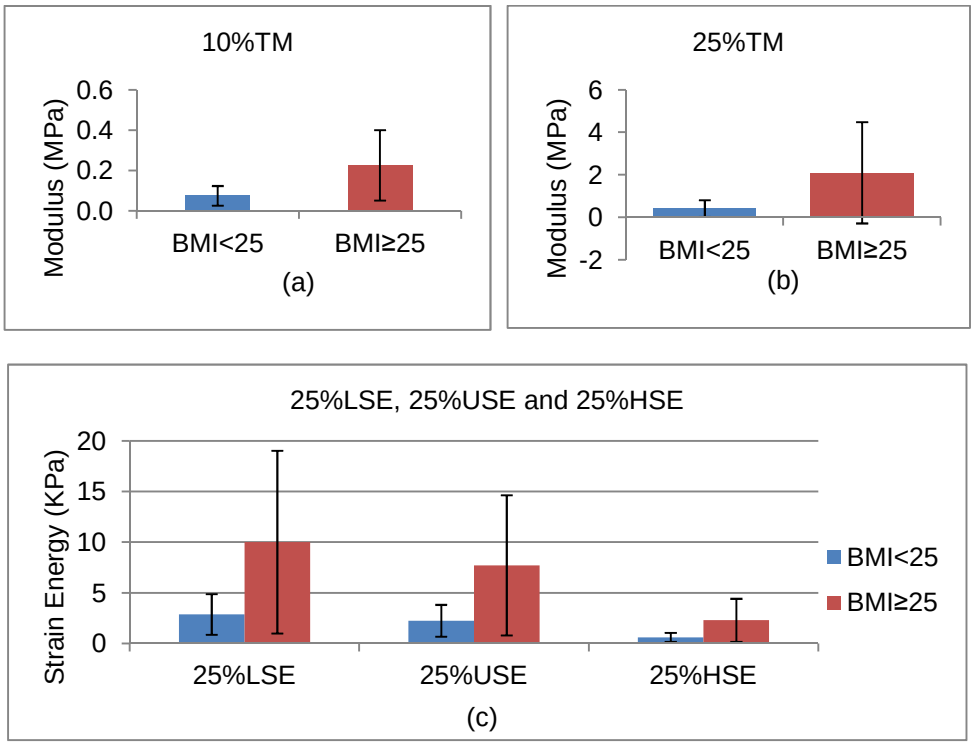

Figure 17 Mean ± SD of cyclic tensile loading parameters of each BMI group: (a) 10%TM (b) 25%TM (c) 25%LSE, 25%USE and 25%HSE

Furthermore, the stored energy at 25% strained state (25%LSE) was higher for patients in group with BMI≥25 than the other group. The recovered strain energy (25%USE) from this same group was also higher. The strain energy loss (25%HSE) was significantly higher for group 2. The mean and SD of these parameters is shown in Figure 17c. The loading-unloading up to 25% stretch of each patient is plotted in Appendix F1. A clear difference in response for each BMI group is shown up to 25%stretch.

The mean stress-strain response (a) and its corresponding modulus (b) of the stretching up to failure test for each BMI group is shown in Figure 18.

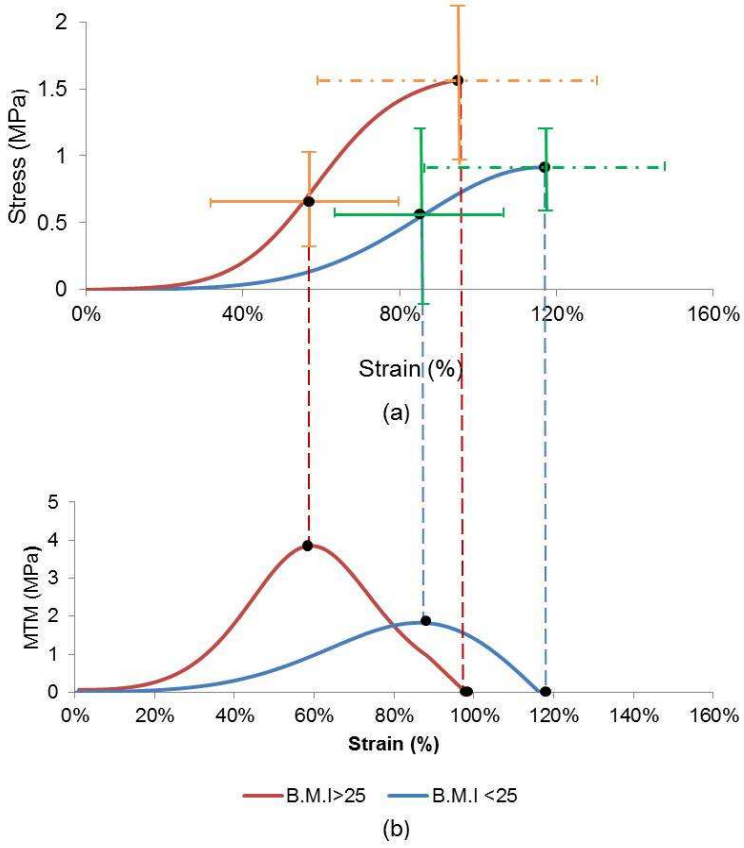

Figure 18 (a) Comparison of stress-strain curve mean ± SD responses by BMI group. (b) Comparison by MTM of stress-strain curve. SD is represented with a solid line for statistically significant data, and dotted for non-significant data.

It can be observed that the MTM becomes maximal at lower strain and at higher stress for BMI≥25 group 2 than the other group 1, which resulted in a statistically different stress-strain response. Both responses were non-linear, but the elasticity of tissues from patients with BMI<25 was significantly higher, as shown by the differences in the yielding point in Figure 18. The same situation is observed in the failure point, since the specimens from BMI≥25 group 2 reached failure at lower strains than group 1. An illustration of the yielding point, the failure point and the MTM for each patient is shown in Appendix G1, and plots of all the patient stress-strain responses up to the yielding point and failure point are shown in Appendices F2 and F3, respectively. Between groups, the MTM difference was statistically significant, with patents with BMI≥25 having a higher MTM than the other group. The mean yielding stress and the mean yielding strain also were statistically different between BMI groups, establishing the difference between the groups yielding points. The YSE did not present a significant difference between groups.

The failure point for each group presented significant differences in stress but not in strain mean values, with BMI≥25 patients developing higher stress values but similar strains as patients with BMI<25. The FSE were statistically different, since the stresses developed were high and resulted in greater areas under the curve for group 2.

4.1.3 Correlating BMI sensitivities between in-vivo and in-vitro test results

Parameters from cyclic tensile loading were plotted against peak tissue uplift from the BTC-2000^{TM} (Figure 19). A similar trend was observed in all parameters. For group 2, as the peak tissue uplift increases the parameter values tend to decrease, showing that even though the tissue of these patients is stiffer compared to group 1, among patients with BMI≥25 the properties of the tissue decrease as it becomes more compliant at higher levels of prolapse. For group 1 however, the trend suggests that

patients with BMI<25 are relatively insensitive to tissue uplift increase, indicating that a high BMI may have an influence in the prevalence of POP.

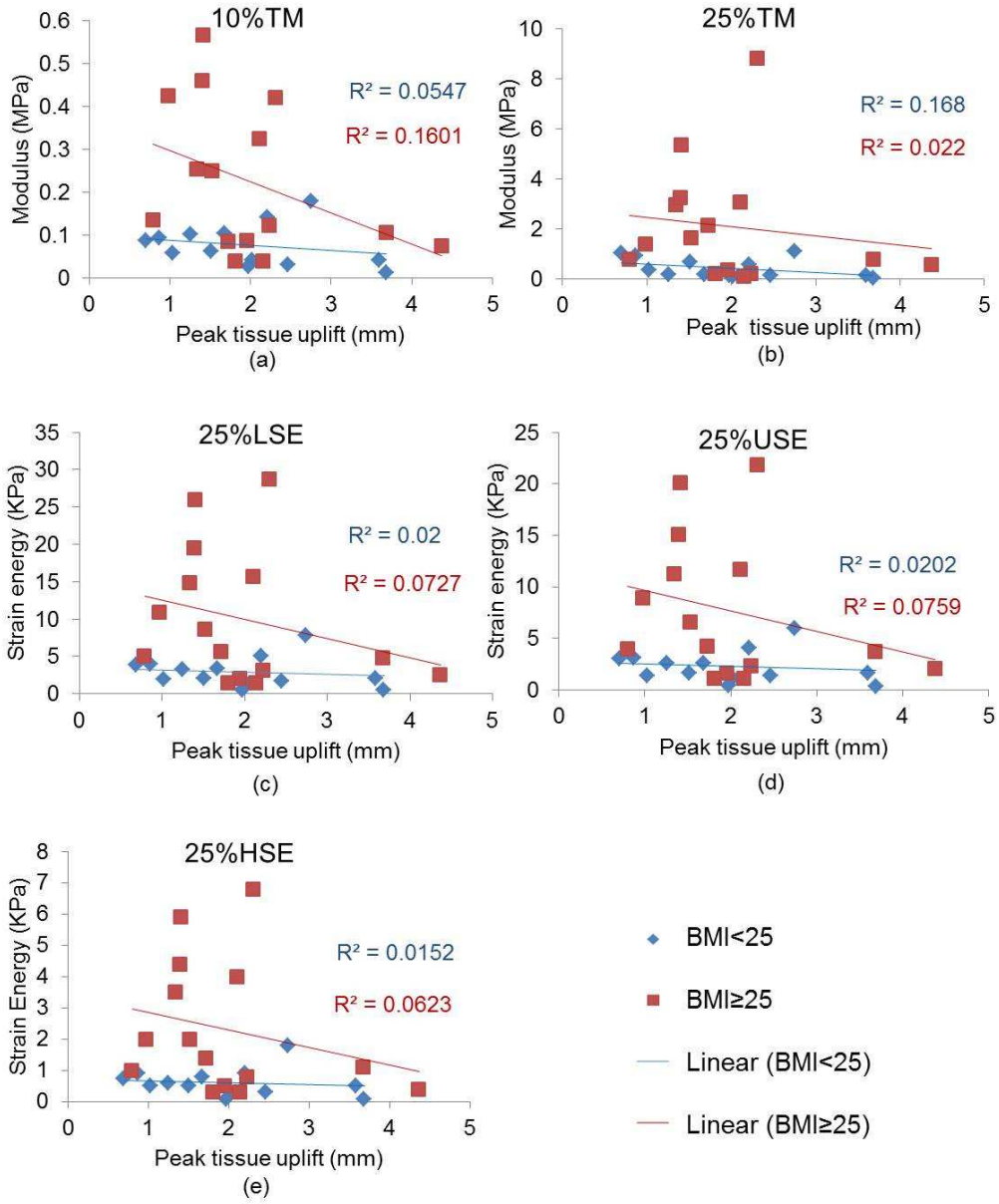

Figure 19 Plots of (a) 10%TM (b) 25%TM (c) 25%LSE (d) 25%USE (e) 25%HSE vs. BTC 2000^{TM} peak tissue uplift for BMI analysis and trend line for each group with coefficient of determination (R^2)

The parameters obtained from the failure test were also plotted against peak tissue uplift to find trends for each BMI group (Figure 20 and 21).

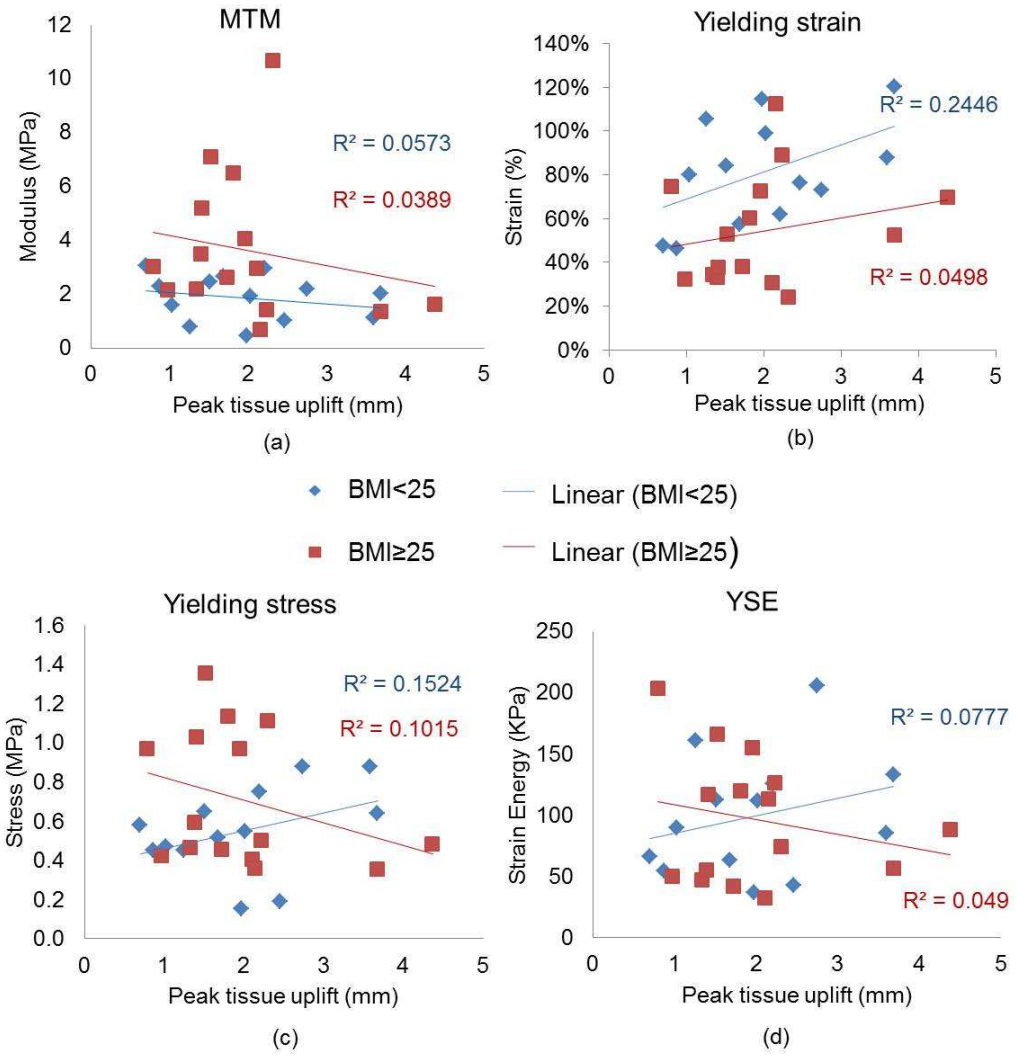

Figure 20 Plots of (a) Maximum tangent modulus (b) Yielding strain (c) Yielding stress (d) Yielding strain energy from Instron testing up to failure vs. BTC-2000^{TM} peak tissue uplift for BMI groups with coefficient of determination for the linear regression (R^2)

The MTM plot (Figure 20a) showed the same trend than the parameters of cyclic loading. MTM from BMI≥25 group decreases as the peak tissue uplift increases, while for group 1, the modulus values remain within the same range, showing that a high BMI alters the compliance of the tissue. As POP becomes more severe, tissue yields at higher strains for both groups, again, suggesting compliance effects in the tissue (Figure 20b). For BMI≥25 group as the severity of POP increases, the yielding stress decreases, while for BMI<25 patients the trend shows that yield stress remain at the same level, or slightly increases as the severity of POP increases (Figure 20c). The YSE (Figure 20d) decreased as the severity of POP increases for group 2, while for patients with BMI<25 it increases due to the changes and trend line observed in stress for both groups.

Failure strain and failure stress for both groups (Figure 20a and b) followed the same trend line as yielding stress and strain, and FSE (Figure 20c) followed the same trend as the YSE for both groups.

Table 4 shows the correlation coefficient of each parameter from Instron testing with the peak tissue uplift from BTC-2000^{TM} test. The correlation coefficients show a weak to medium correlation between tissue uplift and the parameters due to the variability of the data, which could be stronger with a higher sample size for each BMI group. Nevertheless, the coefficient indicates the direction of each trend is as expected.

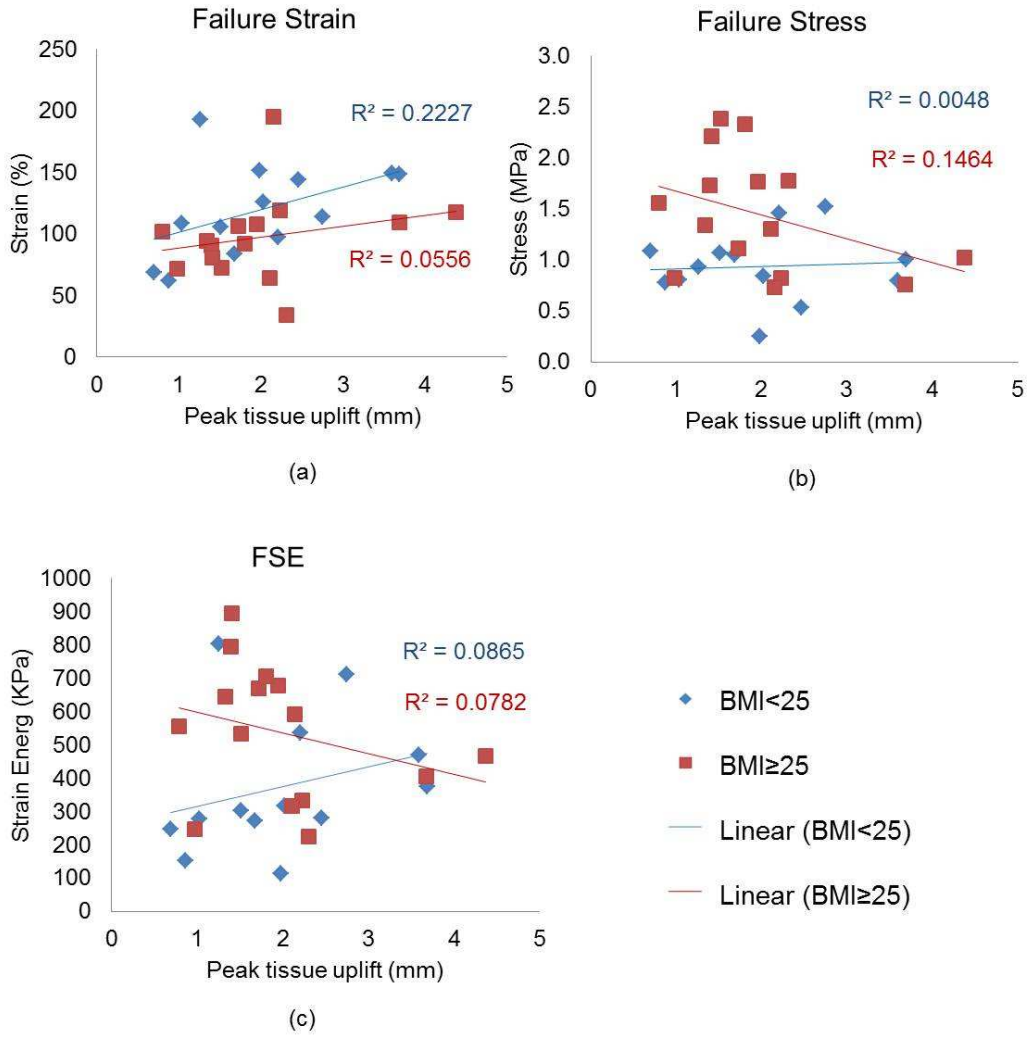

Figure 21 Plots of (a) Failure strain (b) failure stress and (c) failure strain energy from Instron testing up to failure vs. BTC-2000^{TM} peak tissue uplift for BMI groups with coefficient of determination for the linear regression (R^2)

Table 4 Linear correlation coefficient (r) of each parameter from Instron test with BTC-2000^{TM} peak tissue uplift for each BMI group

		BMI<25 (n=13)	BMI≥25 (n=15)
Cyclic stretch to 25%	10%TM	-0.23	-0.4
	25%TM	-0.41	-0.15
	25%LSE	-0.14	-0.27
	25%USE	-0.14	-0.28
	25%HSE	-0.12	-0.25
Stretch to failure	MTM	-0.24	-0.20
	Yielding Strain	0.49	0.21-
	Yielding Stress	0.088	-.29
	YSE	0.28	-0.17
	Failure Strain	0.47	0.25
	Failure Stress	0.069	-0.38
	FSE	0.28	-0.29

4.2 Effect of parity

From the 28 patients, 12 had a parity number between 0 and 2 (group 1) and 16 had a parity number between 3 and 6 (group 2). When comparing patient attributes (Table 5), there were no significant differences between groups due to age and BMI, indicating the differences found in biomechanical parameters only account for differences in parity number. Table 5 also summarizes the data (mean ± SD) for each parameter extracted from in-vivo and in-vitro tests of each parity group with their corresponding P value from the t-test comparison.

4.2.1 Effect of parity from in-vivo test results

Peak tissue uplift and energy absorption extracted from in-vivo BTC-2000^{TM} tests are shown in Figure 22. The means were statistically significant were compared, with group 2 having higher values for both parameters, compared to group 1.

Table 5 Summary of parameters results from in-vivo and in-vitro tests (mean ± SD) for each parity group with corresponding P-values. n= number of patients, values in red represent statistically significant differences between groups ($p<0.05$)

			Parity 0-2 (n=12)	Parity 3-6 (n=16)	P-Value
Patient Attributes		Age	65 ± 11	63± 10	0.69
		BMI	26 ± 5	28 ± 6	0.25
In-vivo (BTC-2000^{TM})		Peak tissue uplift (mm)	1.55 ± 0.59	2.31 ± 1.03	0.022
		Energy absorption (KPa)	6.16 ± 1.83	8.51 ± 4.02	0.048
In-vitro (1D Tensile stretch)	Cyclic stretch to 25%	10%TM (MPa)	0.14 ±0.12	0.17 ± 0.17	0.59
		25%TM (MPa)	0.86 ± 0.85	1.67 ± 2.43	0.23
		25%LSE (KPa)	5.15 ± 4.46	7.85 ± 9.21	0.32
		25%USE (KPa)	4.01 ± 3.48	6.05 ± 7.04	0.32
		25%HSE (KPa)	1.14 ± 1.00	1.80 ± 2.18	0.29
	Stretch to failure	MTM (MPa)	2.38 ± 1.66	3.20 ± 2.55	0.31
		Yielding Strain (%)	72.69± 26.81	63.77 ± 27.58	0.40
		Yielding Stress (MPa)	0.60 ± 0.32	0.64 ± 0.28	0.73
		YSE (MPa)	0.10 ± 0.59	0.10 ± 54.50	0.97
		Failure Strain (%)	106.47 ± 37.02	106.09 ± 39.50	0.98
		Failure Stress (MPa)	1.095 ± 0.55	1.28 ± 0.53	0.37
		FSE (MPa)	0.39 ± 0.21	0.51 ± 0.22	0.13

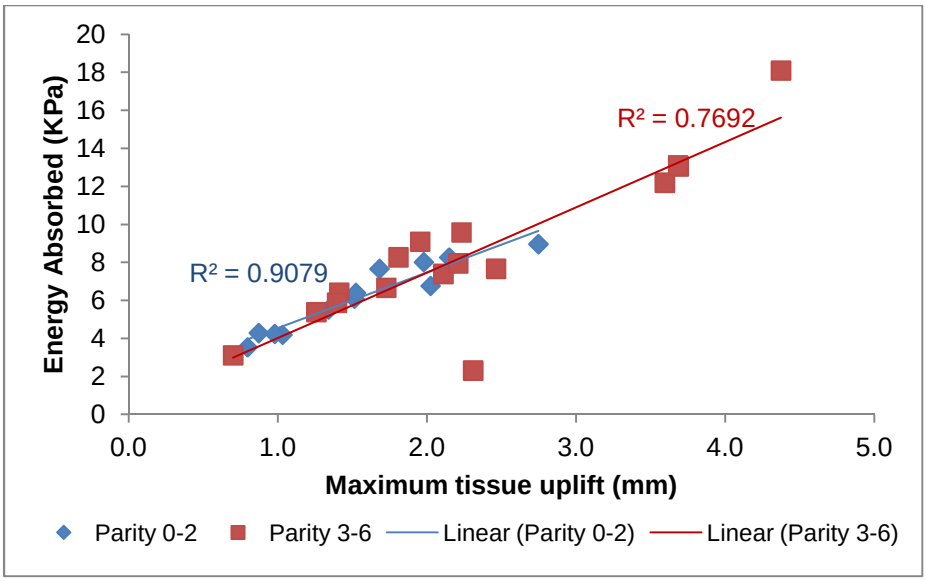

Figure 22 Association between BTC-2000^{TM} parameters (Peak tissue uplift and energy absorption) for each parity group and coefficient of determination (R^2) of each linear regression

The plot showed the same positive correlation between tissue uplift and energy absorption, with coefficients of determination of 90% and 76%, respectively. It is also observed that the peak tissue uplift and energy absorption values do not reach the maximum values that patients from group 2 reach, and their tissue is not as compliant as the level of prolapse increases. These results indicate that parity number is correlated to the severity of prolapse, and thus, patients with low parity that develop prolapse do not develop as highly compliant tissue as patients with higher parity number.

4.2.2 Effect of parity from in-vitro test results

All of the parameters obtained from cyclic loading, 10%TM and 25%TM, 25%LSE, 25%USE and 25%HSE were higher for patients with parity 3-6 than patients of group 1, with parity of 0-2. However, the results were not statistically significant.

The mean ± SD stress-strain response (a) and its corresponding MTM (b) of the stretching up to failure test for each parity group is shown in Figure 23.

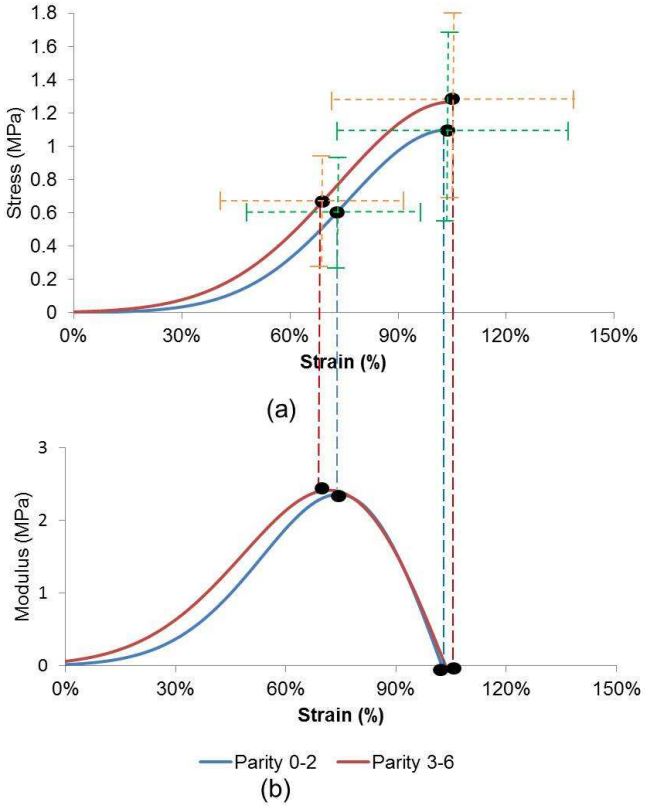

Figure 23 (a) Comparison of stress-strain curve mean + SD responses by parity group (b) Comparison by MTM of stress-strain curve.

The MTM becomes maximal at similar strain and also at similar stress values, leading to similar non-linear stress-strain responses for both groups. The same is observed for the failure point strain and stress values . An illustration of the yielding point, the failure point and the MTM for each patient is shown in Appendix G2. None of the parameters presented any statistical significant differences which may indicate that parity number does not influence the progression of POP.

4.2.3 Correlating parity group sensitivities between in-vivo and in-vitro test results

Instron parameters from cyclic loading were plotted against BTC-2000^{TM} peak tissue uplift (Figure 24).

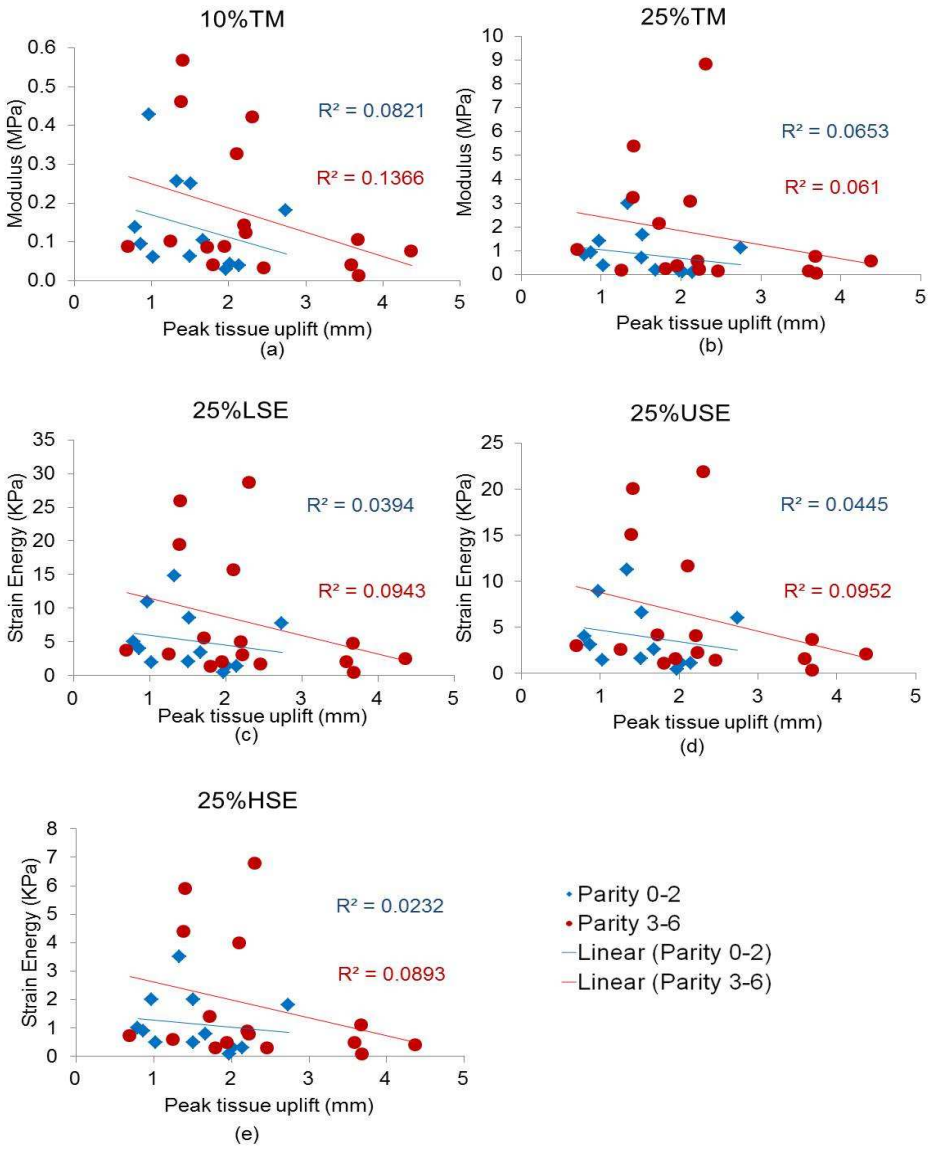

Figure 24 Plots of: (a) 10%TM (b) 25%TM (c) 25%LSE (d) 25%USE (e) 25%HSE for parity analysis vs. BTC-2000^{TM} peak tissue uplift and trend line for each group and coefficient of determination for each linear regression (R^2)

A similar trend is observed for all parameters: For both groups, as the peak tissue uplift increases, the strain energy decreases. This trend line is more pronounced in patients with higher parity. Since the 10% and 25% modulus parameters show the same trend line, results indicate that among patients with higher parity the tissue becomes more compliant when prolapse becomes more severe. Patients with low parity however, do not exhibit as large a compliance shift as patients with higher parity.

The parameters from failure tests were also plotted against peak tissue uplift (Figure 25 and 26). The Modulus plot (Figure 25a) showed the same trend line than the parameters of cyclic loading. Furthermore, as the severity of POP increases, the tissue yields at higher strain for low parity patients, but for high parity patients the opposite was observed (Figure 25b). However, for high parity patients as the severity of POP increases, the yielding stress decreases, while for low parity patients the trend line shows that yield stress remain among the same values as the severity of POP increases (Figure 25c). The strain energy up to yielding point (Figure 25d) remained among the same values as the severity of POP increases for high parity patients, while for low parity patients it increases.

The failure strain and failure stress for both groups (Figures 26a and b) followed the same trend line as yielding stress and strain. The strain energy up to failure point (Figure 26c) followed the same trend as the strain energy up to yield point, for both groups.

Table 6 shows the correlation coefficient of each parameter from tensile testing with BTC-2000^{TM} peak tissue uplift. The correlation coefficients show a weak to medium correlation between peak tissue uplift and the in-vitro parameters due to the variability of the data.

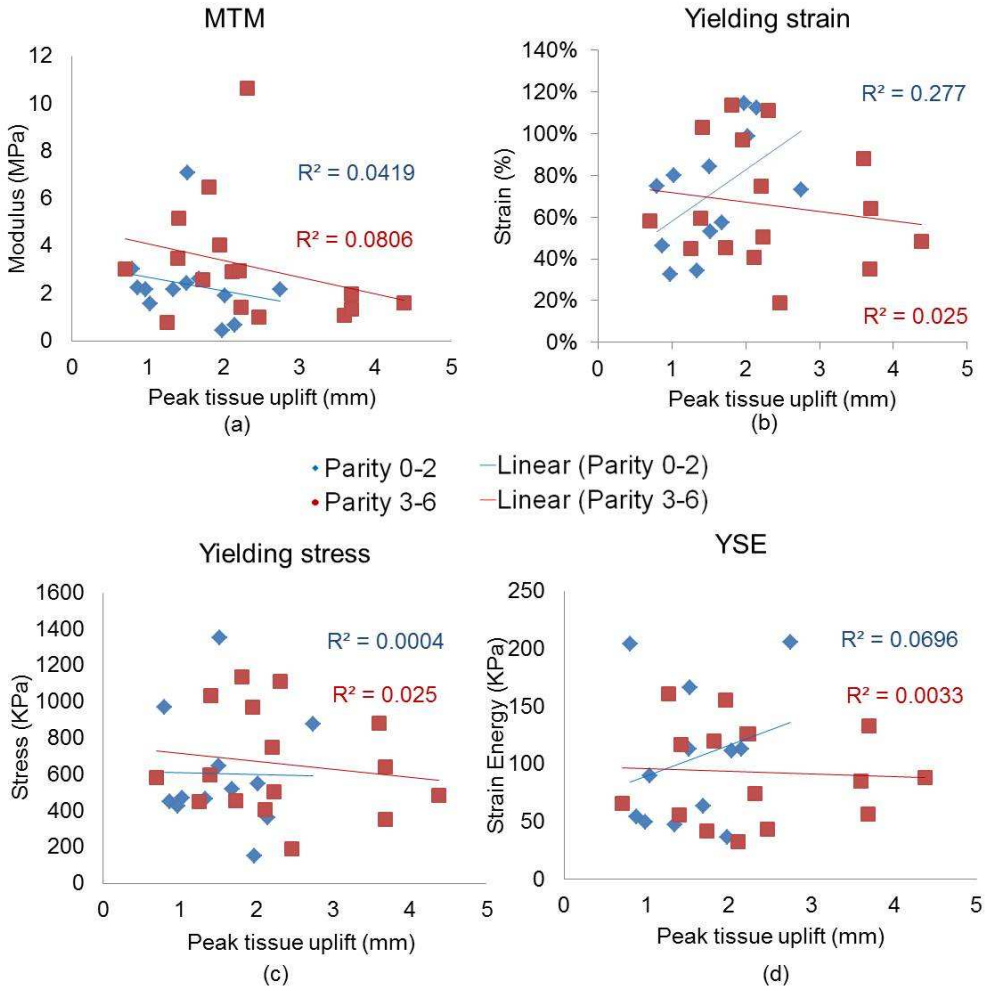

Figure 25 Plot of (a) Maximal tangent modulus (b) Yielding strain (c) Yielding stress (d) Yielding strain energy from Instron testing up to failure vs. BTC-2000^{TM} peak tissue uplift for parity groups. The trend line for each group and coefficient of determination for each linear regression (R^2) is included.

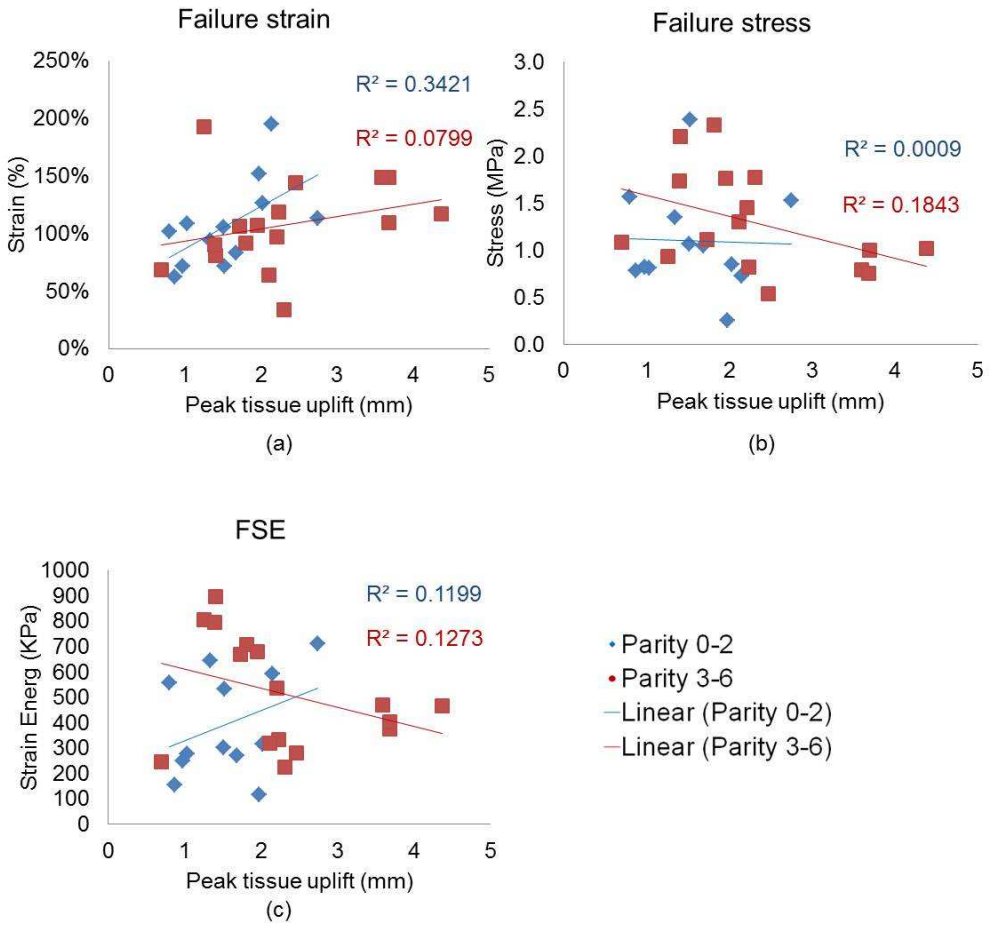

Figure 26 Plot of (a) Failure strain (b) Failure stress (c) Failure strain energy from Instron testing up to failure vs. BTC-2000^{TM} peak tissue uplift for parity groups. The trend line for each group and coefficient of determination for each linear regression (R^2) is included.

Table 6 Linear correlation coefficient (r) of each parameter from Instron test with BTC-2000^{TM} peak tissue uplift for each parity group

		Parity 0-2 (n=12)	Parity 3-6 (n=16)
Cyclic stretch to 25%	10%TM	-0.29	-0.37
	25%TM	-0.26	-0.25
	25%LSE	-0.20	-0.31
	25%USE	-0.21	-0.31
	25%HSE	-0.15	-0.30
Stretch to failure	MTM	-0.21	-0.29
	Yielding Strain	0.52	0.38-
	Yielding Stress	-0.020	-0.28
	YSE	0.26	-0.007
	Failure Strain	0.57	0.30
	Failure Stress	-0.03	-0.43
	FSE	0.32	-0.36

4.3 Effect of geriatric age

From the 28 patients, 14 were between age 40 and 65 (group 1), and 14 were between the age of 66 and 83 (group 2). When comparing patient attributes (Table 7), there were no significant differences between BMI and parity among groups, which indicates the differences found between tissues properties only account for differences in age.

4.3.1 Effect of geriatric age from in-vivo test results

The BTC-2000^{TM} parameters, peak tissue uplift and energy absorption, did not present significant differences between groups. A plot of both BTC-2000^{TM} parameters, shown in Figure 27, indicates that as POP stage increases the compliance of the tissue and the energy absorption increases in a linear fashion for both groups.

Table 7 Summary of parameters results from in-vivo and in-vitro tests (mean ± SD) for each age group with corresponding P-values (n= number of patients)

			Age≤65 (n=14)	Age>65 (n=14)	P-Value
Patient Attributes		BMI	28 ± 7	27 ± 5	0.72
		Parity	2 ± 1	3 ± 1	0.33
In-vivo (BTC-2000^{TM})		Peak tissue uplift (mm)	2.10 ± 1.17	1.87 ± 0.64	0.53
		Energy absorption (KPa)	7.50 ± 4.44	7.51 ± 2.18	0.99
In-vitro (1D Tensile stretch)	Cyclic stretch to 25%	10%TM (MPa)	0.14 ±0.13	0.17 ± 0.18	0.65
		25%TM (MPa)	1.55 ± 2.30	1.09 ± 1.53	0.54
		25%LSE (KPa)	7.03 ± 7.88	6.36 ± 7.51	0.82
		25%USE (KPa)	5.40 ± 5.96	4.96 ± 5.83	0.85
		25%HSE (KPa)	1.63 ± 1.91	1.40 ± 1.68	0.74
	Stretch to failure	MTM (MPa)	3.43 ± 2.77	2.29 ± 1.35	0.19
		Yielding Strain (%)	63.8 ± 24.73	71.36 ± 29.75	0.35
		Yielding Stress (MPa)	0.71 ± 0.34	0.55 ± 0.23	0.15
		YSE (MPa)	0.11 ± 0.63	0.94 ± 0.47	0.33
		Failure Strain (%)	97.78 ± 35.24	114.73 ± 39.53	0.24
		Failure Stress (MPa)	1.31 ± 0.56	1.11 ± 0.51	0.63
		FSE (MPa)	0.43 ± 0.19	0.49 ± 0.25	0.43

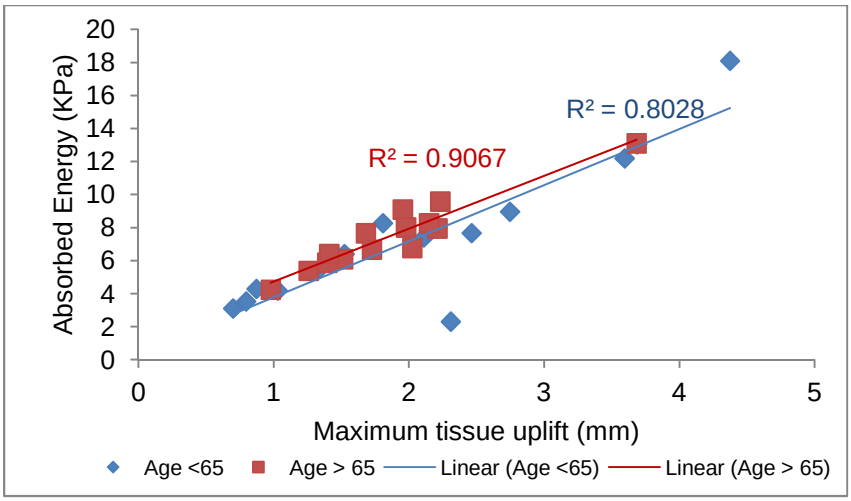

Figure 27 Association between BTC-2000^{TM} parameters (Peak tissue uplift and energy absorption) for each age group and coefficient of determination (R^2) of each linear regression

4.3.2 Effect of geriatric age from in-vitro test results

The 10%TM was lower for group 1 (Age< 65) than group 2 (Age> 65). However, the 25%TM was higher for group 1 (Age< 65) than group 2 (Age> 65). The Stored Energy at 25% Strained State (25%LSE), the recovered strain energy (25%USE) and the strain energy loss (25%HSE) were also higher for group 1 (Age< 65), suggesting a stiffness in group 1 tissue as the strain level increases. However, none of the parameters obtained from cyclic tensile loading presented statistically significant differences among group mean comparisons.

Figure 28 represents the mean stress-strain response (a) and its corresponding Modulus (b) of the stretching up to failure test for each age. It can be observed that mean responses are different, suggesting patients with age< 65 have a stiffer tissue than patients with age> 65, but again this difference was not statistically significant. An

illustration of the yielding point, the failure point and the MTM for each patient is shown in Appendix G3.

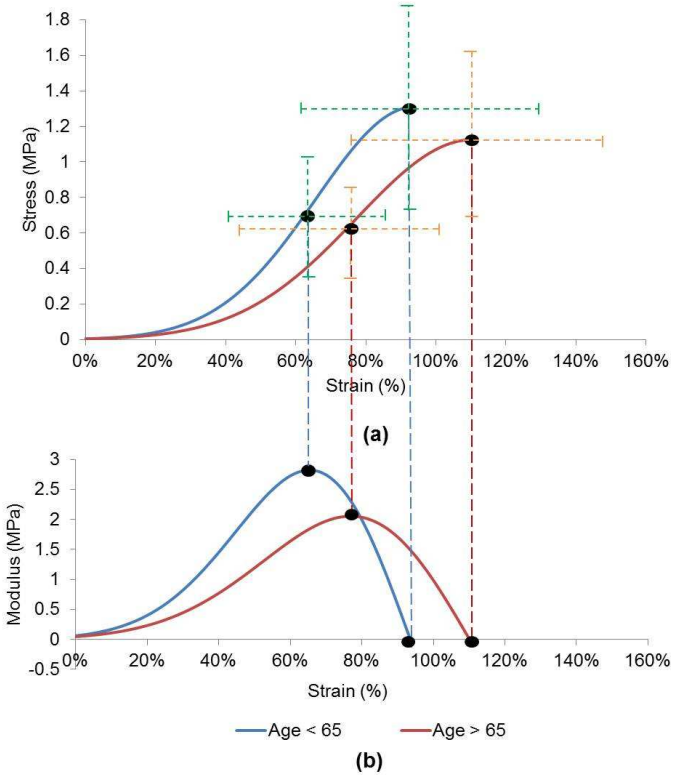

Figure 28 (a) Comparison of stress-strain curve mean ± SD responses from geriatric age groups. (b) Tangent modulus of stress-strain curve.

4.3.3 Correlating age groups sensitivities between in-vivo and in-vitro test results

Instron parameters from cyclic tensile loading were plotted against peak tissue uplift from BTC-2000^{TM} (Figure 29). For group 2 (Age> 65), as the peak tissue uplift increases due to the severity of prolapse, the strain energy decreases. Additionally, peak tissue uplift values do not reach the same compliance values that group 1 reached. Moreover, for group 1 (age< 65), the trend line suggests that even with an increase in peak tissue uplift, the parameters stay essentially the same.

The parameters obtained from the failure test were also plotted against peak tissue uplift to find trend lines among groups (Figure 30 and 31). Comparing the parameters extracted from yielding point, the trends are essentially the same for both groups (Figure 30). FSE (Figure 31c) is the only parameter that showed different trends for each group, but the values of FSE seem to remain within the same range, even with an increase in peak tissue uplift. Table 8 shows the correlation coefficient of each parameter from tensile testing with BTC-2000^{TM} peak tissue uplift. The correlation coefficients show a weak to medium correlation between peak tissue uplift and the in-vitro parameters due to the variability of the data.

Table 8 Linear correlation coefficient (r) of each parameter from Instron test with peak tissue uplift from BTC-2000^{TM} for each geriatric age group

		Age≤65 (n=14)	Age>65 (n=14)
Cyclic stretch to 25%	10%TM	-0.18	-0.45
	25%TM	-0.086	-0.33
	25%LSE	-0.11	-0.36
	25%USE	-0.11	-0.37
	25%HSE	-0.11	-0.33
Stretch to failure	MTM	-0.18	-0.13
	Yielding Strain	0.49	0.13
	Yielding Stress	-0.19	-0.17
	YSE	0.024	-0.006
	Failure Strain	0.56	0.13
	Failure Stress	-0.20	-0.29
	FSE	0.15	-0.22

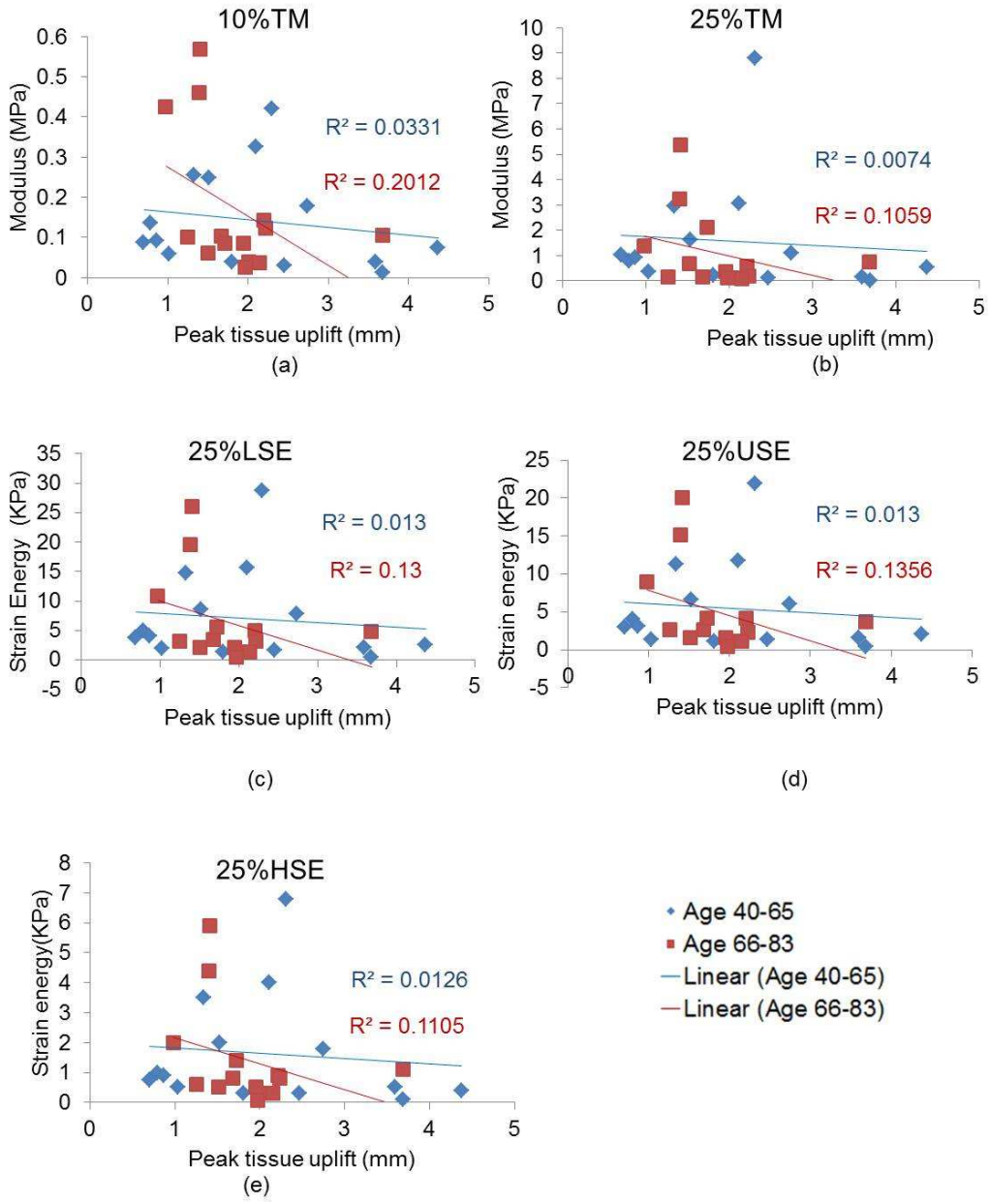

Figure 29 Plot of (a) 10%TM (b) 25%TM (c) 25%LSE (d) 25%USE and (e) 25%HSE vs. BTC-2000^{TM} peak tissue uplift for age analysis and trend line for each group The coefficient of determination for each linear regression (R^2) is included.

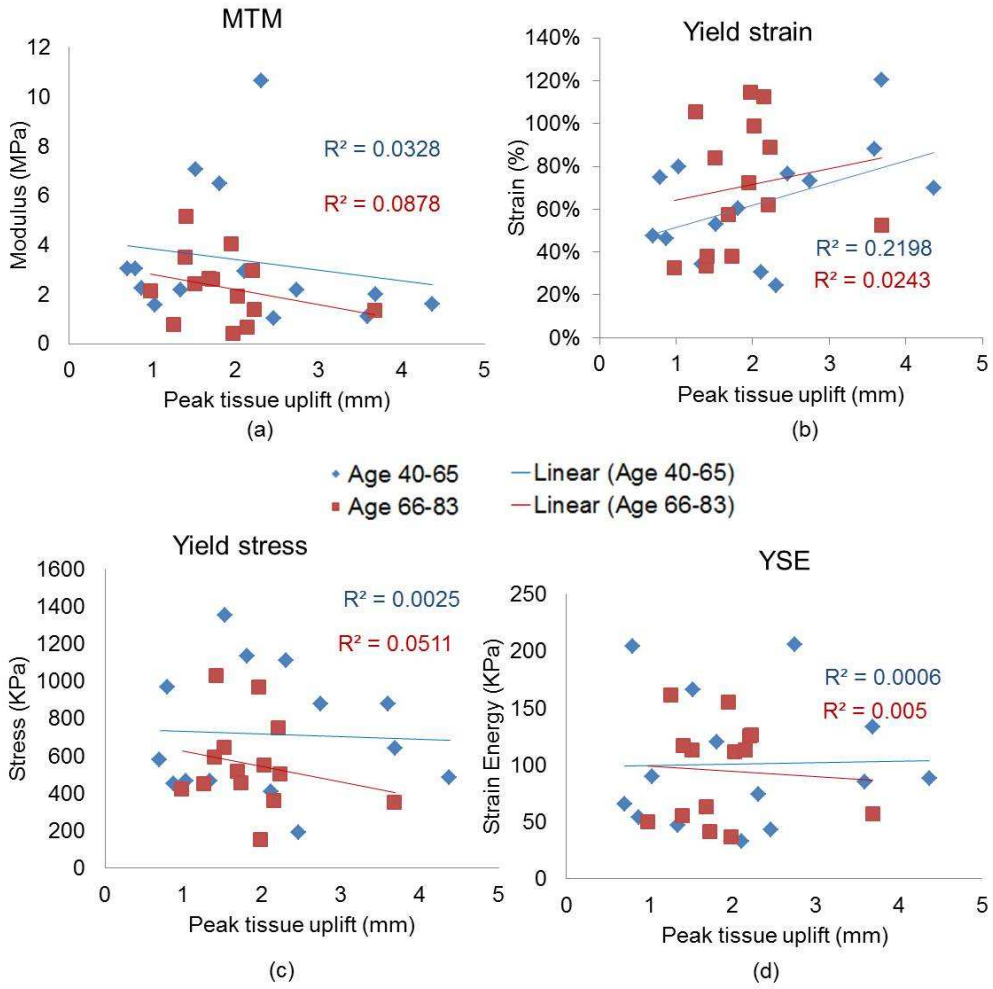

Figure 30 Plots of (a) Maximal tangent modulus (b) Yielding strain (c) Yielding stress (d) Yielding strain energy from Instron testing up to failure vs. BTC-2000^{TM} peak tissue uplift for the geriatric age groups. The trend line for each group and coefficient of determination for each linear regression (R^2) is included.

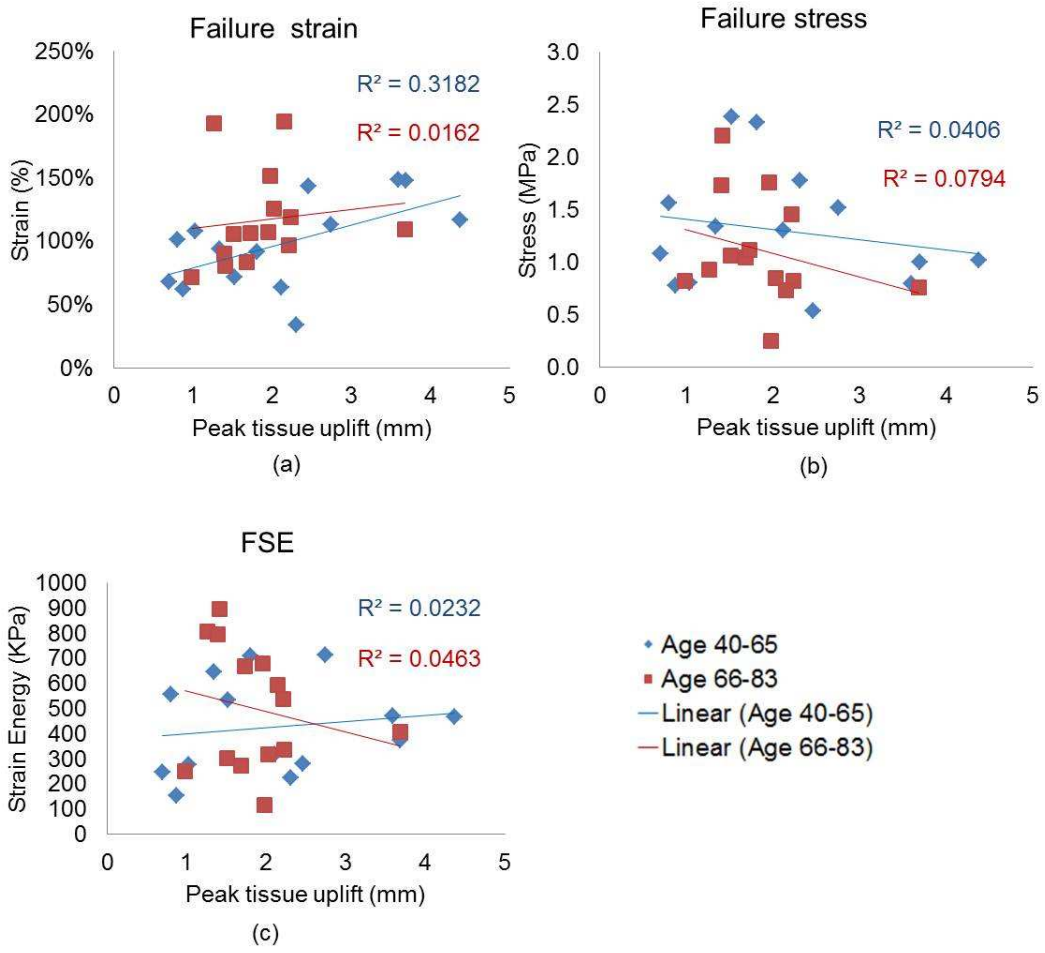

Figure 31 Plots of (a) Failure strain (b) failure stress (c) failure strain energy (d) from Instron testing up to failure vs. BTC-2000^{TM} peak tissue uplift for the geriatric age groups. The trend line for each group and coefficient of determination for each linear regression (R^2) is included.

4.4 Effect of menopause

Of the 28 patients, 7 were between age 40 and 53, and were considered to be premenopausal (group 1); 21 patients were between the ages of 60 to 83 and were considered to be postmenopausal (group 2). When comparing patient attributes (Table 9), there were no significant differences between BMI and parity among groups, which indicates that the differences found between tissues properties can only be accounted by differences in menopause. A summary of all parameters (mean ± SD) is shown in table 9.

4.4.1 Effect of menopause from in-vivo test results

The BTC-2000™ parameters, peak tissue uplift and energy absorption, did not present significant differences between pre and postmenopausal patients, as observed in Table 9. A plot of both parameters, shown in Figure 32, indicates that as POP stage increases the compliance of the tissue and the Energy absorption increases in a linear fashion for both groups.

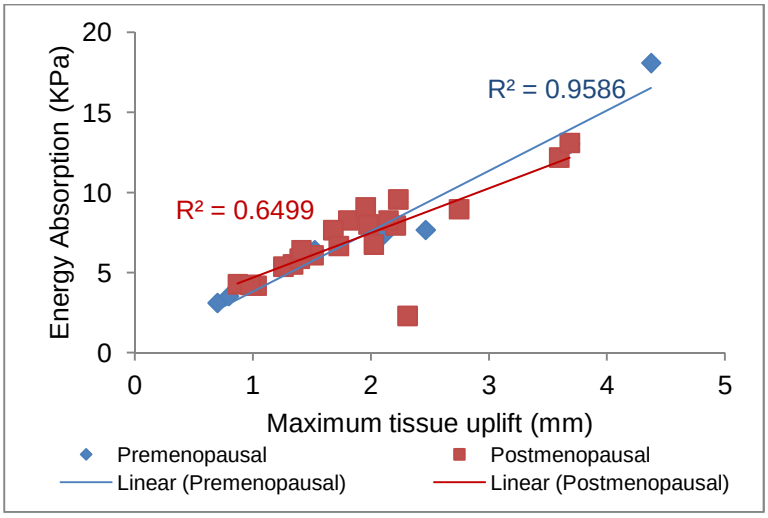

Figure 32 Association between BTC-2000™ parameters (Peak tissue uplift and energy absorption) for each menopause group and coefficient of determination (R^2) of each linear regression

Table 9 Summary of parameters results from in-vivo and in-vitro tests (mean ± SD) of pre and postmenopausal groups with corresponding P-values (n= number of patients, values in red represent statistically significant differences between groups)

			Premenopausal (n=7)	Postmenopausal (n=21)	P-Value
Patient Attributes		BMI	29 ± 8	27 ± 5	0.48
		Parity	3 ± 1	2 ± 1	0.75
In-vivo (BTC-2000^{TM})		Peak tissue uplift (mm)	2.24 ± 1.39	1.90 ± 0.75	0.56
		Energy absorption (KPa)	8.47 ± 5.37	7.18 ± 2.61	0.56
In-vitro (1D Tensile stretch)	Cyclic stretch to 25%	10%TM (MPa)	0.13 ±0.11	0.16 ± 0.16	0.56
		25%TM (MPa)	1.03 ± 1.04	1.42 ± 2.16	0.53
		25%LSE (KPa)	5.40 ± 5.25	7.13 ± 8.24	0.52
		25%USE (KPa)	4.17 ± 3.88	5.52 ± 6.34	0.51
		25%HSE (KPa)	1.22 ± 1.37	1.61 ± 1.91	0.56
	Stretch to failure	MTM (MPa)	3.04 ± 1.99	2.78 ± 2.32	0.78
		Yielding Strain (%)	69.61 ± 25.94	66.92 ± 28.08	0.82
		Yielding Stress (MPa)	0.72 ± 0.37	0.59 ± 0.27	0.45
		YSE (MPa)	0.13 ± 0.71	0.95 ± 0.48	0.71
		Failure Strain (%)	102.24 ± 35.72	107.59 ± 39.16	0.74
		Failure Stress (MPa)	1.26 ± 0.58	1.18 ± 0.53	0.73
		FSE (MPa)	0.39 ± 0.12	0.48 ± 0.24	0.24

4.4.2 Effect of menopause from in-vitro test results

The 10%TM mean was higher for the postmenopausal group, but the 25%TM mean was higher for the premenopausal group. The stored energy at 25% strained state (25%LSE), the recovered strain energy (25%USE) and the strain energy loss (25%HSE) were higher for postmenopausal patients. However, none of these parameters presented statistically significant differences.

Figure 33 represents the mean ± SD stress-strain response (a) and its corresponding modulus (b) of the stretching up to failure test for pre and postmenopausal groups. It can be observed the tangent modulus becomes maximal at a very similar yielding strain and also similar yielding stress mean values, leading to a similar non-linear stress-strain response for both groups. The same is observed for the failure point strain and stress mean values. An illustration of the yielding point, the failure point and the MTM for each patient is shown in Appendix G4. None of the parameters presented statistical significant differences.

4.4.3 Correlating menopausal groups sensitivities between in-vivo and in-vitro test results

Instron parameters from cyclic tensile loading were plotted against BTC-2000^{TM} peak tissue uplift (Figure 34). For each parameter, a similar trend line was observed for both groups: as the peak tissue uplift increases due to the severity of prolapse, the parameter values tend to decrease.

Figure 35 and 36 present the parameters obtained from the failure test plotted against BTC-2000^{TM} peak tissue uplift to find trend lines. The modulus plot (Figure 35a) showed a similar trend line than the parameters of cyclic tensile loading. As POP becomes more severe, the tissue yields at higher strain both groups (Figure 35b). However, for premenopausal patients as the severity of POP increases, yielding stress decreases, while postmenopausal patients the trend line shows that yield stress

increases as the severity of POP increases (Figure 35c). Furthermore, The strain energy up to yielding point (Figure 35d) followed the same trend line as the yield stress for both groups.

The failure strain and failure stress for both groups (Figure 36 a and b) followed the same trend line as yielding stress and strain, and the strain energy up to failure point (Figure 36c) did not present changes in values as the peak tissue uplift increased.

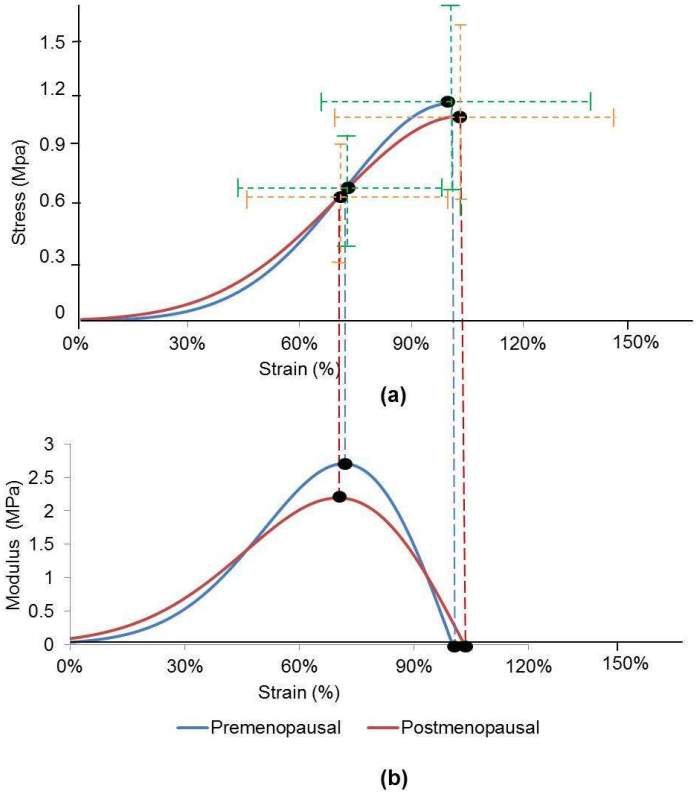

Figure 33 (a) Comparison of stress-strain curve mean ± SD responses from pre and postmenopausal groups (b) Tangent modulus of stress-strain curve mean.

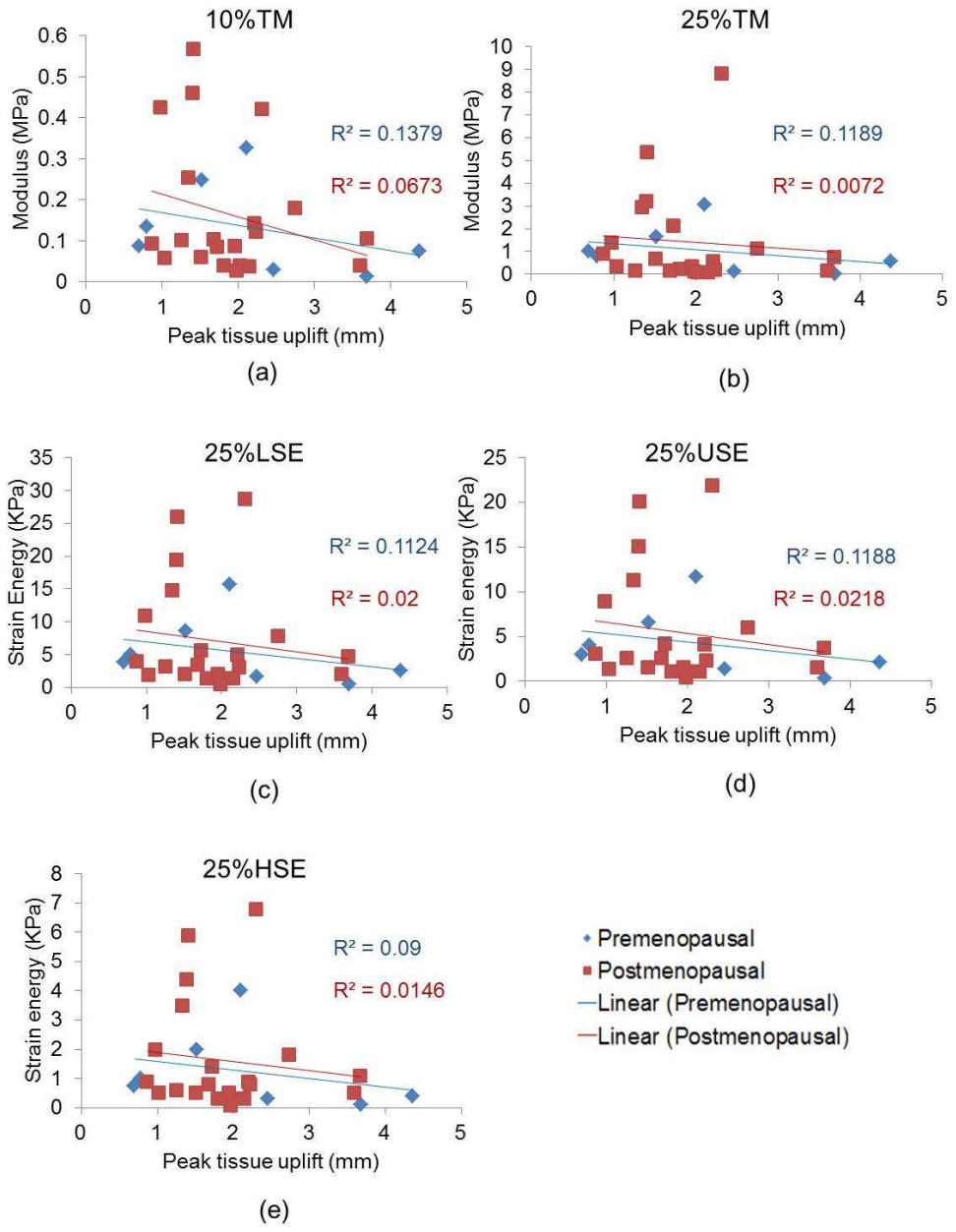

Figure 34 Plots of (a) 10%TM (b) 25%TM (c) 25%LSE (d) 25%USE and (e) 25%HSE for menopause analysis and trend line for each group. The coefficient of determination for each linear regression (R^2) is included.

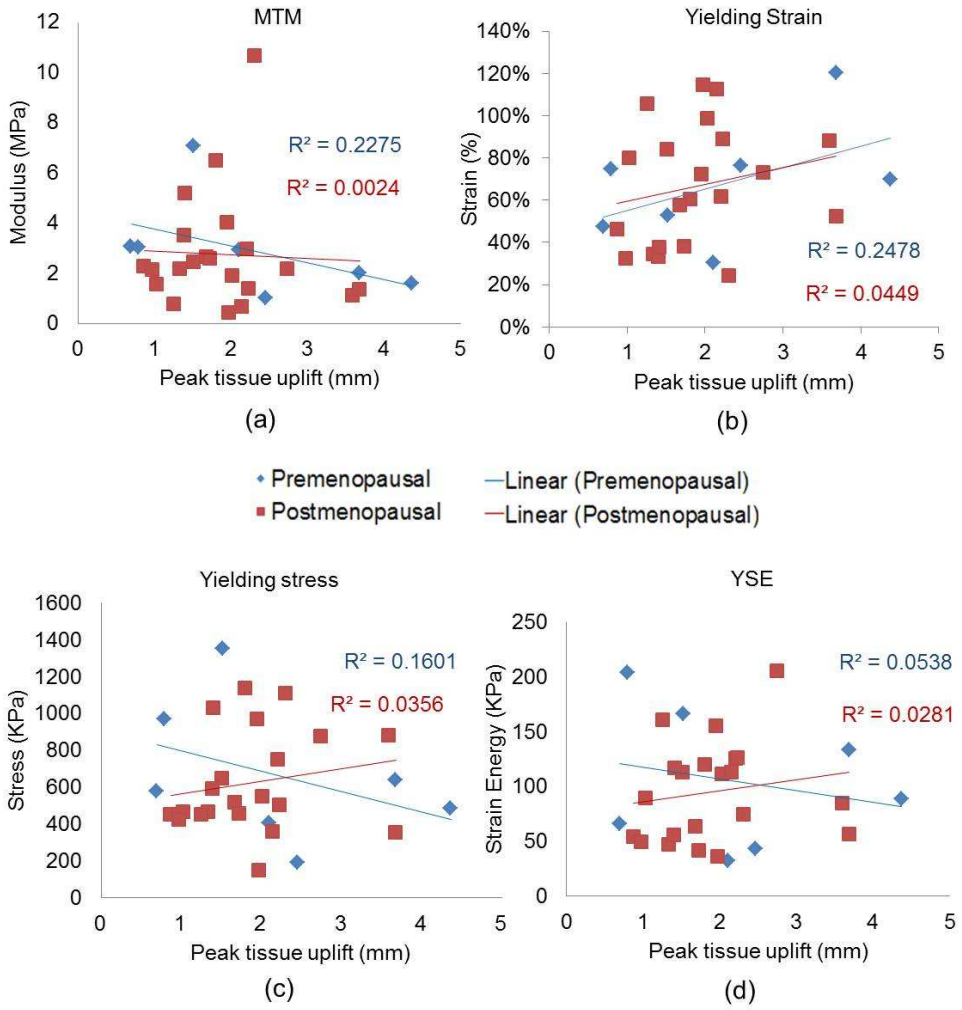

Figure 35 Plots of (a) maximal tangent modulus (b) yielding strain (c) yielding stress and (d) yielding strain energy from Instron testing up to failure vs. BTC-2000^{TM} peak tissue uplift from for pre and postmenopausal groups. The trend line for each group and coefficient of determination for each linear regression (R^2) is included.

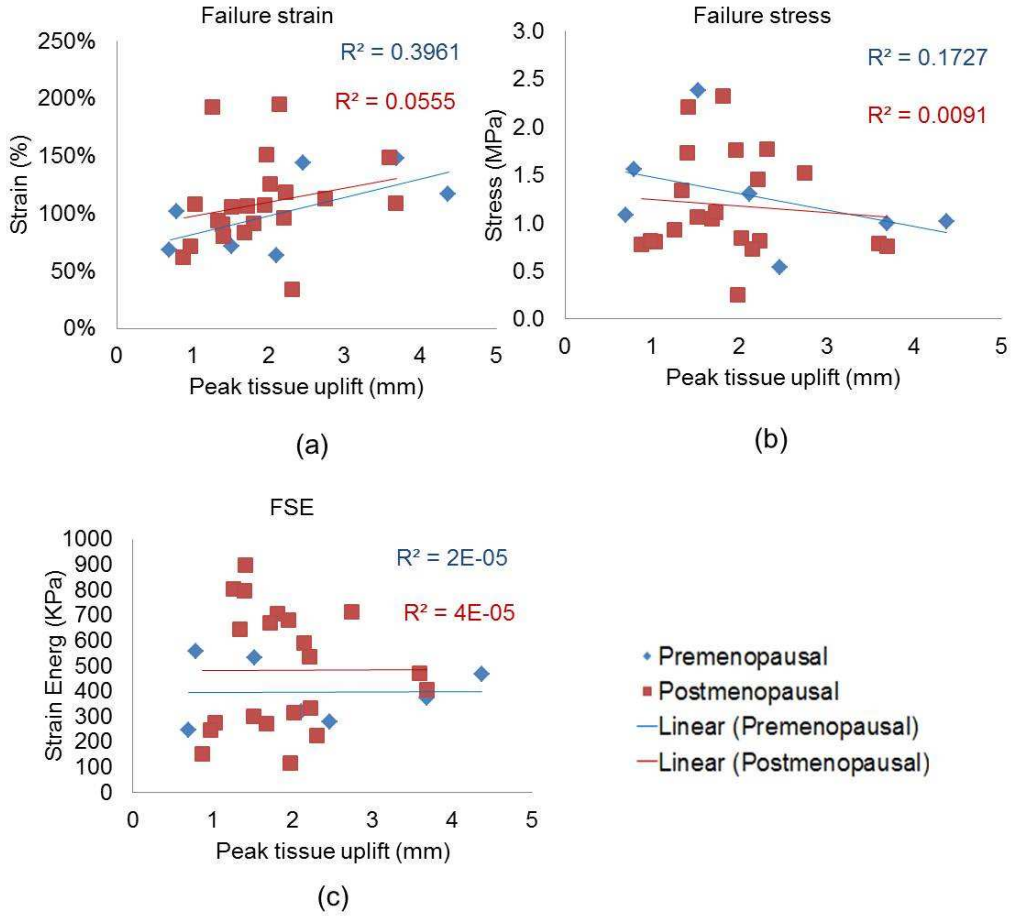

Figure 36 Plots of (a) Failure strain (b) failure stress and (c) failure strain energy from Instron testing up to failure vs. BTC-2000^{TM} peak tissue uplift for menopause groups. The trend line for each group and coefficient of determination for each linear regression (R^2) is included.

Table 10 shows the correlation coefficient of each parameter from tensile testing with BTC-2000^{TM} peak tissue uplift. The correlation coefficients show a weak to medium correlation between peak tissue uplift and the in-vitro parameters due to the variability of the data.

Table 10 Linear correlation coefficient (r) of each parameter from Instron test with peak tissue uplift from BTC-2000^{TM} for each menopause group

		Premenopausal (n=7)	Postmenopausal (n=21)
Cyclic stretch to 25%	10%TM	-0.37	-0.26
	25%TM	-0.34	-0.085
	25%LSE	-0.34	-0.14
	25%USE	-0.35	-0.15
	25%HSE	-0.30	-0.12
Stretch to failure	MTM	-0.48	-0.048
	Yielding Strain	0.54	0.20
	Yielding Stress	-0.43	0.019
	YSE	-0.23	-0.19
	Failure Strain	0.63	0.24
	Failure Stress	-0.42	-0.095
	FSE	0.0039	0.00041

4.5 Power analysis statistics

To estimate the needed sample size for all of the parameters from in-vivo BTC-2000T^{M} and in-vitro Instron tests that did not present significant differences, the effect size was calculated based on Cohen's d analysis [41]. The average of this calculation yields the needed sample size. Based on this analysis, the approximate sample size with an 80% power, a significance level of 0.05 and an effect size calculated of 0.3 is 175 patients.

Chapter 5

Discussion

Initially, the aim of this study was to analyze each risk factor separately and see how much each one altered the biomechanical properties of the tissue and contributed to the development or progression of AVW prolapse. Since parity, menopause and age had been previously analyzed [4,11,12,18,22] and are considered major risk factors [1,10,11], the study was focused on these three parameters. However, after analyzing changes in BMI and observing significant differences in almost every parameter, the study became more focused into how obesity affect the tissue such as it alters its properties during prolapse.

5.1 Alterations in prolapsed AVW tissue due to BMI changes

From in-vivo measurements, the BTC-2000^{TM} cutometer-like device was able to detect the differences in the tissue according to the severity of the prolapse for both groups, as shown by the trends from peak tissue uplift and energy absorption plot. The results from in-vitro tensile cyclic loading and the tensile failure test suggest a stiffer tissue for patients that have higher than normal BMI values (BMI >25). For almost every parameter obtained at different strain levels (25%stretch, stretch up to yielding point, and stretch up to failure point) the group with BMI> 25 showed statistically significant values than patients with BMI< 25, indicating a clear difference in response between groups. When correlating in-vivo and in-vitro measurements, Instron parameters for patients with a BMI>25 show sensitivity to increase in peak tissue uplift from BTC-2000^{TM}, with a negative correlation. Instron parameters for patients with normal BMI (BMI< 25) showed insensitivity to tissue uplift changes, and thus, to the progression of POP. These results

imply that a high BMI may have played a role contributing to the progression of POP in patients, by stiffening the AVW tissue.

Collagen and elastin are the main components that influence the stiffness of AVW connective tissue [42]. As mentioned before, elastin allows tissue deformability and recoil without permanent changes in structure and carries the load during small physiological stress and plays a complementary role with collagen fibers, which confer the tensile strength at higher physiological loads [42,45]. No studies were found that correlated BMI increase, overweight or obesity with alterations in elastin or collagen composition of AVW tissue. However, there were a few studies that related obesity to a decrease in elastin concentration or alterations in elastin fibers in connective tissue of other structures [42,43,44,45,46]. Of particular importance was an immunohistochemical study of Szczesny et al. [46], in which they found a significant reduction of elastin in the fascia of Rectus Abdominis muscle sheath in obese patients, which influences the development of hernias. In a different study, Chen et al. [45] found a relationship between obesity and Lysyl Oxidase (LOX) down regulation due to increased perivascular adipose tissue, leading to elastin fiber fragmentation and defective maturation in fibroblasts from ECM and vascular smooth muscle cells. They concluded that the elastin fibers could be altered due to mechanical factors in the connective tissue of aortas, leading to aortic stiffening [45]. The latter study, even though from a completely different structure, relates LOX down-regulation (a down-regulated protein observed in previous studies of prolapsed AVW tissue [29,42]), with obesity. Alperin et al. [29] related the down regulation of this protein in the sub epithelial and muscularis layers of the vagina of mice to the development of AVW prolapse. Klutke et al. [42] also measured the gene expression for LOX but in actual human patients with and without POP in the uterosacral ligament. The results showed that the mRNA expression of LOX gene was significantly

decreased in patients with prolapse [42]. Other researchers, such as Moon et al., relate the decrease of elastin in pelvic tissues to an increase in the proteases implicated in its degradation [20,43]. A study by Unal et al. related the increase of MMP-9 in adipose connective tissue [52]. Since little adipose tissue is found in the AVW, it is uncertain if it would contribute to the cause of POP.

After looking at all the previous studies, it is logic to hypothesize that a down regulation in LOX enzyme or an inhibition in its expression in AVW connective tissue of patients with high BMI could explain a structural remodeling due to elastin fiber alterations, which could result in stiffness of the tissue. However, there has to be a cause for this down regulation, so this was further investigated.

It is known that fibroblasts, the cells that produce collagen and elastin in the ECM of connective tissue, are major type of mechano-responsive cells [55]. The mechanical regulation of ECM gene expression in fibroblasts aids with the maintenance of connective tissue composition [45,46,55]. Nevertheless, research suggests that other mechanical loads can also interfere with normal cellular gene expression and, consequently, cause the pathogenesis of connective tissue diseases [42,45,55]. An extra mechanical load in the pelvic cavity related to patients with overweight or obesity can be caused by an increased Intra-abdominal pressure (IAP) [48,49]. However, no studies were found that directly related an increased IAP and vaginal prolapse. A study by Nobblet et al. [49] found a significant correlation between BMI increase and IAP increase and concluded that obesity stresses the pelvic floor leading to a chronic state of increased pressure and structural remodeling. This was correlated to the development and recurrence of urinary incontinence [49]. Therefore, the additional stress that the AVW tissue is subjected to, due to extra intra-abdominal pressure (IAP) in patients with high BMI, could be a mechanical load that strains the tissue enough to cause an inhibition of LOX gene

expression and could result in remodeling of vaginal tissue. This is important since LOX protein catalyzes crosslinks in lysine residues in both elastin and collagen [42,45,46] and, therefore, both of these fibers could also be disrupted in obese patients, leading to prolapse progression.

5.1.1 Compound effect of BMI and parity in AVW tissue

Some authors have related the down regulation of LOX with the development of POP after vaginal birth [29,42,47], since it is the only time period when extensive remodeling of elastin fibers is done. They mention that there is vulnerability to other mechanical factors during this period that could lead to alterations in connective tissue composition. In Klutke et al. [42] they analyzed control non-POP and POP groups according to parity number and they observed significant differences in between high parity groups, showing that patients with high parity and with prolapse had lower levels of LOX and desmosine (the elastin specific crosslink) than controls with high parity. For the low parity group there were no significant differences between the levels of desmosine in POP and control patients. Liu [47] and Alperin [29] observed similar differences. To relate this thesis with Klutke, Liu and Alperin findings, for each BMI group, the patients were further subdivided according to parity (Table 11) as they did in Klutke study (parity from 0 to 2 and parity from 3 to 6). The P-values, after comparing the group of higher parity, were consistent with previous research findings, and showed statistically significant differences between the parameters. This suggests that among patients with high parity, when having a BMI≥25, the tissue becomes stiffer than patients with lower BMI. On the other hand, among patients with low parity, the results were not statistically significant, and suggests than an increase in BMI would not significantly alter the properties of the tissue.

Table 11 Mean ±SD of each BMI group subdivided according to parity number, and P-values of t-tests between BMI groups. Red values indicate a statistically significant difference.

		Parity 0-2			Parity 3-6		
		BMI<25 (n=7)	BMI≥25 (n=5)	P-Value	BMI<25 (n=5)	BMI≥25 (n=10)	P-Value
In-vivo (BTC-2000^{TM})	Peak tissue uplift (mm)	1.69 ± 0.64	1.36 ± 0.53	0.34	2.32 ± 1.21	2.30 ± 0.98	0.97
	Energy absorption (KPa)	6.57 ± 1.83	5.59 ± 1.86	0.39	8.23 ± 3.84	8.68 ± 4.33	0.83
In-vitro (1D Tensile stretch)	10%TM (MPa)	0.080 ± 0.05	0.22 ± 0.14	0.096	0.069 ± 0.049	0.23 ± 0.19	0.0311
	25%TM (MPa)	0.49 ± 0.41	1.37± 1.07	0.14	0.34 ± 0.38	2.46 ± 2.80	0.041
	25%LSE (KPa)	3.01 ± 2.41	8.14 ± 5.18	0.092	2.71 ± 1.62	10.94 ± 10.57	0.037
	25%USE (KPa)	2.32 ± 1.86	6.38 ± 4.00	0.085	2.18 ± 1.32	8.38 ± 8.10	0.039
	25%HSE (KPa)	0.70 ± 0.56	1.76 ± 1.21	0.12	0.52 ± 0.29	2.56 ± 2.48	0.029
	MTM (MPa)	1.91 ± 0.74	3.02 ± 2.41	0.37	1.81 ± 1.01	4.03 ± 2.86	0.045
	Yielding Strain (%)	79.22 ± 23.37	63.53 ± 31.27	0.37	83.30 ± 27.18	52.05 ± 21.22	0.04
	Yielding Stress (MPa)	0.52 ± 0.22	0.72 ± 0.43	0.39	0.50 ± 0.19	0.73 ± 0.30	0.086
	YSE (MPa)	0.097 ± 0.056	0.12 ± 0.069	0.61	0.10 ± 0.045	0.085 ± 0.047	0.47
	Failure Strain (%)	106.13 ± 28.01	106.95 ± 50.91	0.97	133.28 ± 44.06	89.78 ± 27.08	0.063
	Failure Stress (MPa)	0.90 ± 0.38	1.36 ± 0.66	0.21	0.97 ± 0.31	1.47 ± 0.56	0.033
	FSE (MPa)	0.29 ± 0.19	0.52 ± 0.16	0.057	0.4 5± 0.20	0.55 ± 0.23	0.39

These results show that the statistical significant values obtained between BMI groups are mainly due to patients with high parity. Additionally, the in-vitro 25%LSE was

plotted against BTC-2000™ peak tissue uplift, but now with each BMI group divided according to parity, in Figure 37. This illustrates again that there is not a defined trend of BMI groups when parity is low (Figure 37a) with an increase in peak tissue uplift; when parity is high, BMI> 25 group exhibits sensitivity to peak tissue uplift increase, while patients with BMI <25 do not (Figure 37b).

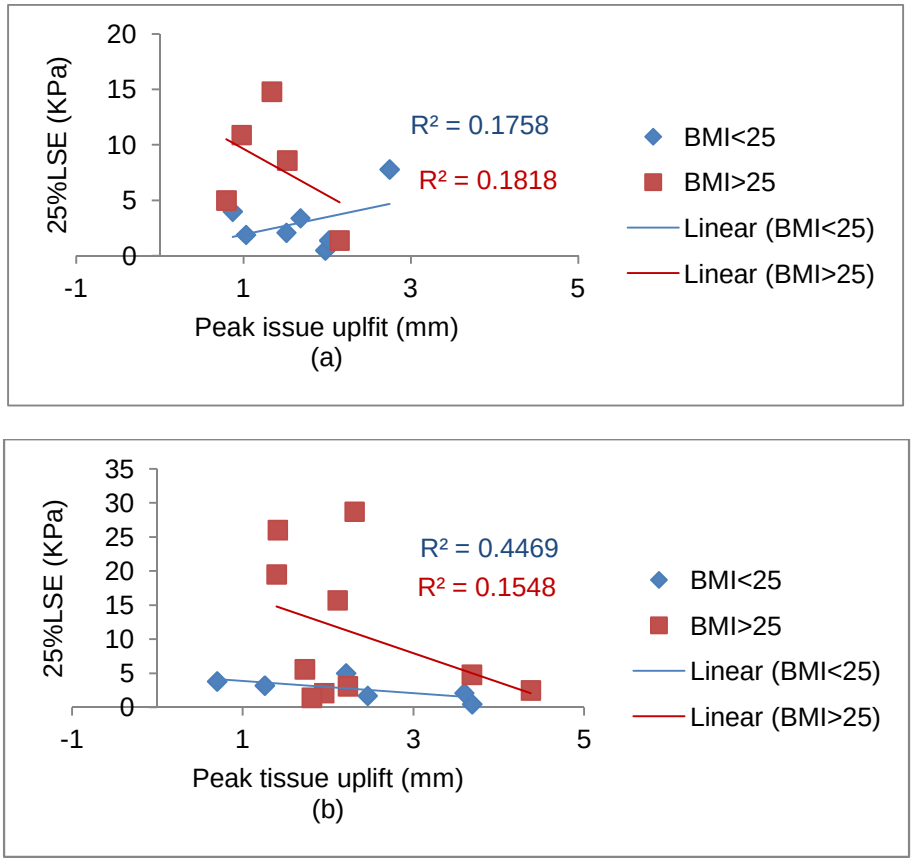

Figure 37 25%LSE from Instron vs. BTC-2000™ peak tissue uplift for each BMI group (a) Parity range from 0 to 2 (b) Parity range from 3 to 6. Coefficient of determination (R^2) for each trend included.

5.1.2 Compound effect of BMI and age and of BMI and menopause in AVW tissue

A correlation between the patients from BMI groups was also done, similar to the one done with parity, subdividing the BMI groups according to age groups and then to menopause groups (Appendix H). For geriatric age, the comparison between BMI groups of the same age range presented did not significant differences in any case (Appendix H1). For postmenopausal patients, the results were statistically significant between BMI groups, (Appendix H2) suggesting that when patients are postmenopausal and have a BMI>25 they develop a significantly stiffer tissue than postmenopausal patients with BMI<25. There were no statistically significant results between premenopausal BMI groups.

These results implicate that having a BMI>25 increases the risk of progression of POP, and when other risk factors, such as menopause and high parity, are present the risk of prolapse progression becomes even higher. A compound effect with age does not seem to alter the progression of prolapse.

5.2 Alterations in prolapsed AVW tissue due to parity

Parity is considered the primary risk factor for the onset of POP due to the trauma to the vaginal tissue associated with vaginal delivery [1,10]. This was related to the statistically significant results between parity groups that the BTC-2000^{TM} provided. Patients with high parity develop more complaint AVW tissue, detected by in-vivo testing.

The results from in-vitro testing were not statistically significant between groups of different parity number. This suggests that the mechanical properties of the tissue remain similar among diseased patients even when the number of deliveries increases, when no other risk factor is present. Therefore, parity may not be related to the progression of POP, but rather could be just an onset for the disease, as suggested by other research [1,10]. However, when other factors are present, POP could progress to

the point where the mechanical properties of the tissue change. This was demonstrated with the parity-obesity compound effect discussed above. Age and menopause were also correlated with parity to analyze any differences caused by these factors. The differences between parity number groups with same age ranges presented no statistical significant results (Appendix I1). On the other hand, the differences between parity groups in postmenopausal patients presented significant differences in yielding stress and failure stress (Appendix I2), suggesting that postmenopausal patients with high parity develop a stiffer AVW tissue. This could also be related with previous research findings about lower elastin content on tissue from postmenopausal women [44].

5.3 Alterations in prolapsed AVW tissue due to age and menopause

In this study, the age analysis did not presented differences in- vivo nor in-vitro testing. The post hoc analysis suggests an increase in sample size might be useful to determine if these results could have clinical relevance. However, when analyzing the compound effect of age with parity and age with obesity the difference in between groups did not present significant differences either. These suggest that aging do not alter the progression of pop and the biomechanical properties of the tissue. The pot-hoc analysis suggests a sample size of 175 would be appropriate to avoid missing an effect due to a smaller sample size. However, obtaining patients' consent is challenging and that sample size might be difficult to obtain.

On the other hand, menopause groups showed no statistically significant results. Since premenopausal group only included 7patients, an increase in sample size might give a better result. Postmenopausal patients showed to have a compound effect with high parity, in the development of POP (Appendix I2).

5.4 Reliability of in-vitro and in-vivo testing protocols

The aim of this study was firstly to analyze a better protocol for in-vitro testing, simulating forces that AVW prolapsed tissue undergoes and analyzing parameters that have not been analyzed in previous studies that define the nature of the tissue. It can be proved that the results from Instron cyclic tensile testing show significant differences in parameters with a comparable sample size, which indicate this testing protocol could be used to effectively determine the properties of AVW tissue.

Since the BTC-2000^{TM} only detect structural changes of the tissue, the correlation between in-vitro and in-vivo test and results was done in order to see if BTC-2000^{TM} would allow detection of differences among POP patients. Even though the mean values of the BTC-2000^{TM} parameters did not yield statistically significant differences for most of the risk factor groups, the trend lines from the correlation of in-vitro vs. BTC-2000^{TM} peak tissue uplift indicated that this cutometer-like instrument can detect differences in tissue compliance according to the severity of POP, which may be useful in the clinical diagnosis setting.

5.5 Limitations of the current study

One important limitation was the small sample size for premenopausal patients. This could have contributed to the lacking of clear statistical differences in the effect of menopause. Another important limitation was that the patients' information about hormone therapy was not provided, a factor that could alter the results obtained.

Another limitation was that there were no histological testing of the samples which could offer insights in elastic, collagen compositions and structure architecture, and their roles in varying biomechanical properties under different risk factors (BMI, parity, age, menopause, etc.).

Finally, although uniaxial tensile test is reliable for testing the mechanical properties of materials, a biaxial test might be more accurate since, physiologically, the tissue is strained in different directions.

Chapter 6

Conclusion and future studies

Anterior vaginal wall prolapse is a bothersome condition that affects thousands of women. In this study, biomechanical parameters from two different tests, performed in same patient group (in-vivo BTC-2000^{TM} suction pressure test, and in-vitro uniaxial tensile test), were systematically extracted and compared within the context of four prolapse risk factors. Both tests were designed to match the physiological conditions of maximal straining that AVW tissue is subjected to. Therefore, parameters from both tests were correlated, to verify if BTC-2000^{TM} can detect differences in tissue compliance and could be used as a diagnosis tool.

From all of the risk factors analyzed, an increased BMI showed to alter the biomechanical properties of tissue in patients with prolapse. This was the only risk factor whose parameters from in-vitro tensile test were statistically different, when compared in between groups. Patients with AVW prolapse and high BMI develop stiffer tissue than patients with low BMI.

Based on the results, it was hypothesized that an additional intra-abdominal pressure transferred to AVW tissue in obese patients may lead to the progression of POP due alterations in elastin composition and structure. Further histological tests are proposed for future studies, in addition to the biomechanical tests in obese patient. Additionally, a histological-biomechanical study of obese patients with POP before and after weight loss, could aid to determine if the connective tissue composition, that is causing these biomechanical property changes, is altered permanently.

Nevertheless, this study provided useful clinical information about a patient's weight and their progression of AVW prolapse, leading to the conclusion that having a healthy body weight may aid patients delay the progression of POP and it could be helpful to determine the patient's therapy or surgical options.

Parity number was correlated to the severity of prolapse, due to the statistical difference between means from BTC-2000^{TM} measurements. The behavior of the tissue showed that patients with high parity develop a more compliant tissue as the severity of POP increased. In-vitro test parameters did not present statistically significant differences. This could be related to other studies that suggest that parity is only linked to the onset and not to the progression of POP.

Age and menopause did not show significant differences in this study between groups. A greater sample size, especially for premenopausal patients, is proposed. Additionally, a record of hormone therapy of patients would help control other variables that could alter the tissue properties, and provide a better result

There was a compound effect of BMI and parity in the properties of AVW tissue: Patients with high BMI and high parity develop stiffer tissue than patients with low BMI and high parity. Patients with low parity did not present differences in between BMI groups. There was also a compound effect of BMI and menopause in the properties of AVW tissue: Postmenopausal patients with high BMI develop stiffer tissue than postmenopausal patients with low BMI. Premenopausal patients did not present differences between BMI groups.

The BTC-2000^{TM} by itself was able to detect differences between tissue compliance in POP patients. It was proved that it can be correlated linearly to the severity of POP. From the correlation between in-vitro and in-vivo test results, there were some in-vitro parameters from risk factor subgroups that exhibited sensitivities to an increase in

POP severity. Other in-vitro parameters showed to have insensitivity to POP severity. This could provide useful information about the behavior of the tissue, and could provide a better preoperative assessment for AVW repair.

Appendix A

Pictures of BTC-2000™ cutometer-like device and probe

A. 1 BTC-2000^{TM} device with target laser hand piece assembly (2 meter cord), AC/DC power supply with AC input cord from SRLI technologies [34]

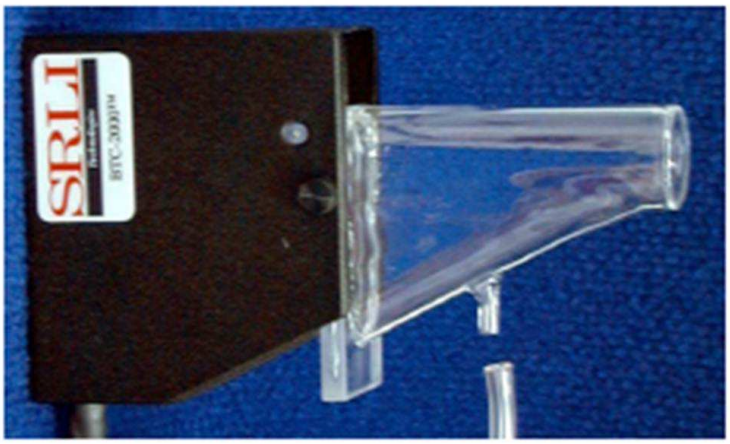

A. 2 The BTC-2000^{TM} probe. Trapezoidal glass chamber is fixed to a rectangular plastic endplate that fits into the black laser optics chamber. The orifice at the right is fit with a two-sided sticky tape washer to seal the AVW tissue to the chamber edge.

Appendix B

Description of in-vitro tissue strip test

Provided by Dr. Cheng-Jen Chuong

Harvesting tissue samples and preparation

With IRB approval, harvest of tissue samples was performed by Dr. Zimmern follow steps as previously described (Zimmern N&U 2009). Tissue samples approximately 1 cm x 3 cm were taken from the same area of AVW along anterior-posterior axis where In-vivo measurements were taken. A suture mark was applied at the top corner of the sample for reference of orientation. Tissue samples were placed in a dish covered with sterile gauze soaked with sterile media and transported to the facility for uni-axial tensile test performed within two hours from harvest.

1D tensile properties measurement of tissue specimen using Instron

Before testing, two reference marks in non-bleached India ink were applied to the sample surface approximately 10 mm apart along the longitudinal direction for reference during the test. After measuring the cross-sectional dimensions, tissue samples were loaded for tensile strength testing on an Instron^{TM} 5565 (Instron, Norwood, MA, USA). Samples were loaded between two grips with jaws to prevent slippage during test. We identified the tissue reference dimension corresponds to zero load by gently increased the grip distance until the force reading deviated from zero. The distances between two reference marks correspond to zero load were carefully measured with a caliper and used as the reference dimension for strain calculation.

Cross-sectional dimensions correspond to the midpoint of the tissue were measured for stress calculation. To precondition tissue specimen, each sample was stretched at a rate of 0.5 mm/s to 25% stretch and returned to the initial length for a total of 3 cycles after which the tissue sample was stretched until failure. The rationale for choosing 25% stretch is offered in Appendix B. Three cycles were used for preconditioning since our preliminary tests showed that tissue responses quickly converged. During tissue testing, tensile force and grip distance were digitized and recorded at a rate of 10 Hz. Raw data including that from all three loading-

unloading cycles and failure test were imported to a PC running MS Excel where Cauchy stresses and tissue strains were calculated for further data analysis.

Appendix C

Mathematical analysis that correlates in-vitro cyclic loading with in-vivo suction pressure force

A summary of note from Dr. Cheng-Jen Chuong

This analysis provides an approximation for tissue strain under BTC-2000TM pressure load. From the BTC-2000TM measurement, when the suction pressure load reaches maximum value, a maximum strain develops at the crown region of the distended tissue, as shown in figure C1. .

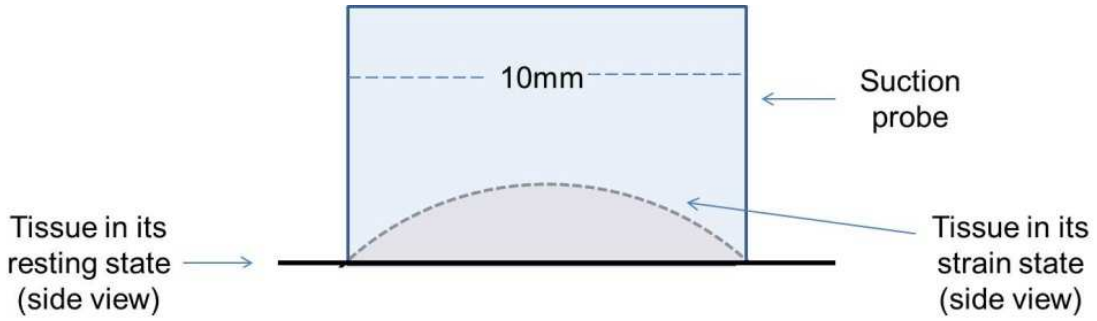

C.1 Side view representation of 1D peak tissue uplift

A geometric 1D analysis can be done to approximate the stretched area by assuming an uplift of 4mm, which is the approximate maximum uplift values reported in the experiments carried out for this thesis and previous experiments. If half of the strained tissue is represented by an arc $\overset{\frown}{CD}$ shown in Figure C2, then it can be calculated as a portion of the circumference with origin 0 by the size of its corresponding angle θ and the length of the radius R=$\overline{CO}$ of the circumference.

To find the angle θ from isosceles triangle DOC the other two angles, α, have to be subtracted. To obtain α from right angle BDC, the inverse tangent, knowing that$\overline{BC} = 5$, which represents half of the diameter of the probe, and $\overline{BD} = 4$, which is the peak tissue uplift, can be used as described in equation C1 and C2.

$$\alpha = tan^{-1}\left(\frac{\overline{BC}}{\overline{BD}}\right) = tan^{-1}\left(\frac{5}{4}\right) = 51.34° \quad \text{Eq. (C1)}$$

$$\theta = 180° - 2 \propto = 77.32° \quad \text{Eq. (C2)}$$

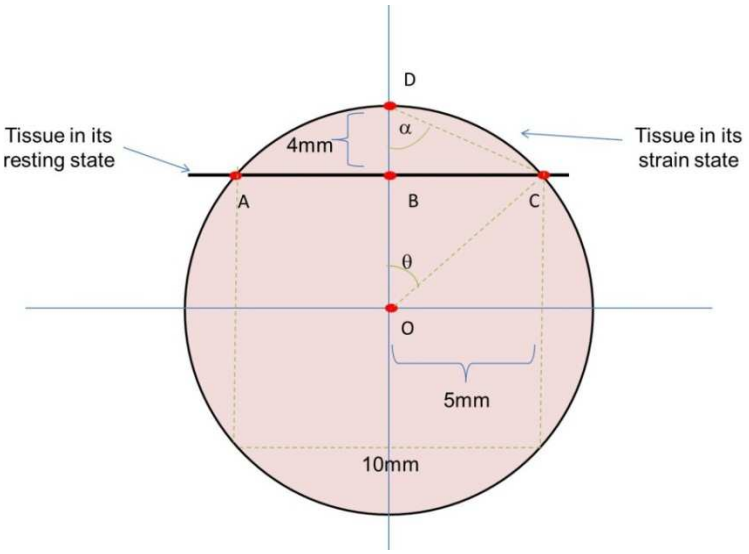

C.2 Geometric 1D analysis of peak tissue uplift

To obtain the radius R, from the triangle BCO the Pythagorean theorem can be used, where:

$$\overline{BC}^2 + \overline{BO}^2 = \overline{CO}^2 \qquad \text{Eq. (C3)}$$

Substituting and solving for R,

$$(R-4)^2 + 5^2 = R^2 \qquad \text{Eq. (C4)}$$

$$R^2 - 8R + 16 + 25 = R^2$$

$$R = \frac{41}{8} = 5.125\ mm$$

Now, the length of the arc *S* can be calculated as follows:

$$S = R\theta = 5.125 * \left(\frac{77.32}{180} * \pi\right) = 6.92mm \qquad \text{Eq. (C5)}$$

The strain can then be derived as the length of the arc and the tissue without strain ratio:

$$Strain = \left(\frac{6.92}{5} - 1\right) * 100 = 38\% \qquad \text{Eq. (C6)}$$

Moreover, with the same rationale, but since the strain is a quadratic elongation, the area strain at this region can be calculated from the ratio between the area at the uplifted, state

(A_{uplift}), and its initial state (A). The area at the initial state can be obtained by the area of a circle with a 10mm diameter, since this is the diameter of the suction probe:

$$A = \pi \left(\frac{d}{2}\right)^2 \quad \text{Eq. (C7)}$$

Were *d* is the probe diameter. The area at the uplifted state can be represented by:

$$A_{uplift} = \pi \left[\left(\frac{d}{2}\right)^2 + u_{Peak}^2\right] \quad \text{Eq.(C8)}$$

Were u_{peak} represents the maximum peak tissue uplift. The equivalent linear strain can then be derived from the square root of the area ratio,

$$e = \left(\sqrt{\frac{A_{Uplift}}{A}} - 1\right) * 100 = 28\% \quad \text{Eq. (C9)}$$

The same analysis was repeated for a peak tissue uplift of 3mm, and the results showed a 1D linear strain of 22.7% for the 1D analysis and an equivalent linear strain of 16.6%. Therefore after several experimental testing it was determined that a 25% strain in Instron would capture the same properties captured by the 150mmHg of suction pressure applied to the probe of BTC-2000TM, which gave peak tissue uplift results from the range from 1 to 4mm.

Appendix D

Matlab function that computes yielding point, maximal tangent modulus and failure point from Instron testing up to failure data

```
function [YStrain,YStress,MTM,YSE,errorYSE,StrainEnd,UTS,FSE,errorFSE]
= ComputeYieldAndFailureEnergy( x,y )
%ComputeYieldAndFailureEnergy returns:
    %YStrain: Strain at Yielding point
    %YStress: Stress at Yielding Point
    %MTM: Maximal Tangent Modulus
    %YSE: Strain Energy at Yielding Point
    %StrainEnd: Strain at Failure point
    %UTS: Stress at Failure Point
    %FSE: Strain Energy at Failure Point
 %For inputs it needs:
    %x:vector of strain values from Instron test
    %y:vector of Stress Values from Instron test
UTS=max(y); %Largest Stress measured from stress-strain Instron data
L=length(y); %Number of Stress Values
c=1;%Counter
while y(c)~=UTS & y<=L
    c=c+1;
end
StressEnd=y(c); %Use data up to the UTS
StrainEnd=x(c);
NewStress=y(1:c); %use Stress- Strain Values up to UTS
NewStrain=x(1:c);
p=polyfit(NewStrain,NewStress,6); %Fit the data with a 6th order polynomial
StressFit=polyval(p,NewStrain);
```

```
%%%%%COMPUTE MODULUS FROM 6th ORDER POLYNOMIAL
a=diff(StressFit)./diff(NewStrain) ;%dStrain/dStress
xp=NewStrain(2:end); % map the slope to the ending point (backward difference)
MTM=max(a); %Yielding Modulus
YStrain= xp(a==max(a(:))); %Yielding Strain
plot(x,y,'.',NewStrain,StressFit,'red');
xlabel('Strain')
ylabel('Stress')
 %%%COMPUTE YIELD STRAIN ENERGY FROM ORIGINAL DATA
 d=1;%Counter
while NewStrain(d)~=YStrain
    d=d+1;
end
YStress=NewStress(d);
YSE=trapz(NewStrain(1:d),NewStress(1:d))*1000;
 %%%COMPUTE YIELD STRAIN ENERGY FROM FIT TO OBTAIN ERROR %
YSEFit=trapz(NewStrain(1:d),StressFit(1:d))*1000;
errorYSE=100*((abs(YSEFit-YSE))/YSEFit);
 %%%COMPUTE FAILURE STRAIN ENERGY FROM ORIGINAL DATA
FSE=trapz(NewStrain,NewStress)*1000;
 %%%COMPUTE FAILURE STRAIN ENERGY FROM FIT TO OBTAIN ERROR %
FSEFit=trapz(NewStrain,StressFit)*1000;
errorFSE=100*((abs(FSEFit-FSE))/FSEFit);
 end
```

.

Appendix E

Outliers analysis

Two patients were considered as possible outliers because their stress-strain curves from Instron testing for the third cycle showed noise during the experiment (Figure E1). Their maximum stress values seem to be lower with respect to the other experiments during the cyclic loading, as shown in Figure E2.

Another patient, P36, was also considered as a possible outlier when comparing the BTC-2000^{TM} parameters. It was clearly observed a linear increase in energy absorption with an increase in peak tissue uplift except for this patient, as shown in Figure E3. When analyzing this same patient in other parameters, such as 25%LSE from Instron, it did not follow the trend line shown by the rest of the patients. Therefore it was also considered as a possible outlier.

A plot of the stress-strain response up to yielding point (Figure E4) and up to failure point (Figure E5), highlighting these 3 patient's responses was done. Since the plots during the responses did not show noisy curves and were within the expected values of response, all of the patients were considered for the study and there were no patients considered as outliers, since removing them may cause undesired and inaccurate alterations in the analysis.

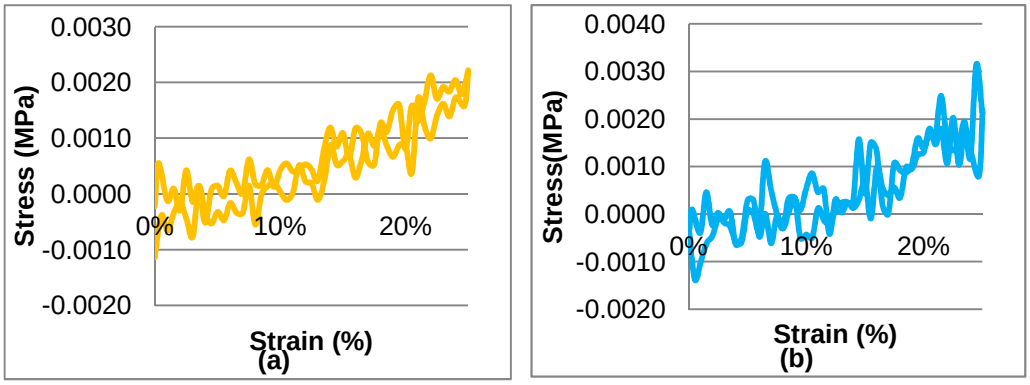

E.1Third loading-unloading cycle for two patients (a) P74 and (b) P75 considered as outliers due to experiment errors.

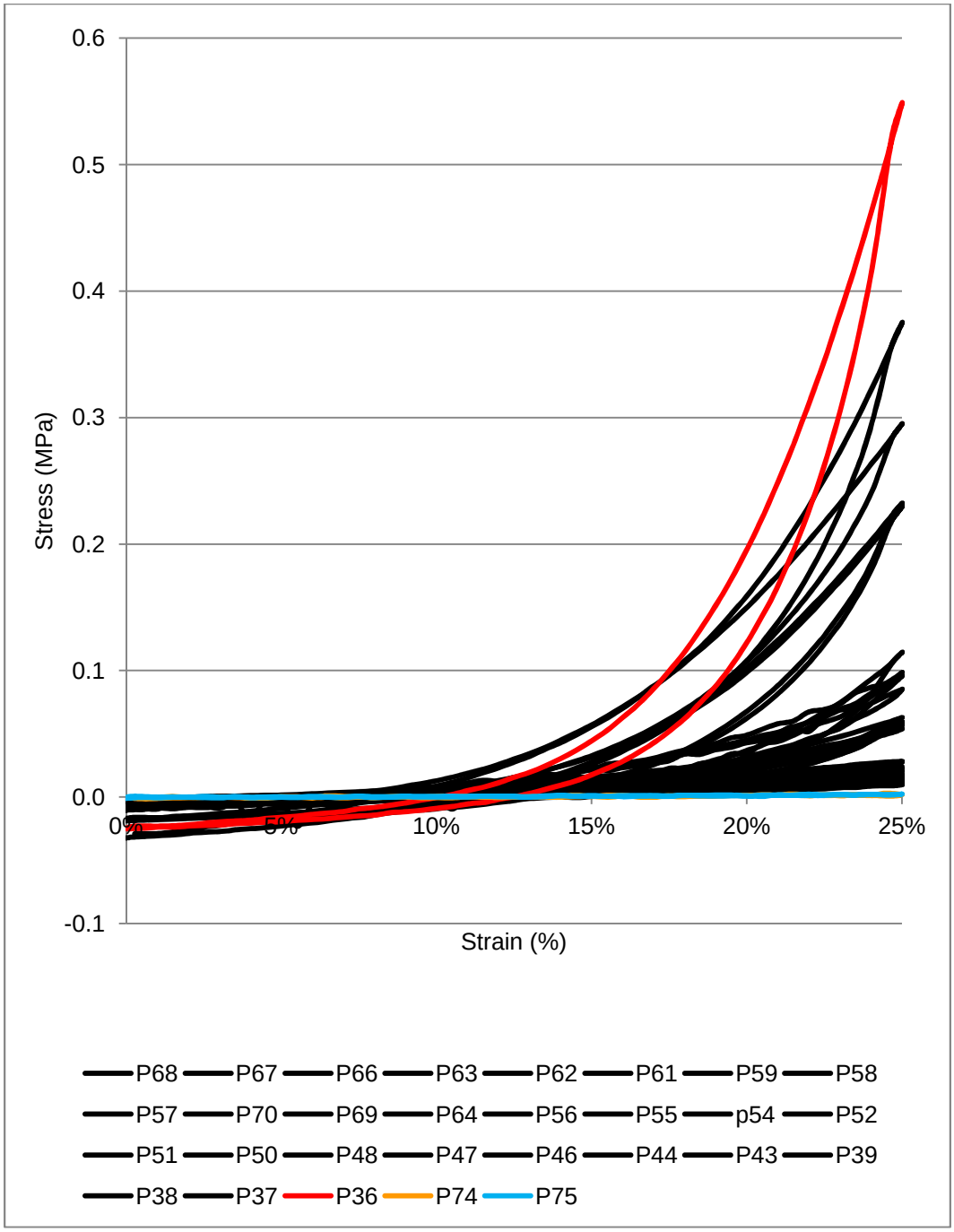

E.2 Instron stress-strain response up to 25%stretch for all patients. The 3 possible outliers are highlighted in red, orange and blue color respectively.

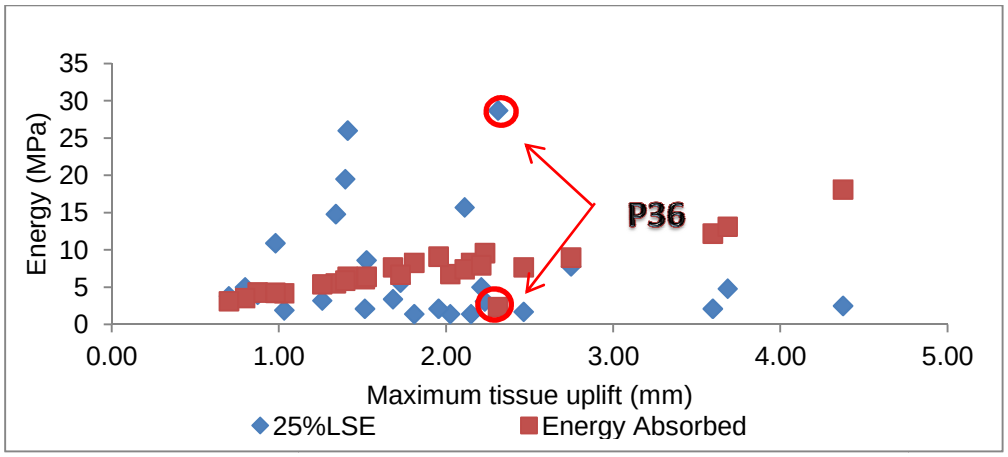

E.3 Plot of BTC-2000^{TM} parameters and 25%LSE against peak tissue uplift to show one patient as an outlier.

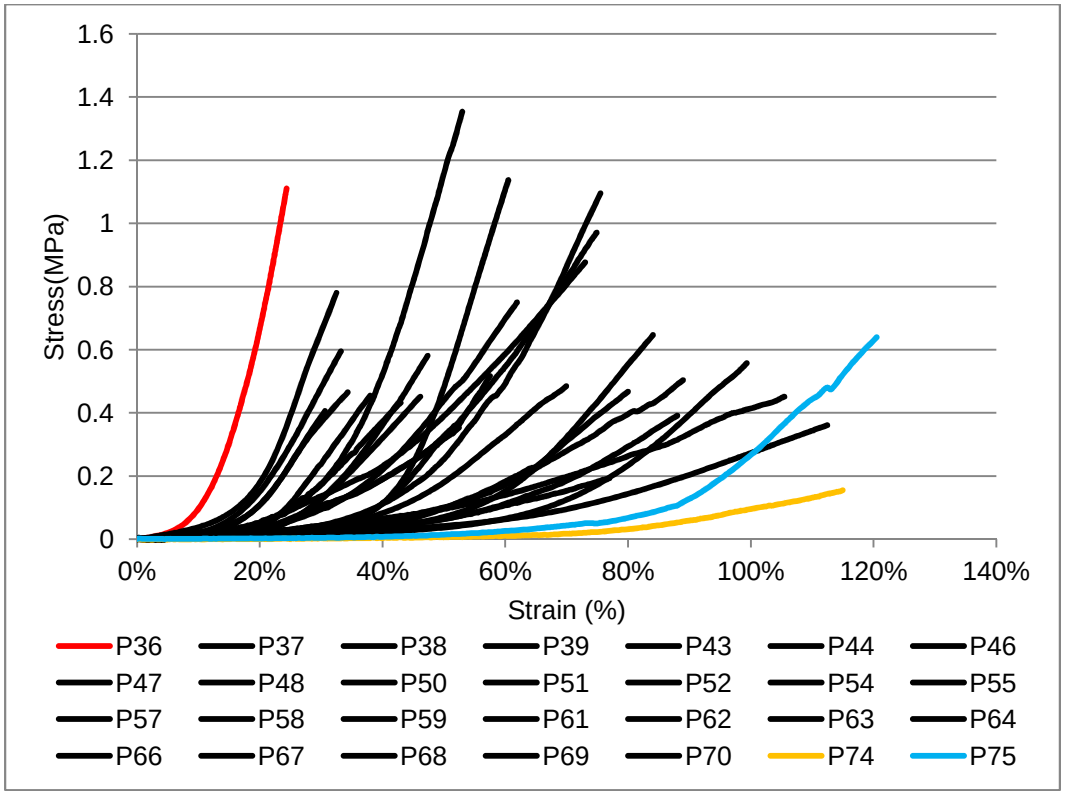

E.4 Instron stress-strain response up to yielding point for each patient. The 3 possible outliers are highlighted in red, orange and blue color respectively.

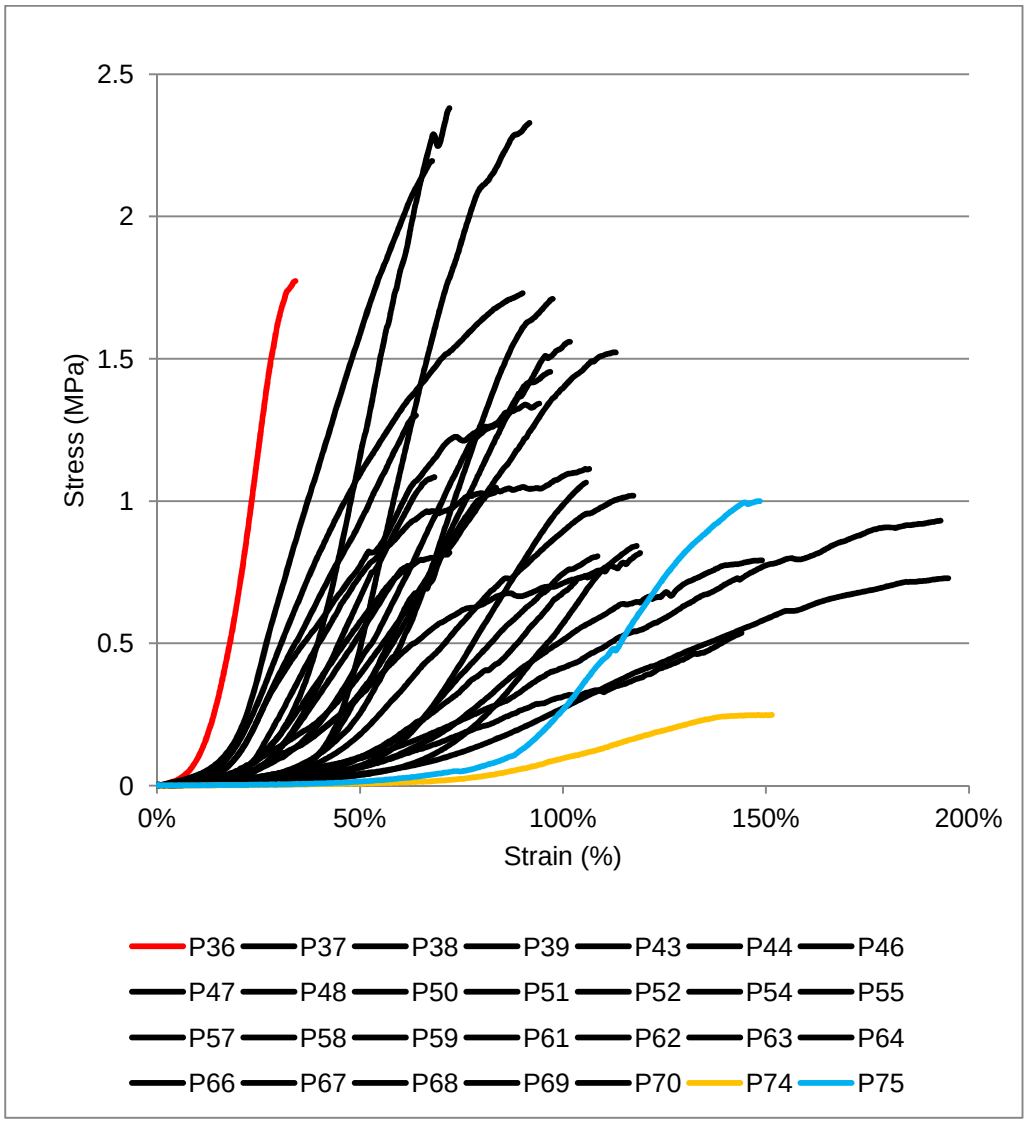

E.5 Instron stress-strain response up to failure point for each patient. The 3 possible outliers are highlighted in red, orange and blue color respectively.

Appendix F

Plot of each patient’s Instron stress-strain response divided into BMI groups

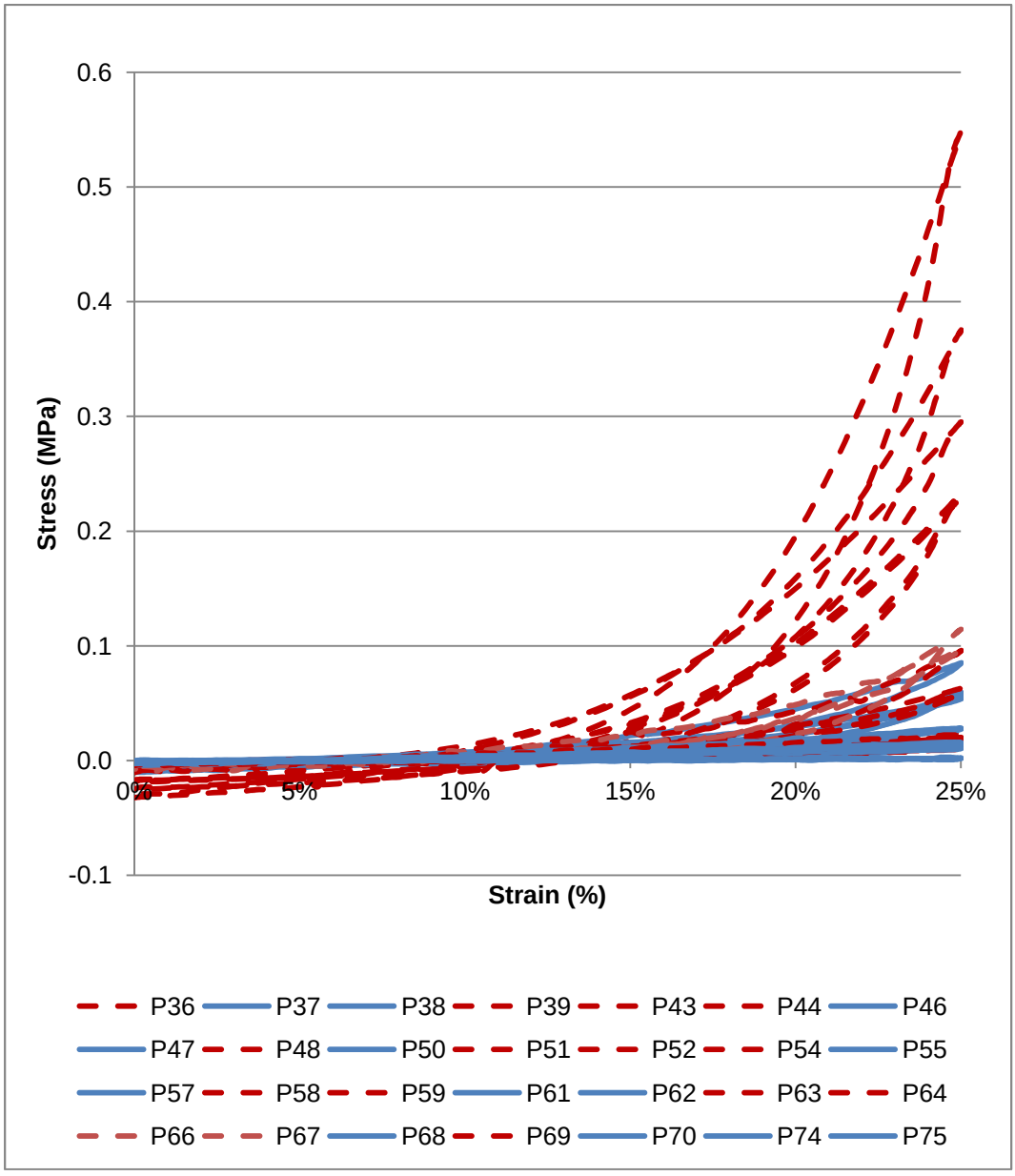

F.1 25% loading-unloading from Instron stress-strain response of each patient. Patients with BMI<25 are displayed in solid blue lines and patients with BMI≥25 in dashed red lines.

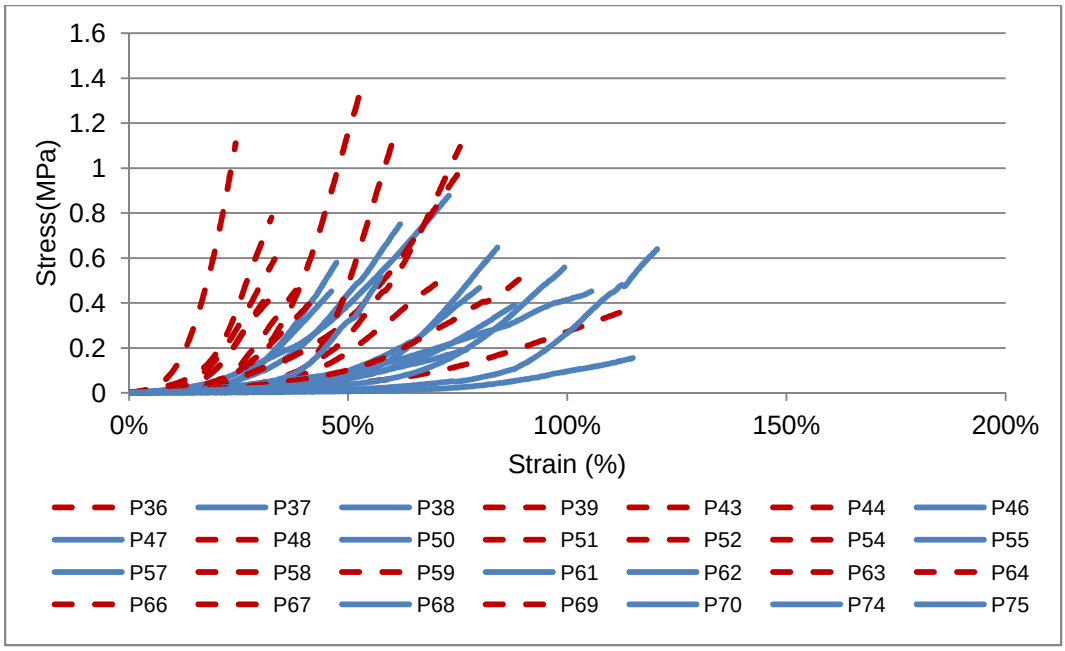

F.2 Instron stress-strain response up to yielding point of each patient. Patients with BMI<25 are displayed in solid blue lines and patients with BMI≥25 in dashed red lines.

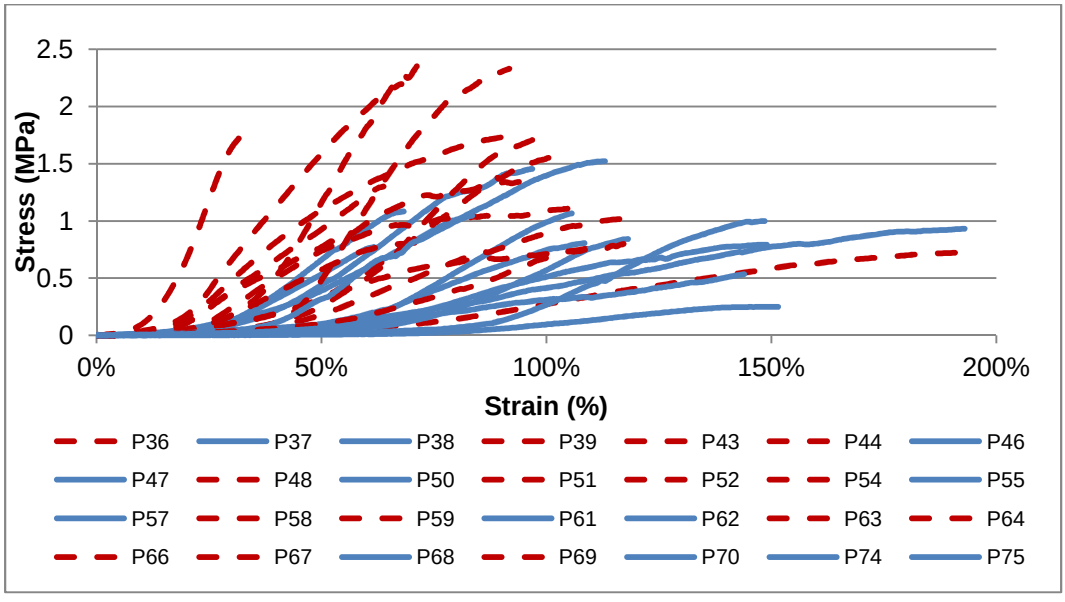

F.3 Instron stress-strain response up to failure point of each patient. Patients with BMI<25 are displayed in solid blue lines and patients with BMI≥25 in dashed red lines.

Appendix G

Yielding point, failure point and maximal tangent modulus from each patient divided by each risk factor group

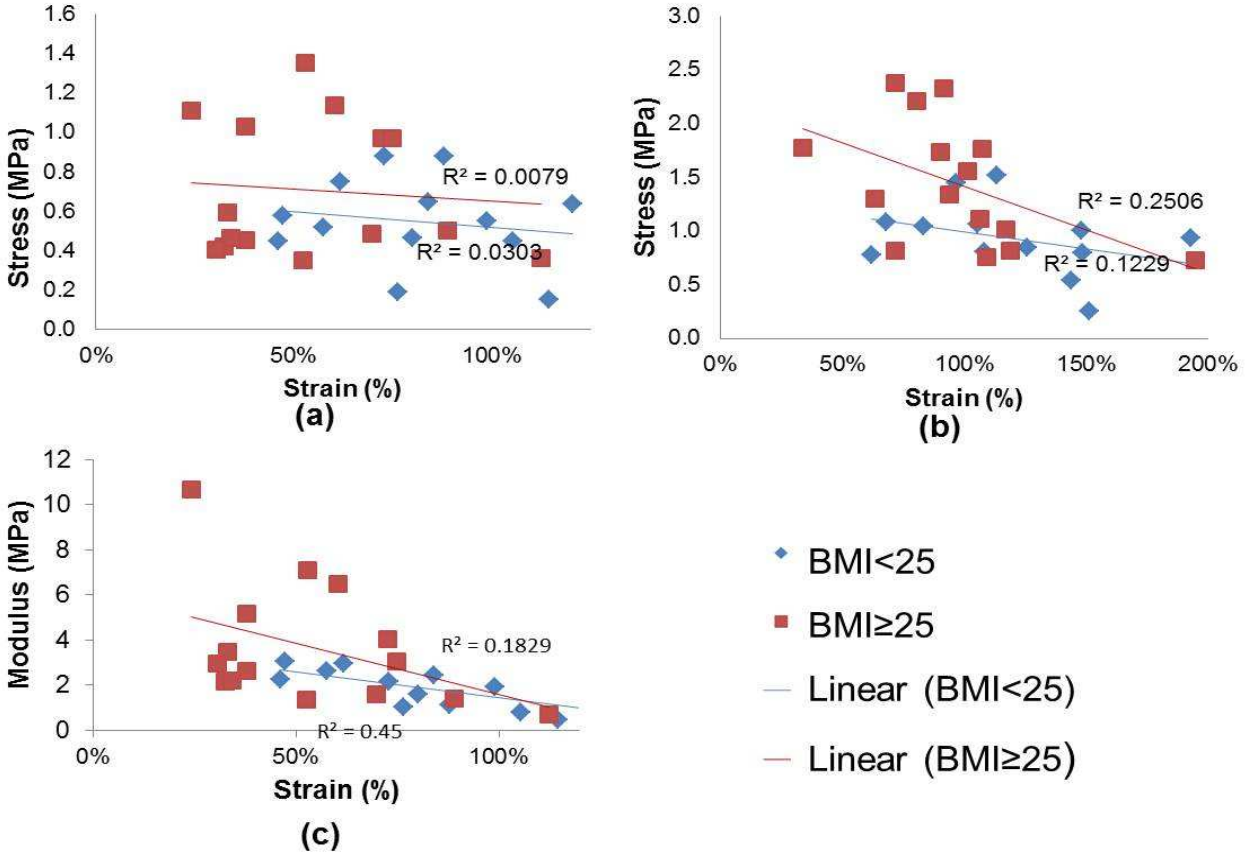

G.1 (a) Yielding Point (b) Failure Point (c) MTM for each patient of each BMI group and linear trend line for each group

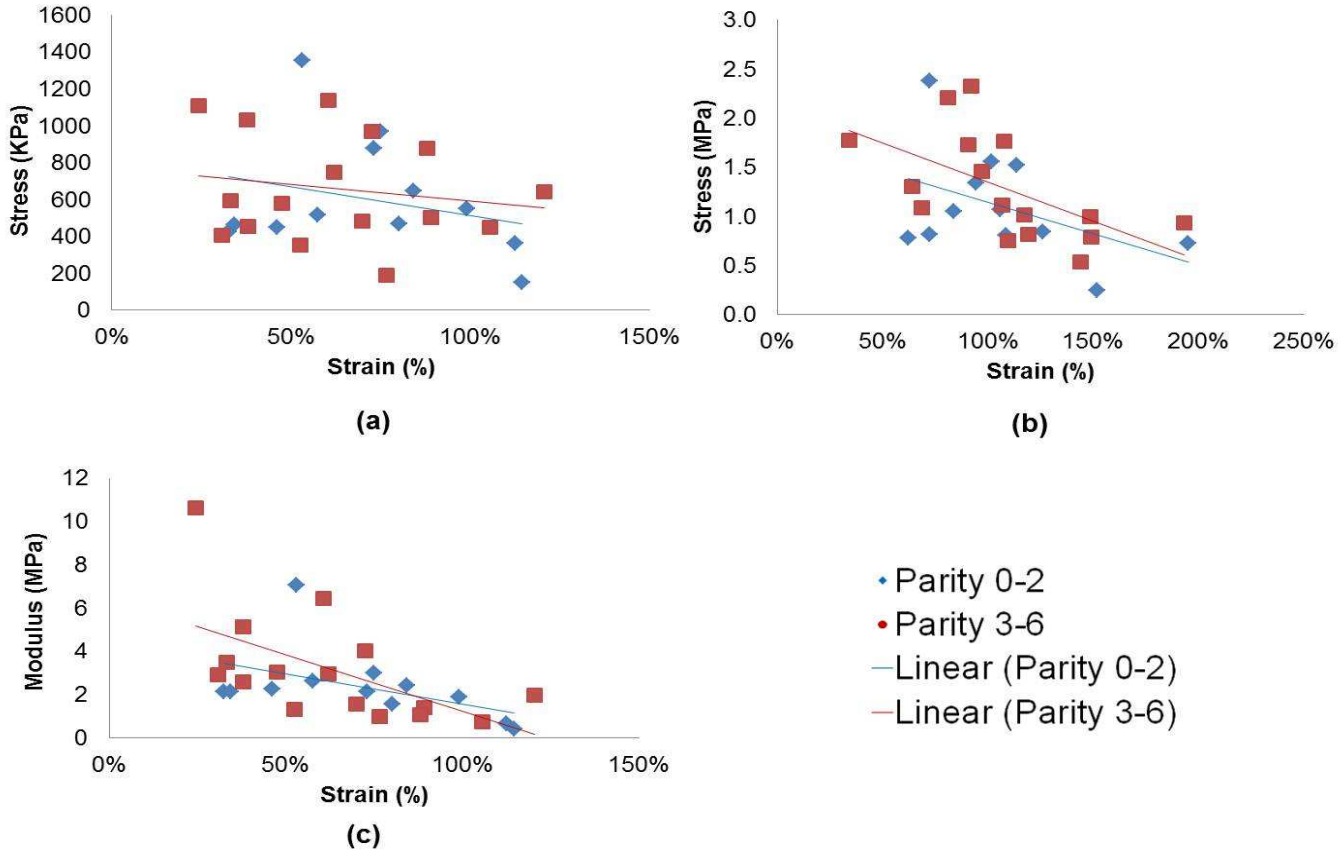

G.2 (a) Yielding Point (b) Failure Point (c) MTM for each patient of each Parity group and linear trend line for each group

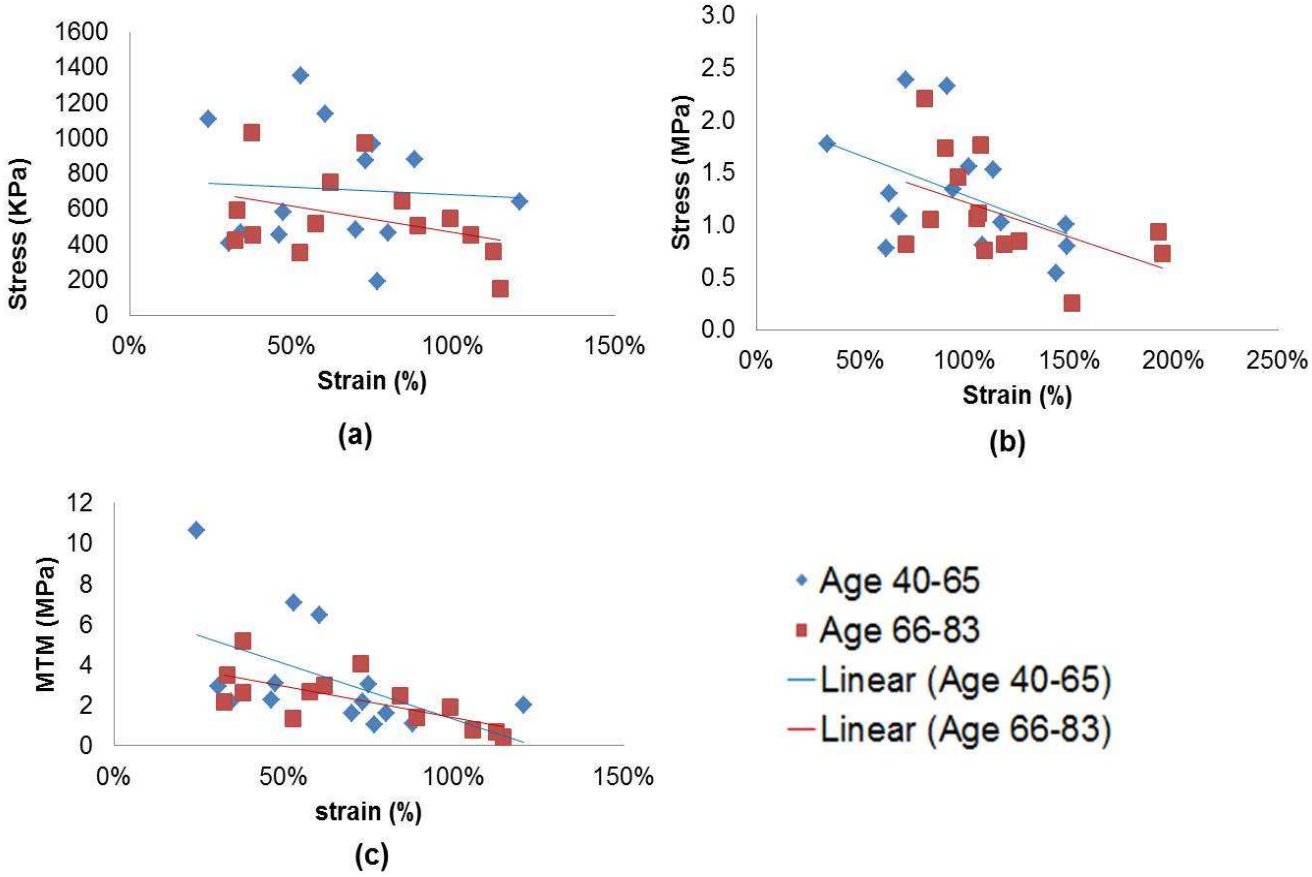

G.3 (a) Yielding Point (b) Failure Point (c) MTM for each patient of each age group and linear trend line for each group

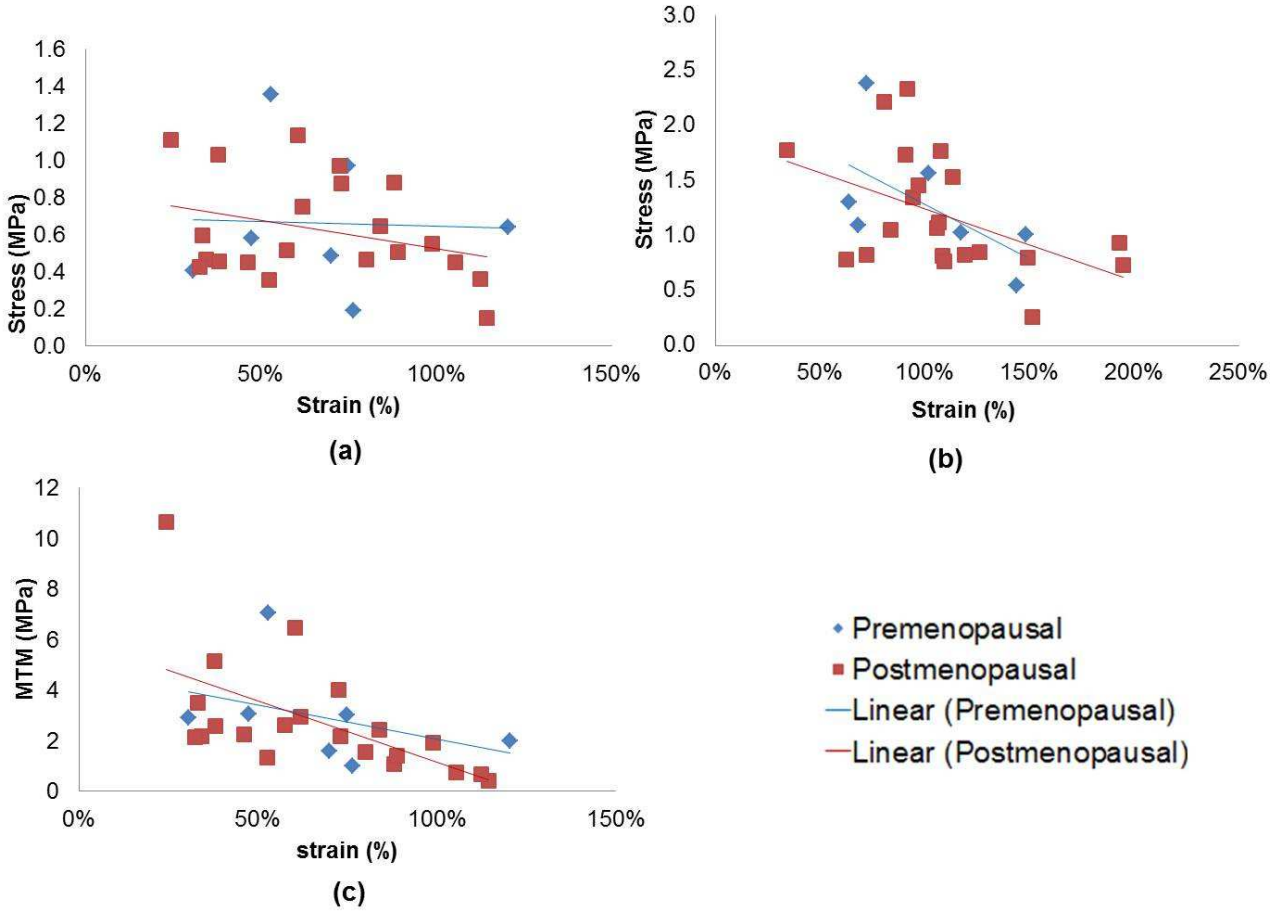

G.4 (a) Yielding Point (b) Failure Point (c) MTM for each patient of pre and postmenopausal groups and linear trend lines

Appendix H

Correlation of BMI with age and BMI with menopause

H.1. Mean ±SD of each BMI group subdivided according to same age range for geriatrics analysis, and P-values of t-tests between BMI groups. Red values indicate a statistically significant difference.

		Age ≤ 65			Age > 65		
		BMI<25 (n=7)	BMI≥25 (n=7)	P-Value	BMI<25 (n=6)	BMI≥25 (n=8)	P-Value
In-vivo (BTC-2000™)	Peak tissue uplift (mm)	2.16 ± 1.28	2.04 ± 1.14	0.85	1.78 ± 0.35	1.94 ± 0.82	0.62
	Energy absorption (KPa)	7.64 ± 3.99	7.36 ± 5.17	0.91	6.98± 1.08	7.91 ± 2.74	0.40
In-vitro (1D Tensile stretch)	10%TM (MPa)	0.07± 0.05	8.14 ± 5.18	0.035	0.08 ± 0.043	0.24 ± 0.21	0.074
	25%TM (MPa)	0.53 ± 0.47	6.38 ± 4.00	0.11	0.30 ± 0.25	1.69 ± 1.84	0.070
	25%LSE (KPa)	3.11 ± 2.40	10.96 ± 9.62	0.076	2.60 ± 1.60	9.18 ± 9.03	0.080
	25%USE (KPa)	2.41 ± 1.85	8.39 ± 7.27	0.074	2.07 ± 1.31	7.13 ± 7.02	0.083
	25%HSE (KPa)	0.69 ± 0.56	2.57± 2.36	0.081	0.53 ± 0.31	2.05 ± 2.02	0.072
	MTM (MPa)	1.87 ± 0.71	3.36 ± 3.31	0.056	1.85 ± 1.04	2.61 ± 1.52	0.29
	Yielding Strain (%)	75.93 ± 25.35	52.55 ± 20.06	0.053	87.06 ± 23.44	58.50 ± 29.85	0.068
	Yielding Stress (MPa)	0.58 ± 0.24	0.74 ± 0.39	0.15	0.51 ± 0.20	0.59 ± 0.26	0.55
	YSE (MPa)	0.096± 0.056	0.11 ± 0.063	0.80	0.10 ± 0.04	0.09 ± 0.04	0.61
	Failure Strain (%)	113.42 ± 36.78	89.81 ± 27.69	0.099	126.10 ± 40.52	110.08 ± 37.77	0.46
	Failure Stress (MPa)	0.93 ± 0.31	1.52 ± 0.52	0.009	0.93 ± 0.39	1.24 ± 0.57	0.25
	FSE (MPa)	0.36 ± 0.18	0.50 ± 0.17	0.18	0.39 ± 0.24	0.58 ± 0.23	0.17

H.2 Mean ±SD of each BMI group subdivided according to pre and postmenopausal groups, and P-values of t-tests between BMI groups. Red values indicate a statistically significant difference.

		Premenopausal			Postmenopausal		
		BMI<25 (n=3)	BMI≥25 (n=4)	P-Value	BMI<25 (n=10)	BMI≥25 (n=11)	P-Value
In-vivo (BTC-2000™)	Peak tissue uplift (mm)	2.28 ± 1.50	2.20 ± 1.54	0.94	1.89 ± 0.83	1.91 ± 0.68	0.96
	Energy absorption (KPa)	7.95 ± 4.97	8.86 ± 6.37	0.91	7.15 ± 2.39	7.21 ± 2.77	0.95
In-vitro (1D Tensile stretch)	10%TM (MPa)	0.04 ± 0.038	0.20 ± 0.11	0.066	0.08 ± 0.04	0.24 ± 0.19	0.029
	25%TM (MPa)	0.39 ± 0.55	1.51 ± 1.13	0.15	0.43 ± 0.37	2.32 ± 2.59	0.044
	25%LSE (KPa)	1.99 ± 1.68	7.95 ± 5.75	0.12	3.14 ± 2.09	10.75 ± 9.62	0.032
	25%USE (KPa)	1.59 ± 1.32	6.10 ± 4.16	0.11	2.45 ± 1.64	8.30 ± 7.39	0.032
	25%HSE (KPa)	0.38 ± 0.33	1.85 ± 1.58	0.15	0.69 ± 0.47	2.45 ± 2.23	0.032
	MTM (MPa)	2.01 ± 1.01	3.65 ± 2.37	0.27	1.82 ± 0.83	3.65 ± 2.90	0.069
	Yielding Strain (%)	81.45 ± 36.81	57.11 ± 19.99	0.37	80.95 ± 21.85	53.38 ± 27.75	0.020
	Yielding Stress (MPa)	0.47 ± 0.24	0.81 ± 0.44	0.26	0.57 ± 0.22	0.67 ± 0.32	0.42
	YSE (MPa)	0.081 ± 0.046	0.12 ± 0.07	0.41	0.10 ± 0.05	0.090 ± 0.040	0.2
	Failure Strain (%)	120.26 ± 45.05	88.72 ± 25.09	0.35	118.98 ± 37.68	100.6 ± 39.03	0.27
	Failure Stress (MPa)	0.87 ± 0.29	1.56 ± 0.59	0.10	0.95 ± 0.36	1.40 ± 0.59	0.049
	FSE (MPa)	0.30 ± 0.06	0.47 ± 0.11	0.051	0.40± 0.23	0.56 ± 0.23	0.11

Appendix I

Correlation of parity with age and parity with menopause

I.1 P-values of t-tests between parity groups of the same age range for all tested parameters

		Age 40-65 (P-Value) Parity:0-2=6 patients Parity:3-6 =8 patients	Age 66-80 (P-Value) Parity:0-2=6 patients Parity:3-6 =8 patients
In-vivo (BTC-2000$^{TM)}$	Peak tissue uplift	0.032	0.43
	Energy absorption	0.11	0.30
In-vitro (1D tensile test)	10%TM	0.62	0.33
	25%TM	0.70	0.12
	25%LSE	0.99	0.15
	25%USE	0.99	0.16
	25%HSE	0.97	0.13
	MTM	0.70	0.14
	Yield Strain	0.74	0.2
	Yield Stress	0.66	0.1
	YSE	0.18	0.30
	Failure Strain	0.58	0.68
	Failure Stress	0.60	0.02
	FSE	0.39	0.0044

I.2 P-values of t-tests between BMI groups of the same menopausal status for all tested parameters

		Premenopausal (P-Value) Parity:0-2=2 patients Parity:3-6 =5 patients	Postmenopausal (P-Value) Parity:0-2=10 patients Parity:3-6 =11 patients
In-vivo (BTC-2000$^{TM)}$	Peak tissue uplift	0.096	0.11
	Energy absorption	0.15	0.18
In-vitro (1D tensile test)	10%TM	0.35	0.33
	25%TM	0.72	0.20
	25%LSE	0.54	0.22
	25%USE	0.54	0.22
	25%HSE	0.67	0.21
	Yield Strain	0.80	0.30
	Yield Stress	0.12	0.025
	MTM	0.37	0.075
	YSE	0.022	0.51
	Failure Strain	0.40	0.81
	Failure Stress	0.22	0.025
	FSE	0.004	0.022

References

1. Pelvic Organ Prolapse Statistics. National Association for Continence, 2012. Web. 1 March 2013. Retrieved from http://www.nafc.org/media/statistics/pelvic-organ-prolapse/
2. Rubod C, Boukerrou M, Brieu M, et al. Biomechanical properties of vaginal tissue: Preliminary results. Int Urogynecol J Pelvic Floor Dysfunct. 2008 Jun;19(6):811-6. DOI 10:1007/s00192-007-0533-3
3. Anterior Vaginal Repair (Bladder repair) A Guide for Women,2011. Web. 1 March 2013. International Urogynecological Association.Retrieved from www.iuga.org
4. Abramowitch SD, Feola A, Jallah Z et al. Tissue mechanics, animal models, and pelvic organ prolapse: A review. Eur Journal Obstet Gynecol and Reprod Biol.144S: S146, 2009.
5. Rubod C, Boukerrou M, Brieu M, et al. Biomechanical Properties of Vaginal Tissue. Part 1: New Experimental Protocol. J Urol 178: 320, 2007.
6. Chen, Luyun (2008) biomechanical analyses of anterior vaginal Wall prolapse: mr imaging and computer modeling studies. Dissertation from The University of Michigan.Web. Retrieved 1 Nov, 2012.
7. Baggish M, Karram,M (2001). Anatomy of the Vagina. Atlas of Pelvic Anatomy and Gynecologic Surgery. Section B- Vaginal surgery P336-348. ISBN 0721683185
8. Goh JT. Biomechanical and biochemical assessments for pelvic organ prolapse. Curr Opin Obstet Gynecol. 2003 Oct;15(5):391-4.

9. Walters, Mark (2005). Anterior vaginal wall prolapse: Innovative surgical approaches. Cleveland clinic journal of medicine volume 72 supplement 4
10. Lei L, Song Y and Chen R et al. Biomechanical properties of prolapsed vaginal tissue in pre- and postmenopausal women. Int Urogynecol J Pelvic Floor Dysfunct. 18 (6): 603,2007.
11. Moalli PA, Debes KM, Meyn LA, et al. Hormones restore biomechanical properties of the vagina and supportive tissues after surgical menopause in young rats. Am J Obstet Gynecol.199:161.e1,2008
12. Kudish, et al. (2009). Effect of Weight Change on Natural History of Pelvic Organ Prolapse. Obstet Gynecol. 2009 January ; 113(1): 81–88. Doi:10.1097/AOG.0b013e318190a0dd.
13. Krissi H, Eitan R, Ram E, Peled Y (2012) How Accurate Is Preoperative Evaluation of Pelvic Organ Prolapse in Women Undergoing Vaginal Reconstruction Surgery? Plos ONE 7(10): e47027. Doi:10.1371/journal.pone.0047027
14. Egorov Et Al.: Vaginal Tactile Imaging IEEE Transactions On Biomedical Engineering, Vol. 57, No. 7, July 2010 Digital Object Identifier 10.1109/Tbme.2010.2045757
15. Bump, Richard, et al. (1996) The standardization of terminology of female pelvic organ prolapse and pelvic floor dysfunction. Volume 175, Number 1 Bump eta[. 11 Amj Obstet Gynecol
16. Moore, et. al. Single-incision vaginal approach to treat cystocele and vault prolapse with an anterior wall mesh anchored apically to the sacrospinous ligaments. Int Urogynecol J (2012) 23:85–91. DOI 10.1007/s00192-011-1536-7

17. FDA Report (2011) Urogynecologyc Surgical Mesh: Update on the safety and effectiveness of transvaginal placement for pelvic organ prolapse. July 2011.Retrieved Sep 1, 2012.
18. Feola A, Abromowitch S, Jones K, et al. Parity negatively impacts vaginal mechanical properties and collagen structure in rhesus macaques. Am J Obstet Gynecol;203:595.e1-8, 2010.
19. Epstein LB., Graham , Carol A., Heit, Michael H. Correlation between vaginal stiffness index and pelvic floor disorder quality-of-life scales. Int Urogynecol J 19:1013–1018, 2008.
20. Mosier E, Lin V and Zimmern P. Extracellular Matrix Expression of human prolapsed Vaginal Wall. Neourology and Urodynamics.2009 Apr;29(4):582-6. DOI10.002/nau20806
21. Epstein LB, Graham CA, Heit MH. Systemic and vaginal biomechanical properties of women with normal vaginal support and pelvic organ prolapse. Am J Obstet Gynecol;197:165.e1-165e6, 2007.
22. Rahn, David D. Et al. Biomechanical properties of the vaginal wall: effect of pregnancy, elastic fiber deficiency, and pelvic organ prolapse. Am J Obstet Gynecol 198:590.e1-590.e6 2008.
23. Karam JA, Vazquez DV, Lin VK et al: Elastin expression and elastic fibre width in the anterior Vaginal wall of postmenopausal women with and without prolapse. BJU Int 2007; 100: 346.
24. Phillips CH, Anthony F, Benyon C, Monga AK. Collagen metabolism in the uterosacral ligaments and vaginal skin of womenwith uterine prolapse. BJOG 2006;113:39–46.

25. Zong, et al. Alteration of vaginal elastin metabolism in women with pelvic organ prolapse. Obstet Gynecol. 2010 May ; 115(5): 953–961. Doi:10.1097/AOG.0b013e3181da7946.
26. Alperin, Marianna and Moalli, Pamela (2006). Remodeling of vaginal connective tissue in patients with prolapse. Curr Opin Obstet Gynecol 18:544–550. _ 2006 Lippincott Williams & Wilkins.
27. Northington, et al. (2011)Contractile Response of Human Anterior Vaginal Muscularis in Women With and Without Pelvic Organ Prolapse. Reproductive Sciences 18(3) 296-303 DOI: 10.1177/1933719110392054
28. Bump, Richard, et al. (1996) The standardization of terminology of female pelvic organ prolapse and pelvic floor dysfunction. Volume 175, Number 1 Bump eta[. 11 Amj Obstet Gynecol
29. Alperin, Marianna et al. LOXL1 deficiency negatively impacts the biomechanical properties of the mouse vagina and supportive tissues. Int Urogynecol J Vol 19:977–986, 2008.
30. Epstein LB, Graham CA, Heit MH. Systemic and vaginal biomechanical properties of women with normal vaginal support and pelvic organ prolapse. Am J Obstet Gynecol;197:165.e1-165e6, 2007.
31. Mosier E, Jerome R, Xie XJ, Chuong CCJ, Yan J, et al. (2011) In Vivo Btc-2000™ Measurement of Anterior Vaginal Wall Biomechanical Properties in Prolapse Patients Undergoing Surgical Repair. J Biotechnol Biomaterial 1:117. doi:10.4172/2155-952X.1000117
32. Zimmern, et al. (2009).Methodology for biomechanical testing of fresh Anterior Wall Vaginal samples from Postmenopausal Women Undergoing Cystocele Repair. DOI 10.1002/nau.20657 Neurology and Urodynamics 28:325-329.

33. Chuong C, Towns R, Eberhart R, et al. Development of a biomechanical finite element model to predict prolapsed anterior vaginal wall compartment properties. UTSW medical center. PDF. Retrieved Sep 1, 2012 from www.ics.org/Abstracts/Publish/105/000095.pdf
34. SLRI Technologies (2003). Biomechanical Tissue Characterization. BTC-2000™User Manual. PDF. Retrieved from Www.srli.com
35. Matlab Tutorial –Numerical Integration. Mathworks. Web Retrieved March1, 2013 from www.ee.hacettepe.edu.tr/.../Matlab/Matlab%20Tutorial/Matlab
36. Chuong et al. (1991). On the Anisotropy of the Canine diaphragmatic Central TendonJ Biomech.1991;24(7):563-76. doi.org/10.1016/0021-9290(91)90289-Y
37. Wood, G (1982) Data smoothing and differentiation procedures in Biomechanics.
38. Ogden C, Carroll, MD, Kit BK, et al. Prevalence of Obesity in the United States, 2009–2010. NCHS data brief. 82, 2012. Web. March 2013.
39. Biancalana A, Veloso LA and Gomes L. Obesity Affects Collagen Fibril Diameter and Mechanical Properties of Tendons in Zucker Rats. Connect Tissue Res. 51;171, 2010.
40. Aging Statistics. Administration of Aging.Web. Sep 01, 2011. Retrieved March 01,2013. from http://www.aoa.gov/Aging_Statistics/
41. Cohen, J. Statistical Power Analysis for the Behavioral Sciences. USA 1977. LEA Inc. 2nd Edition P66-73. ISBN 0.8058—283-5.
42. Klutke J,Ji Q, Campeau J, et al. Decreased endopelvic fascia elastin content in uterine prolapse. Acta Obstetricia et Gynecologica. 87: 111,2008
43. Moon YJ, Choi JR, Jeon MJ et al. Alteration of Elastin Metabolism in Women With Pelvic Organ Prolapse. J Urol. 185: 1786, 2011.

44. Goepel C: Differential elastin and tenascin immunolabeling in the uterosacral ligaments in postmenopausal women with and without pelvic organ prolapse. Acta Histochem. 110: 204,2008
45. Chen JY, Tsai PJ, Tai HC, et al. Increased Aortic Stiffness and Attenuated Lysyl Oxidase Activity in Obesity. Arterioscler Thromb Vasc Biol.Web. Published online before print 14 Feb 2013.
46. Szczesny W, Bodnar M, Dabrowiecki S et al. Histologic And Immunohistochemical Studies Of Rectus Sheath In Obese Patients. J Surg Res. E1-E6,2011.
47. Liu X, Zhao Y, Gao J, Pawlyk B, Starcher B, Spencer JA, et al. Elastic fiber homeostasis requires lysyl oxidase-like 1 protein. Nat Genet. 2004;36:178_82.
48. Myers DL, Sung VW, Richter HE et al. Prolapse Symptoms in Overweight and Obese Women Before and After Weight Loss. Female Pelvic Med Reconstr Surg. 18 (1) :55, 2012
49. Noblett KL, Jensen JK and Ostergard Dr. The Relationship of Body Mass Index to Intra-abdominal Pressure as Measured by Multichannel Cystometry. Int Urogynecol J Pelvic Floor Dysfunct . 8:323, 1997.
50. Greer WJ, Richter HE, Bartolucci AA, et al. Obesity And Pelvic Floor Disorders: A Review Of The Literature. Obstet Gynecol. 112:341, 2008.
51. Mangera, et. Al. Are biomechanical properties predictive of the success of prostheses used in stress urinary incontinence and pelvic organ prolapse? A systematic review. Neurourology And Urodynamics 2012 Jan; Vol. 31 (1), pp. 13-21. Date of Electronic Publication: 2011 Oct 28. DOI 10.1002/nau.21156

52. Unal R, Yao-Borengasser A, Varma V, ET AL. N Matrix Metalloproteinase-9 Is Increased in Obese Subjects and Decreases in Response to Pioglitazone .J Clin Endocrinol Metab, June 2010, 95(6):2993–3001
53. Ashton-Miller J. and DeLancey J. On the Biomechanics of Vaginal Birth and Common Sequelae. Annu Rev Biomed Eng. 2009 ; 11: 163–176. doi:10.1146/annurev-bioeng-061008-124823.
54. Fung YC (1993). Biomechanics: Mechanical properties of living tissues, 2nd Edition Spring Verlag, USA. ISBN: 978-1-4419-3104-7
55. Wang J, Thampatty B, Lin, JS et al. Mechanoregulation of gene expression in fibroblasts. *Gene*. 2007 April 15; 391(1-2): 1–15. doi:10.1016/j.gene.2007.01.014.
56. Mouritsen L. Classification and evaluation of prolapse. Best Practice and Research Clinical Obstetrics and Gynaecology. Vol. 19, No. 6, pp. 895-911, 2005. doi:10.1016/j.bpobgyn.2005.08.007
57. Feola A, Moalli P, Alperin M, et al. Impact of Pregnancy and Vaginal Delivery on the Passive and Active Mechanics of the Rat Vagina. Ann Biomed Eng. 2011 January ; 39(1): 549–558. doi:10.1007/s10439-010-0153-9.
58. Nahum A, Melvin J. Accidental Injury. Biomechanics and prevention. 2nd edition. 2002. Springer, USA.ISBN-110: 0-387-98820-3.Ch11 :228-253.
59. Griffiths D.J., Van Mastrigt R, Van Duyl W, et al. Active mechanical properties of the smooth muscle of the urinary bladder. Med & Biol. Eng. & Comput., 1979, 17, 281-290.
60. David J. Tensile testing. ASM International: The Materials Information Society. 2004. Second Edition. USA. Chapter 3, 33-78. ISBN:0-87170-806-X

61. Cornelis S, Pastore J, MacKintosh F, et al. Nonlinear elasticity in biological gels.Cornell University Library, 2004. Retrieved March 1, 2013. Web. From http://arxiv.org/abs/cond-mat/0406016
62. Bhatt A. Biomechanical properties of anterior vaginal wall tissue in post-menopausal women. Thesis presented to the University of texas at Arlington. 2005. Web. Retrieved Sep 1, 2012. From UTA library.
63. Akins, M, Luby-Phelps, K., Bank, R., and Mahendroo, M. Cervical softening during pregnancy- regulated changes in collagen cross-linking and composition of matricellular proteins in the mouse. Biol. of Reprod 2011 84 1053-62
64. Timmons, B.C., Fairhurst, A.M.F., and Mahendroo, M. Temporal changes in myeloid cells in the cervix during pregnancy and parturition. J of Immunology 2009 182 2700-2707
65. Ruscheinsky M., De la Motte C., and Mahendroo M.Hyaluronan and its binding proteins during cervical ripening and parturition: Dynamic changes in size, distribution and temporal sequence.Matrix Biology Summer 2008 27 487-497

Biographical Information

Sandra Gabriela Ochoa Lopez completed her Bachelor of Science in Biomedical Engineering from the Monterrey Institute of Technology and Higher Education, in Monterrey Campus at Mexico, in December 2008. After graduating she worked for two and a half years in the hospital environment for a company that provided Minimal Invasive Surgery Service to Public and Private hospitals in Mexico as the North Mexico Coordinator. Her main responsibilities were training of technicians that assisted in surgeries, and preventive and corrective maintenance of equipment. She obtained a scholarship from the Mexican National Council of Science of Technology and enrolled in the Masters joint program of Biomedical Engineering at University of Texas at Arlington/University of Texas Southwestern Medical center, in August 2011. During the course of her education she worked on various class projects and presentations related to the biomechanics track. The outcome of this research and thesis is important clinically, since it provides useful information regarding the biomechanics of the Anterior Prolapsed Vaginal Wall that could provide much needed quantitative preoperative assessment and might also turn out to be very useful in the design and development of better prosthetic meshes for vaginal wall repairs. She looks forward to applying and expanding the knowledge and abilities she obtained into her professional development by working in the biomechanics field. Additionally she plans to aid in the expansion of this area of knowledge, which is emerging in Mexico, by possibly becoming a teacher and also being involved in more research projects.